

AD-756 547

FORCES ON A HORIZONTAL CYLINDER DUE TO
NON-LINEAR WAVES

Fred Herman Gehrman, Jr.

Naval Postgraduate School
Monterey, California

December 1972

DISTRIBUTED BY:

NTIS

National Technical Information Service
U. S. DEPARTMENT OF COMMERCE
5285 Port Royal Road, Springfield Va. 22151

AD 756547

NAVAL POSTGRADUATE SCHOOL

Monterey, California



THESIS

D D C
RECEIVED
MAR 12 1973
RECEIVED

FORCES ON A HORIZONTAL CYLINDER
DUE TO NON-LINEAR WAVES

by

Fred Herman Gehrman Jr.

Reproduced by
NATIONAL TECHNICAL
INFORMATION SERVICE
U.S. Department of Commerce
Springfield VA 22151

Thesis Advisor:

C.J. Garrison

December 1972

Approved for public release; distribution unlimited.

107

DOCUMENT CONTROL DATA - 2 & D

(Security classification of title, body of abstract and indexing annotation must be entered when the overall report is classified)

1. ORIGINATOR'S ACTIVITY (Corporate author) Naval Postgraduate School Monterey, California 93940		2a. REPORT SECURITY CLASSIFICATION Unclassified	
		2b. GROUP	
3. REPORT TITLE Forces on a Horizontal Cylinder Due to Non-Linear Waves			
4. DESCRIPTIVE NOTES (Type of report and, inclusive dates) Master's Thesis; December 1972			
5. AUTHOR(S) (First name, middle initial, last name) Fred Herman Gehrman Jr.			
6. REPORT DATE December 1972		7a. TOTAL NO. OF PAGES 107	7b. NO. OF REFS 13
8a. CONTRACT OR GRANT NO.		8b. ORIGINATOR'S REPORT NUMBER(S)	
b. PROJECT NO.			
c.		9b. OTHER REPORT NO(S) (Any other numbers that may be assigned this report)	
d.			
10. DISTRIBUTION STATEMENT Approved for public release; distribution unlimited.			
11. SUPPLEMENTARY NOTES		12. SPONSORING MILITARY ACTIVITY Naval Postgraduate School Monterey, California 93940	
13. ABSTRACT A horizontal cylinder, located near the floor of a two dimensional wave channel was subjected to a train of non-linear gravity waves. The horizontal and vertical forces were measured and presented in dimensionless form. Experimental values of horizontal and vertical force coefficients are presented as functions of dimensionless wave height and dimensionless wave period. The dimensionless force coefficients predicted by a modified Morrison equation and a Froude-Krilov force are compared to experimental data. Fluid particle velocity and acceleration values were calculated from Stokes fifth-order gravity wave theory. Experimental dimensionless wave periods from 10 to 200 were investigated. The horizontal force coefficients were found to vary linearly with wave height for dimensionless period values from 60 to 120. The vertical force coefficients were found to be inertia dominated at low dimensionless wave heights and dominated by a lift force at higher wave heights. The theory predicted experimental values of force coefficients with good accuracy, especially at greater water depths.			

14. KEY WORDS	LINK A		LINK B		LINK C	
	ROLE	WT	ROLE	WT	ROLE	WT
gravity wave forces						
non-linear						
wave interaction with underwater cylindrical bodies						

Forces on a Horizontal Cylinder Due
to Non-Linear Waves

by

Fred Herman Gehrman, Jr.
Lieutenant, United States Navy
B. S., The Creighton University, 1966

Submitted in partial fulfillment of the
requirements for the degree of

MASTER OF SCIENCE IN MECHANICAL ENGINEERING

from the

NAVAL POSTGRADUATE SCHOOL
December 1972

Author

F. H. Gehrman Jr.

Approved by:

C. J. Garrison

Thesis Advisor

Robert W. Mum

Chairman, Department of Mechanical Engineering

Milton H. Clauser

Provost

ABSTRACT

A horizontal cylinder, located near the floor of a two dimensional wave channel was subjected to a train of non-linear gravity waves. The horizontal and vertical forces were measured and presented in dimensionless form. Experimental values of horizontal and vertical force coefficients are presented as functions of dimensionless wave height and dimensionless wave period. The dimensionless force coefficients predicted by a modified Morrison equation and a Froude-Krilov force are compared to experimental data. Fluid particle velocity and acceleration values were calculated from Stokes fifth-order gravity wave theory. Experimental dimensionless wave periods from 10 to 200 were investigated.

The horizontal force coefficients were found to vary linearly with wave height for dimensionless period values from 60 to 120. The vertical force coefficients were found to be inertia dominated at low dimensionless wave heights and dominated by a lift force at higher wave heights. The theory predicted experimental values of force coefficients with good accuracy, especially at greater water depths.

TABLE OF CONTENTS

I.	INTRODUCTION -----	9
II.	THEORETICAL ANALYSIS -----	13
	A. PROBLEM DEFINITION -----	13
	B. DIMENSIONAL ANALYSIS -----	13
	C. WAVE THEORY -----	16
	D. STOKES FIFTH ORDER SOLUTION -----	18
	E. FORCES ON THE CYLINDER -----	22
	F. DISCUSSION OF COMPUTER PROGRAM -----	26
III.	DESCRIPTION OF APPARATUS AND EXPERIMENTAL PROCEDURE -----	27
	A. WAVE CHANNEL -----	27
	B. TEST MODULE -----	31
	C. WAVE HEIGHT PROBE -----	36
	D. TEST PROCEDURE -----	37
IV.	PRESENTATION OF RESULTS AND CONCLUSIONS -----	41
APPENDIX A:	STOKES FIFTH ORDER WAVE THEORY COEFFICIENTS -----	53
APPENDIX B:	EXPERIMENTAL DATA -----	56
APPENDIX C:	WAVE HEIGHT-FORCE PLOTS -----	79
APPENDIX D:	COMPUTER PROGRAM -----	92
	LIST OF REFERENCES -----	104
	INITIAL DISTRIBUTION LIST -----	105
	FORM DD 1473 -----	106

LIST OF FIGURES

NUMBER	TITLE	PAGE
1.	Definition of Geometry	14
2.	Inertial Force Geometry	25
3.	Wave Channel	28
4.	Wave Channel Truss Arrangement	29
5.	Test Module	32
6.	Horizontal Force Cantilever	33
7.	Vertical Force Cantilever	34
8.	Force Cantilever	35
9.	Wave height Probe Circuit Schematic	38
10.	Cantilever Calibration Arrangement	40
11.	Wave height-Force Traces $h/a = 4.0$	42
12.	Wave height-Force Traces $h/a = 5.5$	43
13.	Wave height-Force Traces $h/a = 7.0$	44
14.	Wave height-Force Traces $h/a = 9.0$	45
15.	Horizontal Wave Force	49
16.	Horizontal Wave Force	50
17.	Horizontal Wave Force	51

LIST OF SYMBOLS

SYMBOL	DEFINITION	UNITS
a	cylinder radius	ft.
a_x	horizontal acceleration	ft./sec. ²
\bar{a}_x	dimensionless horizontal acceleration	
a_y	vertical acceleration	ft./sec. ²
\bar{a}_y	dimensionless vertical acceleration	
c	wave celerity	ft./sec.
\bar{c}	dimensionless wave celerity	
C_D	drag coefficient	
C_L	lift coefficient	
C_M	added mass coefficient	
d	depth to wave length ratio	
F_x	horizontal force component	lbf.
\bar{F}_x	dimensionless horizontal force component	
F_y	vertical force component	lbf.
\bar{F}_y	dimensionless vertical force component	
F_i	vertical inertial force	lbf.
\bar{F}_i	dimensionless vertical inertial force	
F_L	vertical lift force	lbf.
\bar{F}_L	dimensionless lift force	
g	gravitational constant	ft./sec. ²

SYMBOL	DEFINITION	UNITS
gT^2/h	dimensionless period parameter	
h	water depth	ft.
\bar{h}	dimensionless water depth	
H	peak to trough wave height	ft.
\bar{H}	-wave height to diameter ratio, dimensionless wave height	
Hd	wave height to depth ratio	
L	wave length	ft.
l	cylinder length	ft.
P	pressure	lb./ft. ²
\bar{P}	dimensionless pressure	
S	position measured from bottom	ft.
u	horizontal velocity	ft./sec.
\bar{u}	dimensionless horizontal velocity	
v	vertical velocity	ft./sec.
\bar{v}	dimensionless vertical velocity	
y	distance from mean water line	ft.
\bar{y}	dimensionless distance from mean water line	
ρ	fluid density	lbm./ft. ³
ϕ	velocity potential	ft. ² /sec.
$\bar{\phi}$	dimensionless velocity potential	

SYMBOL	DEFINITION	UNITS
λ	arbitrary constant in Stokes Wave Theory	
η	distance from mean water line to free surface	ft.
θ	phase angle	degrees

ACKNOWLEDGEMENTS

The author wishes to express his appreciation, first of all to his advisor, Professor C. J. Garrison, for his enlightenment, encouragement and patience throughout this study. In addition, special thanks is also given to Mr. Tom Christian, who designed the wave height probe without which this study could not have been completed. Finally and most deeply, to Claire, Chris and Karen, for their patience, understanding and long-suffering during this undertaking, the author expresses his love.

I. INTRODUCTION

Exploration for and use of ocean resources has received increasing attention in the scientific community in recent years. A considerable effort has resulted in the development of technology in areas such as off-shore oil exploration, recovery of petroleum and deployment of underwater habitats. Oil production often involved the use of very large submerged oil storage tanks and associated piping systems. In some locations, oil is transferred long distances in submerged piping systems, often leading through the surf zone to facilities ashore. Also, waste disposal systems usually involve deployment of large diameter outfall pipes which are laid through the surf zone. Proposals for large scale mining and food gathering activities indicate the trend toward design and construction of large submerged structures.

This activity has generated considerable interest in the interaction of gravity waves with submerged objects and particularly in the forces induced. Most previous investigations [1,2,3] in this area center on the use of a so-called Morrison Equation [3], which involves both a drag and inertial component of force. Unfortunately, the drag and added mass coefficients are found to be neither constant nor simply shape - or Reynolds number - dependent in the unsteady flow that occurs in the interaction of waves with fixed bodies. In addition, where the amplitude of wave motion is large compared to the body dimensions, flow separation occurs,

and the coefficients vary as the flow in a given direction develops. Finally, for small depth to characteristic dimension ratios, the proximity of the free surface may influence the value of the coefficients, even if no flow separation occurs.

In spite of these difficulties, the Morrison Equation will, with certain restrictions, provide a complete description of the horizontal forces acting on a large horizontal cylinder in contact with a plane boundary. If the cylinder is large in comparison to the amplitude of the fluid motion, separation does not occur, and the resulting wave-induced oscillatory flow may be considered an unseparated potential flow about the cylinder. This has been verified by Kuelegan and Carpenter [2] and by Sarpkaya and Garrison [4]. For such cases, the drag component of force is negligible, while the added mass coefficient is a constant.

Application of the Morrison Equation to determine the vertical components of force for a bottom-mounted cylinder yields a vertical force component of zero, an obviously invalid result. It is recognized that the vertical force should be composed of two components; one associated with the inertia effects and a second which accounts for the lift force caused by the increased velocity and hence decreased the pressure over the top of the cylinder.

The inertial component of vertical force can be approximated by what is commonly known as a Froude-Krilov force. This is the force caused by the pressure distribution around

the surface of the cylinder existing in the wave if the cylinder was not present. This is an approximation which does not account for the presence of the body and is therefore considered to be an underestimate of the force.

The lift component of vertical force can be approximated by use of the unseparated, potential flow model used in the analysis of the horizontal forces, i.e., that of a uniform flow past a cylinder in contact with a rigid boundary. The lift coefficient for this case has been determined by Dalton and Helfenstein [5].

A study carried out by Johnson [6] for horizontal forces acting on a bottom-mounted, horizontal cylinder in long waves, assumed that at long wave lengths, the horizontal forces depended on wave height and water depth only. This assumption is, however, of doubtful validity in the range of Johnson's test.

Shiller [7] measured wave forces on a submerged horizontal cylinder due to small amplitude waves. Over the range of wave heights considered, the magnitude of the horizontal force was found to vary linearly with wave height. The magnitude of the vertical force was found to increase in proportion to the wave height squared.

Perkinson [8] extended Shiller's investigation to include larger wave heights and periods. His study indicates that horizontal forces increased linearly with wave heights and becomes independent of wave period for large wave periods. The vertical forces were found to contain two regimes: the

lower wave lengths where lift force predominates; and the higher wave lengths where inertial force is dominant.

In order to evaluate any forces using the above analyses, it is necessary to first evaluate fluid velocities, accelerations and pressure by use of some wave theory. Fairly simple expressions may be derived for the forces by use of Airy wave theory. However, for finite amplitude waves in finite depth water, a non-linear wave theory is considered to be necessary. Stokes fifth-order wave theory has been chosen for this study.

Stokes originally developed a second-order theory [9] for the case of a non-linear wave in water of finite depth. This method has been extended by Borgman and Chappellear [10] to third order. Skjelbreia and Hendrickson [11] have extended the solution to third and fifth order. Bretschneider [12] has presented a method for extension to any order.

The purpose of this study is to compare the analytical results of Stoke's fifth-order wave theory with experimental values at longer wave periods. The transition section of the wave channel used by Perkinson was extended approximately forty feet to provide a slope of 1:20. This provided the possibility of extending Perkinson's work to include longer wave periods. This study, then, is an extension of the work of Shiller [7] and Perkinson [8].

II. THEORETICAL ANALYSIS

A. PROBLEM DEFINITION

The problem under consideration is illustrated in Figure 1. A train of gravity waves is considered to progress in the positive x-direction in water of depth h , with rate of propagation C . The fluid particle velocity is expressed in terms of the horizontal and vertical components, u and v . It is of primary interest to determine the horizontal and vertical components of wave force acting on the horizontal cylinder which is in contact with the rigid bottom.

B. DIMENSIONAL ANALYSIS

An exact analytical solution to this problem is quite formidable and, therefore, an approximate solution is considered in this work. However, first it is instructive to carry out a dimensional analysis of all pertinent parameters involved.

In general, the maximum of the wave force per unit length acting on a submerged cylinder due to wave motion is known a priori to depend on the following parameters:

$$F_{\max}/l = f_1(h, H, T, L, a, \rho, g, u) \quad (1)$$

where

F = wave force
 h = water depth
 H = wave height
 T = wave period
 L = wave length

$T = \text{Wave Period}$

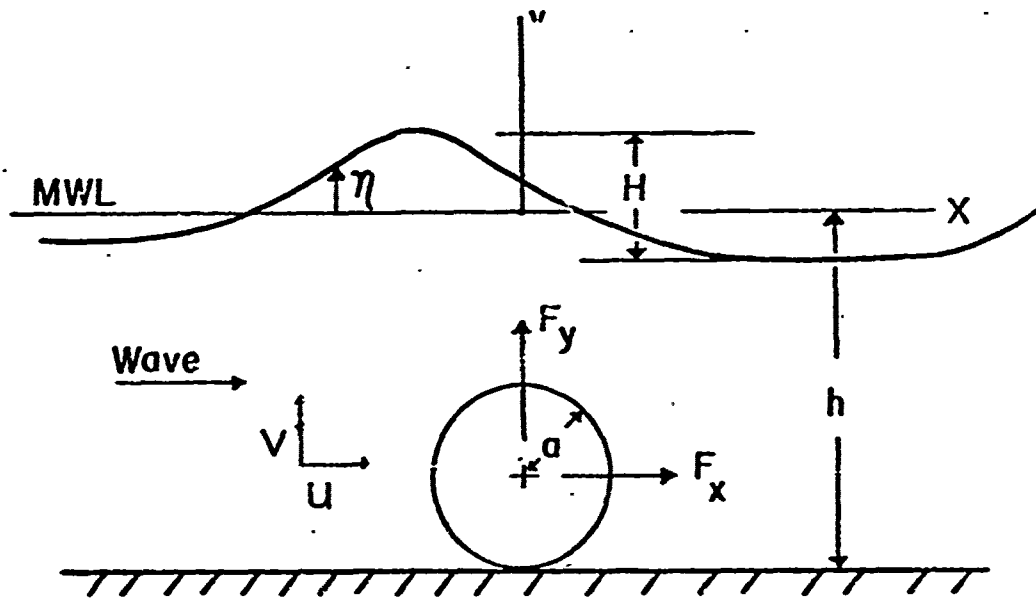


Fig. I. DEFINITION OF GEOMETRY

a = cylinder radius
 ρ = fluid density
 g = gravitational constant
 μ = fluid viscosity
 l = cylinder length

However, a relationship exists between the parameters associated with the incident wave (i.e. h, H, T and L). Consequently, only three of these parameters (e.g. h, H and T) are needed to completely specify the incident wave. A dimensional analysis of the parameters in equation (1) yields the following groups:

$$F_{\max}/\rho g a^2 l = f_2(gT^2/h, h/a, H/2a, \mu/l \sqrt{gha^2}) \quad (2)$$

The last term on the right side of equation (2) represents the ratio of Froude number to Reynolds number, indicating the ratio of viscous to inertial forces. It is believed that, if this number is small, it may be neglected from further consideration, and equation (2) may be rewritten

$$\tilde{F}_{\max} = f_3(gT^2/h, \tilde{H}, \tilde{h}) \quad (3)$$

where

$$\begin{aligned} \tilde{F}_{\max} &= F_{\max}/\rho g a^2 l \\ \tilde{H} &= H/2a \\ \tilde{h} &= h/a \end{aligned}$$

The approximate analytical approach of this study seeks:

1. To develop expressions for the fluid particle motion in the gravity wave as functions of the incident wave parameters, and

- 2). To develop expressions for the forces on the submerged cylinder as functions of the fluid particle motion.

The assumptions upon which this analysis is based are:

- 1). Water will be considered inviscid and incompressible,
- 2). The cylinder radius will be considered small in comparison to the dimensions (h and L) of the incident wave.

C. WAVE THEORY

The motion of fluid particles in a gravity wave based on assumptions 1) and 2) above is specified by the following boundary value problem.

1). Governing Equation

Assumption 1) implies that Laplace's Equation governs the fluid motion. That is:

$$\nabla^2 \phi = 0 \quad (4a)$$

where ϕ is the velocity potential and the two velocity components are given in terms of ϕ as

$$u = \frac{\partial \phi}{\partial x}, \quad v = \frac{\partial \phi}{\partial y} \quad (4b)$$

2). Boundary Conditions

The boundary condition on the bottom is that of a non-porous wall, i.e.,

$$\frac{\partial \phi}{\partial y} = 0 \quad \text{at } y = -h \quad (5)$$

Two boundary conditions are encountered at the water surface, one dynamic and one kinematic.

The dynamic boundary condition is obtained from Bernoulli's Equation by setting the pressure equal to zero. That is:

$$u^2 + v^2 + 2\frac{\partial\phi}{\partial t} = -2g(\Pi - y) \quad \text{at } y = \eta \quad (6)$$

where Π is the total energy head, a constant.

Assuming the wave travels without change in form, it is then possible to choose a reference system moving in the positive x direction with wave celerity C . This makes the fluid motion steady with respect to the moving reference system. The Bernoulli Equation in such a reference system is:

$$(u - C)^2 + v^2 = 2g(\Pi - y) \quad \text{at } y = \eta \quad (7)$$

The kinetic boundary condition imposes the condition that no fluid be transported across the free surface. Or, in other words, the free surface must be a streamline. This may be expressed mathematically in the form:

$$\frac{\partial y}{\partial x} = \frac{v}{u - C} \quad \text{at } y = \eta \quad (8)$$

Equations (4a), (5), (7), and (8) completely specify the boundary value problem.

There are, historically, several approximate solutions to this problem. The solution to be considered further in this analysis is that commonly known as Stokes fifth-order wave theory.

D. STOKES FIFTH ORDER SOLUTION

Stokes proposed [9] a power series type of solution to the above problem and proved the validity of the second order solution based on this power series. Skjelbreia and Hendrickson [9] have extended this theory to fifth-order, yielding a solution to the boundary value problem of the form:

$$\begin{aligned}\phi = \frac{C}{\beta} \{ & A_1 \cosh(\beta S) \sin \theta + A_2 \cosh(2\beta S) \sin(2\theta) \\ & + A_3 \cosh(3\beta S) \sin(3\theta) + A_4 \cosh(4\beta S) \sin(4\theta) \\ & + A_5 \cosh(5\beta S) \sin(5\theta) \} \quad (9a)\end{aligned}$$

where A_1 through A_5 are as given in Appendix A.

This equation may be written in dimensionless form as:

$$\tilde{\phi} = \tilde{C} \{ A_1 \cosh(\beta S) \sin \theta + A_2 \cosh(2\beta S) \sin(2\theta) + \dots \} \quad (9b)$$

where: $\tilde{\phi} = \beta \phi / \sqrt{gh}$

$$\tilde{C} = C / \sqrt{gh}$$

Differentiation of equation (9a) with respect to time yields

$$\begin{aligned}\frac{\partial \phi}{\partial t} = C^2 \{ & A_1 \cosh(\beta S) \cos \theta + 2A_2 \cosh(2\beta S) \cos(2\theta) \\ & + 3A_3 \cosh(3\beta S) \cos(3\theta) + 4A_4 \cosh(4\beta S) \cos(4\theta) \\ & + 5A_5 \cosh(5\beta S) \cos(5\theta) \} \quad (10a)\end{aligned}$$

or, in dimensionless form

$$\frac{\partial \phi}{\partial t} = \bar{C}^2 \{ A_1 \cosh(\beta S) \cos(\theta) + 2A_2 \cosh(2\beta S) \cos(2\theta) + \dots \} \quad (10b)$$

where $\frac{\partial \phi}{\partial t} = \frac{\partial \phi}{\partial t} / \sqrt{gh}$

The series form of the wave profile is assumed to be:

$$y = \frac{1}{\beta} \{ \lambda \cos(\theta) + B_2 \cos(2\theta) + B_3 \cos(3\theta) + B_4 \cos(4\theta) + B_5 \cos(5\theta) \} \quad (11a)$$

where B_2 through B_5 are as given in Appendix A and λ is an arbitrary constant.

Equation (11a) can be expressed in dimensionless form as

$$\bar{y} = \frac{1}{\bar{d}} \{ \lambda \cos(\theta) + B_2 \cos(2\theta) + \dots \} \quad (11b)$$

where $\bar{y} = y/d$
 $\bar{d} = 2\pi h/L$

The series form for Π is assumed to be:

$$\Pi = \frac{1}{\beta} \{ \lambda^2 C_3 + \lambda^4 C_4 \} \quad (12)$$

where C_3 and C_4 are as given in Appendix A.

The wave celerity expressed in series form is

$$C = \frac{y}{\beta} C_0^2 \{ 1 + \lambda^2 C_1 + \lambda^4 C_2 \} \quad (13a)$$

or, in dimensionless form

$$\bar{C} = \frac{1}{\bar{d}} C_0^2 \{1 + \lambda^2 C_1 + \lambda^4 C_2\} \quad (13b)$$

where C_1 and C_2 are as given in Appendix A.

Using equations (4b) and (9b) we find the horizontal particle velocity to be:

$$\begin{aligned} \bar{u} = \left(\frac{\partial \phi}{\partial x}\right) = \bar{C} \{ & A_1 \cosh(\beta S) \cos(\theta) + 2A_2 \cosh(2\beta S) \cos(2\theta) \\ & + 3A_3 \cosh(3\beta S) \cos(3\theta) + 4A_4 \cosh(4\beta S) \cos(4\theta) \\ & + 5A_5 \cosh(5\beta S) \cos(5\theta) \} \end{aligned} \quad (14)$$

where $\bar{u} = u/\sqrt{gh}$

Also, from equations (4b) and (9a):

$$\begin{aligned} \bar{v} = \left(\frac{\partial \phi}{\partial y}\right) = \bar{C} \{ & A_1 \sinh(\beta S) \cos(\theta) + 2A_2 \sinh(2\beta S) \cos(2\theta) \\ & + 3A_3 \sinh(3\beta S) \cos(3\theta) + 4A_4 \sinh(4\beta S) \cos(4\theta) \\ & + 5A_5 \sinh(5\beta S) \cos(5\theta) \} \end{aligned} \quad (15)$$

where $\bar{v} = v/\sqrt{gh}$

Differentiation of equations (14) and (15) with respect to time yields the particle accelerations

$$\begin{aligned} \bar{a}_x = \left(\frac{\partial \bar{u}}{\partial t}\right) = \bar{d}\bar{C}^2 \{ & A_1 \sinh(\beta S) \sin(\theta) + 2A_2 \sinh(2\beta S) \sin(2\theta) \\ & + 3A_3 \sinh(3\beta S) \sin(3\theta) + 4A_4 \sinh(4\beta S) \sin(4\theta) \\ & + 5A_5 \sinh(5\beta S) \sin(5\theta) \} \end{aligned} \quad (16)$$

where $\bar{a}_x = a_x/g$

and

$$\begin{aligned} \tilde{a}_y = \tilde{d}\tilde{C}^2 \{ & A_1 \sinh(\beta S) \cos(\theta) + 2A_2 \sinh(2\beta S) \cos(2\theta) \\ & + \dots \} \end{aligned} \quad (17)$$

where $\tilde{a}_y = a_y/g$

The potential function and its derivatives, as well as the wave profile are now known in terms of the unknown quantities λ and \tilde{d} . Specifying equations for these parameters are found by developing equations for the peak-to-trough wave height and the wave period. That is, the dimensionless wave height is defined as:

$$\tilde{Hd} = \tilde{y}_{\theta=0} - \tilde{y}_{\theta=\pi} \quad (18)$$

where $\tilde{Hd} = H/h$

Substitution of equation (13b) into equation (18) yields:

$$\tilde{Hd} = \frac{2}{\tilde{d}} \{ \lambda + \lambda^3 B_{33} + \lambda^5 (B_{35} + B_{55}) \} \quad (19)$$

where B_{33} , B_{35} , and B_{55} are as given in Appendix A.

Now, the wave period and the wave celerity are related by the relationship:

$$C = L/T \quad (20)$$

So, equation (15a) becomes

$$(L/T)^2 = \frac{C_0^2}{g} \{ 1 + \lambda^2 C_1 + \lambda^4 C_2 \} \quad (21)$$

or,

$$h/gT^2 = \frac{\tilde{d}}{4E^2} C_0^2 \{1 + \lambda^2 C_1 + \lambda^4 C_2\} \quad (22)$$

The parameter gT^2/h is referred to herein as the period parameter.

Equations (19) and (22), if solved simultaneously, yield values for λ and \tilde{d} in terms of $\tilde{H}\tilde{d}$ and gT^2/h , quantities which are incident wave parameters. Thus the potential function, particle velocities and accelerations are shown to be functions of the dimensionless parameters obtained by dimensional analysis and given by equation (3). (Note that $\tilde{H}\tilde{d} = 2H/h$)

The next step in the analysis is to express the forces acting on the cylinder as functions of the potential function, particle velocities and accelerations.

E. FORCES ON THE CYLINDER

The forces acting on the cylinder are described in terms of their horizontal and vertical components.

1). Horizontal Component

The horizontal component of force acting on the cylinder is expressed in the form of the so-called Morrison Equation as.

$$F_x = \frac{C_D}{2}(\rho 2a\dot{u}^2) + (1.0 + C_M)\pi a^2 \dot{a}_x \quad (23)$$

where C_D = drag coefficient
 C_M = added mass coefficient

For cases where fluid particle motion is small in comparison with the cylinder diameter, flow separation does not occur and the contribution of drag to the total force may be disregarded. In this case, equation (23) may be rewritten

$$\tilde{F}_x = (1.0 + C_M)\tilde{a}_x \quad (24)$$

where $\tilde{F}_x = F_x/\rho g a^2 l$.

The added mass coefficient for a circular cylinder in contact with a rigid wall was given in closed form by Garrison [13] as $C_M = 2.29$.

2). Vertical Force Component

As mentioned previously, application of the Morrison Equation to the vertical component of force yields a result which is clearly erroneous. The vertical force may be considered to arise from two sources: an inertial force and a lift force.

a). Lift Force

The lift force may be expressed as:

$$F_L = 1/2(2a\ell\rho)C_L u|u| \quad (25)$$

where C_L = lift coefficient.

or, in dimensionless form:

$$\tilde{F}_L = \tilde{h}C_L u|u| \quad (26)$$

where $\tilde{F}_L = F_L/\rho g a^2 l$.

Dalton and Helfstein indicate [7] that $C_L = 4.49$ for unseparated flow past a circular cylinder in contact with a rigid wall.

b). Inertial Force

The pressure distribution around the surface of the cylinder existing if the cylinder is not present results in a net vertical force (known as a Froude-Krilov force).

Consider the resultant differential force dF_1 acting on a differential area of the cylinder dA as shown in Figure 2. The above equation, written in dimensionless form, is:

$$\tilde{F}_L = \int_0^{2\pi} \tilde{P}(a, \gamma) \sin \gamma d\gamma \quad (30)$$

The pressure is obtained from the Bernoulli Equation:

$$P = -\rho \left\{ \frac{1}{2} (u^2 + v^2) + \frac{\partial \phi}{\partial t} \right\} \quad (31)$$

or, in dimensionless form:

$$\tilde{P} = -\tilde{h} \left[\frac{1}{2} (\tilde{u}^2 + \tilde{v}^2) + \left(\frac{\partial \tilde{\phi}}{\partial \tilde{t}} \right) \right] \quad (32)$$

where $\tilde{P} = P/\rho g a$

Therefore

$$\tilde{F}_1 = -\tilde{h} \int_0^{2\pi} \left[\frac{1}{2} (\tilde{u}^2 + \tilde{v}^2) + \left(\frac{\partial \tilde{\phi}}{\partial \tilde{t}} \right) \right] \sin \gamma d\gamma \quad (33)$$

And the total vertical force may be written:

$$\tilde{F}_y = \tilde{h} \{ C_L \tilde{u} |\tilde{u}| - \int_0^{2\pi} \left[\frac{1}{2} (\tilde{u}^2 + \tilde{v}^2) + \left(\frac{\partial \tilde{\phi}}{\partial \tilde{t}} \right) \right] \sin \gamma d\gamma \} \quad (34)$$

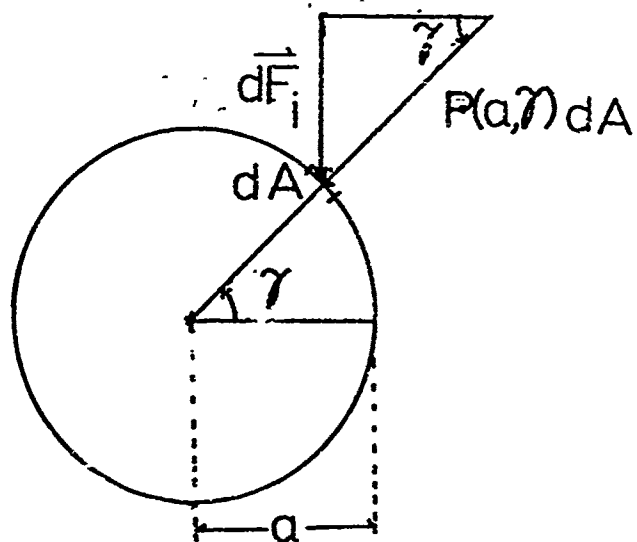


Fig. 2

INERTIAL FORCE GEOMETRY

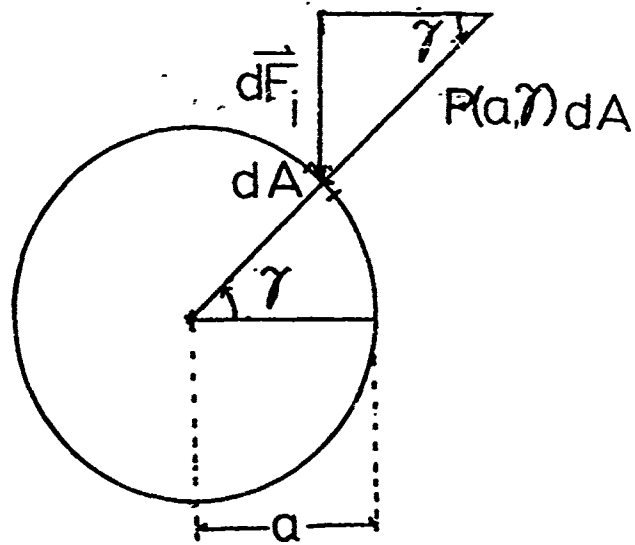


Fig. 2

INERTIAL FORCE GEOMETRY

F. DISCUSSION OF COMPUTER PROGRAM

The equations developed above were programmed for a digital computer as given in Appendix D. The basic inputs to the program are \tilde{H} , \tilde{h} and gT^2/h . The program yields particle velocity, acceleration and computes the horizontal and vertical forces on the cylinder at various wave angles.

The STAKES5 subroutine calculates the coefficients for the Stokes fifth order equations. Simultaneous solution to equations (19) and (22) are obtained by assuming an initial value of λ and \tilde{d} based on linear wave theory and iterating to the actual value using the Newton-Raphson technique.

The main program generates tables of values and in-line graphs of the wave profile, particle velocity vs. depth, vertical and horizontal force vs. phase angle.

III. DESCRIPTION OF APPARATUS AND EXPERIMENTAL PROCEDURE

A. WAVE CHANNEL

Wave forces on the cylinder were measured experimentally in a wave channel. The basic wave channel, as shown in Figure 3, was fifteen inches wide and consisted of two sections: a transition section and a shallow water section. The overall channel length was 87 feet.

Three-quarter inch exterior plywood sheets were used for the channel sides. Vertical rigidity was provided by bracing the plywood sheets with 2x4's at various intervals. The vertical members were placed four feet on centers in the shallow water section and from four feet to eighteen inches in the transition section. Additional rigidity was provided in the transition section by truss arrangements, as shown in Figure 4. Two 2x4's were attached to the top of the vertical studs and extended the length of the channel.

A double floor constructed of two plywood sheets with two half-inch separators was used. The sides of the channel were bolted together, through the spacing of the double bottom, with three-eighths inch threaded rod.

All wooden sections exposed to water were water-proofed and painted with three coats of Morewear Vitri-Glaz 1320A. Dow Corning Sealant 780 was applied to all seams and joints.

A paddle type wave generator was used to generate waves in the channel. An aluminum plate was hinged at the tank

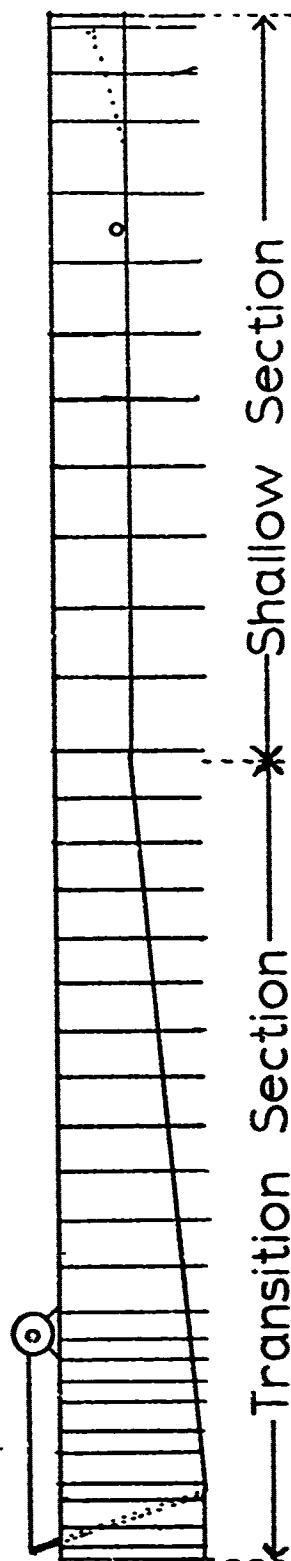


Fig.3 WAVE CHANNEL

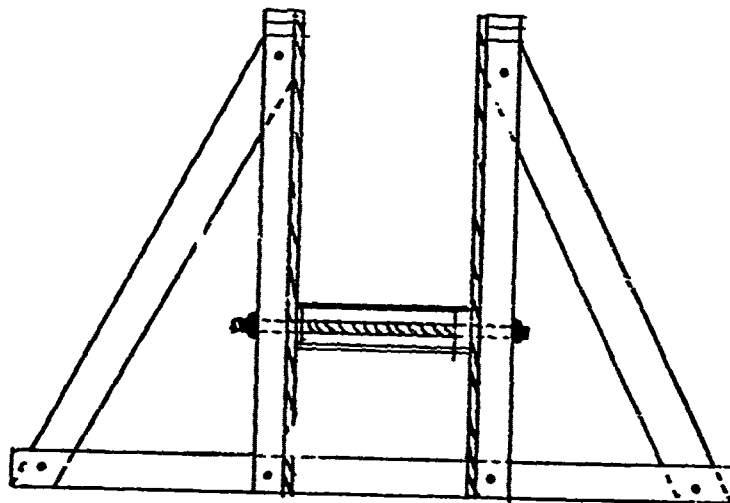


Fig.4

TRANSITION SECTION TRUSS ARR'G'T.

floor and attached by a pin connection at the top to a driving rod. Wave motion behind the paddle was damped by use of baffle plates. A two horse power variable speed drive, with an output speed range of twenty to one hundred eighty revolutions per minute, was mounted on top of the wave channel and fitted with a six and three quarter inch radius face plate. Ways were attached to the plate to adjust the driving rod eccentricity between zero and eight inches.

The transition section contained a ramp with a slope of 1:20 which shoaled the generated wave with a change in depth from four to two feet. The overall length of the transition section was 42 feet.

The shallow water section had a depth of two feet and an overall length of 42 feet. The test module was located twenty four feet from the transition, allowing the waves to reach a fully developed state following the transition before reaching the test section.

A variable slope dissipater beach was located at the end of the test section in order to dissipate the wave motion. The beach was constructed of metal shavings held between two pieces of perforated stainless steel sheet metal, which were separated by two inch wooden spacers. A solid sheet of one-eighth inch aluminum was attached to the bottom of the beach by three and five eighths inch separators. One by one inch aluminum angles were attached to the exposed surface of the beach, parallel to the wave fronts. Maximum slope of the beach was 1:7.

B. TEST MODULE

The test module consisted of the circular cylinder with its own floor and walls, constructed as an integral system to provide easy removal of the model from the tank. The wave channel sides and floor were recessed to provide a smooth transition from channel to test module. The channel walls were made of plexiglass in the test module region to allow maximum visibility of the model. The test module is shown in Figure 5.

A four inch diameter plexiglass cylinder was supported between the walls of the test module by use of cantilever beams and adjusted to approximately one-sixteenth inch above the floor. A thin flexible plastic barrier was installed in this gap to prevent any water motion under the cylinder due to wave motion. The barrier was held in place by 'O' ring material pressed into 0.007 inch slots in the cylinder and test module floor.

The cantilever beams were used to support the cylinder, as shown in Figures 6 and 7. Bulkheads were fixed in the cylinder at approximately two inches from each end, and the fixed ends of the cantilever beams bolted on these bulkheads. The free ends of the two beams protruded slightly beyond the end of the cylinder and into the plexiglass test module walls where they were supported by small self-aligning ball bearings pressed into the plexiglass. Both beams were fitted with strain gauges and waterproofed using ELH Barrier 'C', as shown in Figure 8.



Fig. 5 TEST MODULE

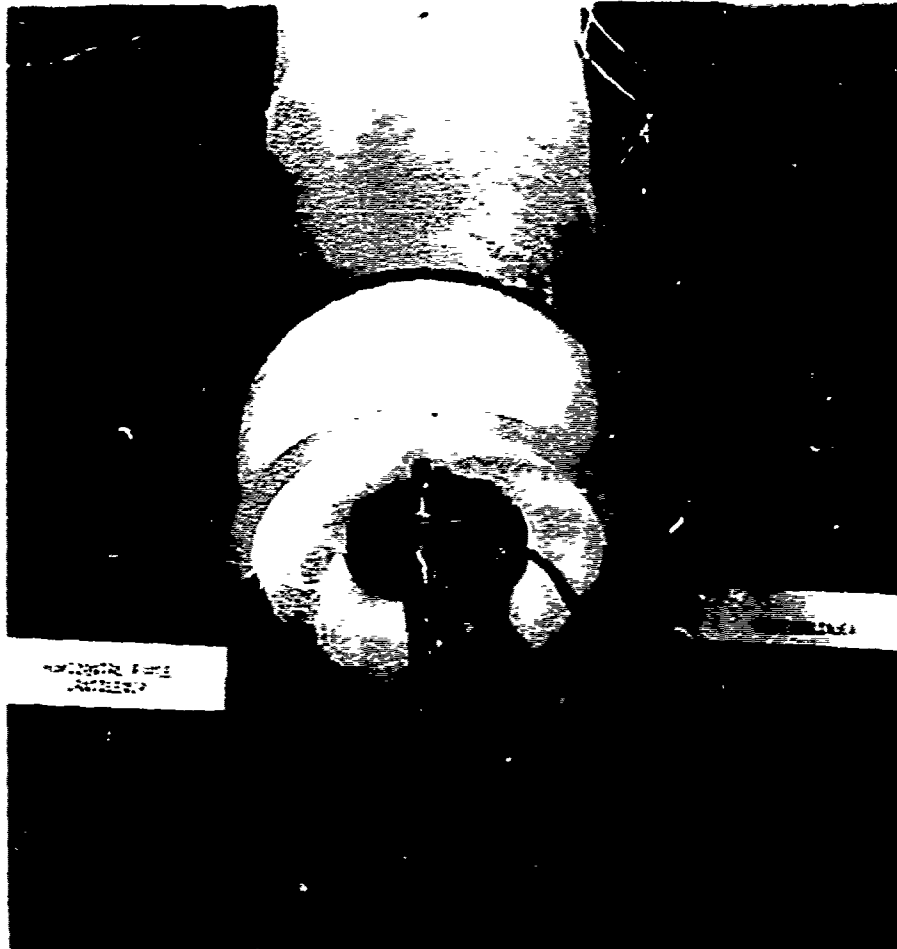


Fig. 6 HORIZONTAL FORCE CANTILEVER

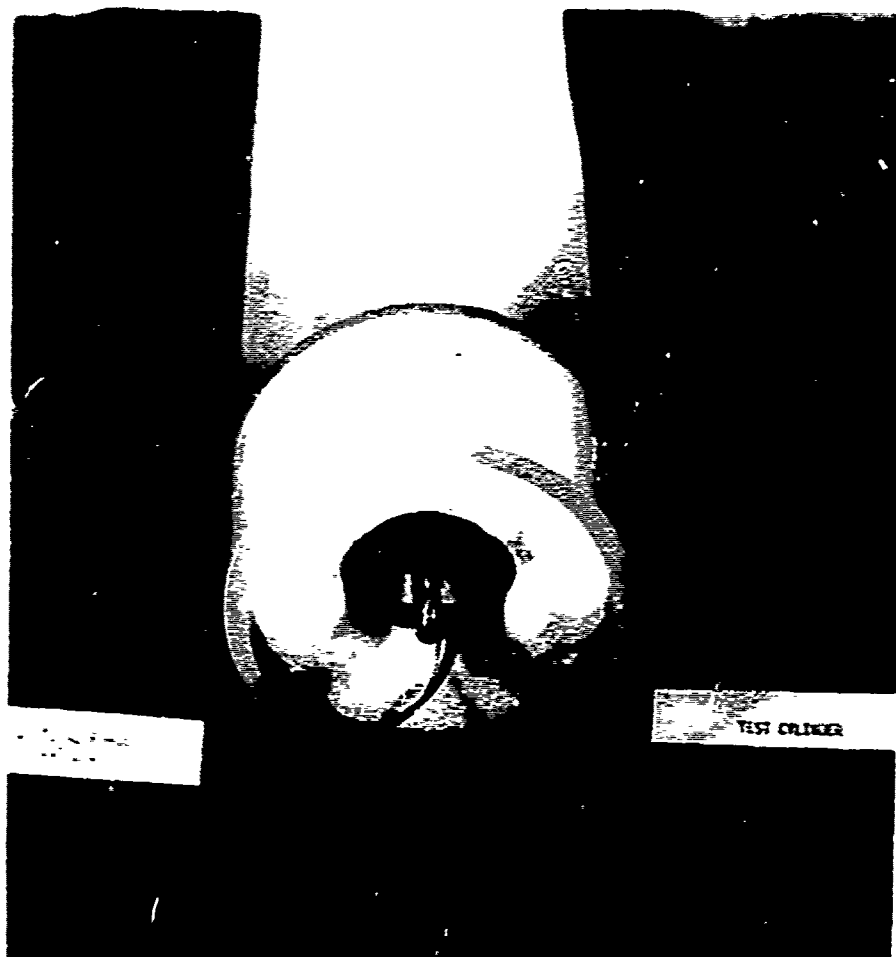


Fig. 7 VERTICAL FORCE CANTILEVER

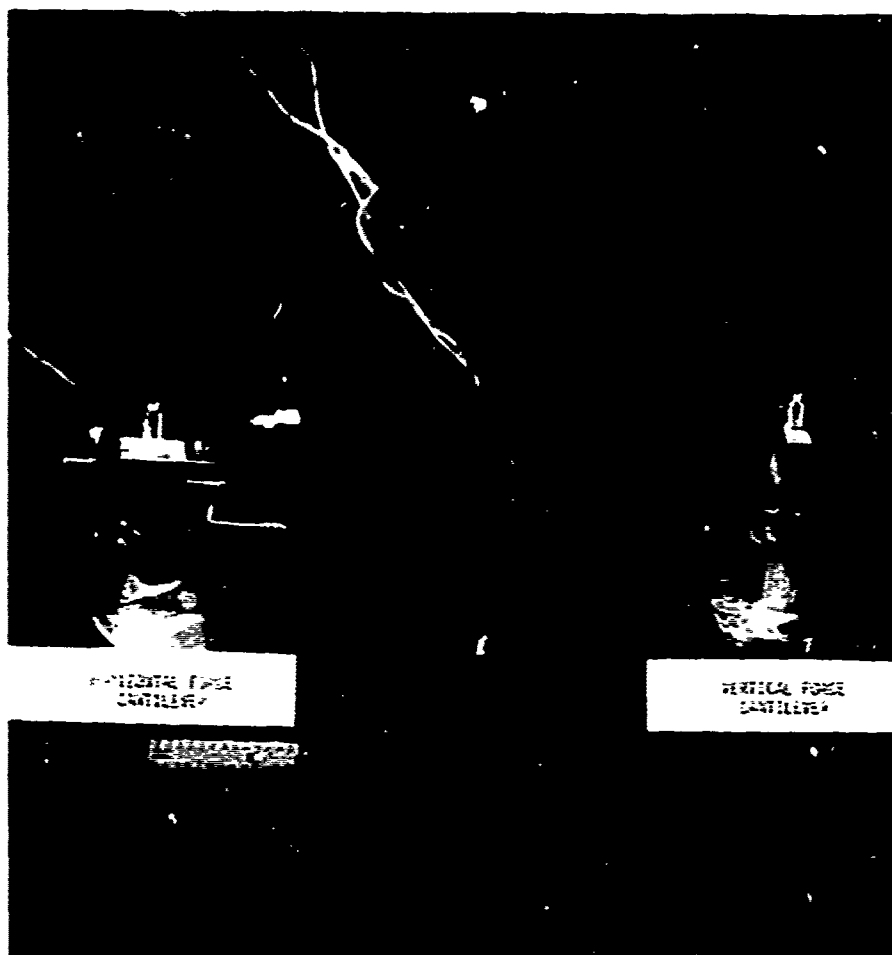


Fig. 8 FORCE CANTILEVER

One beam, positioned with its largest cross sectional dimension vertical, was used to measure horizontal force and the other, with its largest cross section positioned horizontally, was used to measure vertical force. Calibration tests indicated that cross coupling was negligible.

Dimensions of the beams were chosen to provide sufficient flexibility to allow measurement of forces using strain gauges and sufficient stiffness to provide a natural frequency that was large in comparison with the excitation frequency. In addition, the minimum width of the beams was constrained by the width necessary to mount the strain gauges. A reasonable trade-off was arrived at by making use of the maximum sensitivity of the amplifier/recorder and determining a maximum allowable value for the cantilever beam length.

To prevent rotation of the cylinder, an offset arm was used to connect the horizontal force cantilever to the test module. A Farber Bearing, AMS 1K7, was used as a wheel at the test module end of the arm to reduce friction.

C. WAVE HEIGHT PROBE

A capacitance type probe was chosen to measure wave heights in this study. The probe essentially consists of a single insulated wire which acted as one plate of a capacitor, the water acting as the second plate. The capacitance varied as the water level rose and fell. A three-eighths inch diameter acrylic rod was attached to the bottom of the foil-like support member and the sensing wire was attached

at the bottom of the acrylic rod and insulated there. The tip of the acrylic rod was removable to provide easy changing of the sensing wire. The wire was connected at the top to a cable connector mounted on a nylon block. Number 30 A.W.G. wire with poly thermaleze insulation was used.

The schematic of the electronic circuit utilized with this probe is shown in Figure 9. In this circuit, the square wave output of a multi-vibrator is used to drive a capacitance bridge, one leg of which is varied by the wave height probe. The resulting AC error signal is converted to a D.C. output signal by the full wave rectifier. The output signal was found to be insensitive to small multivibrator frequency changes and linear through the range of the wave height probe. A model LD 5211-13 Brush D.C. amplifier was used with the probe circuit.

D. TEST PROCEDURE

Calibration of the probe was conducted with the tank filled to the desired level and the test module and wave height probe in position. With the probe immersed to a depth of nine inches, the amplifier gain was set at desired sensitivity and the recorder pen bias adjusted to position the recorder to mid-scale. The probe immersion was varied over a seven inch range in half inch increments, using a traverse mechanism. This initial calibration was checked at several points before and after each set of runs.

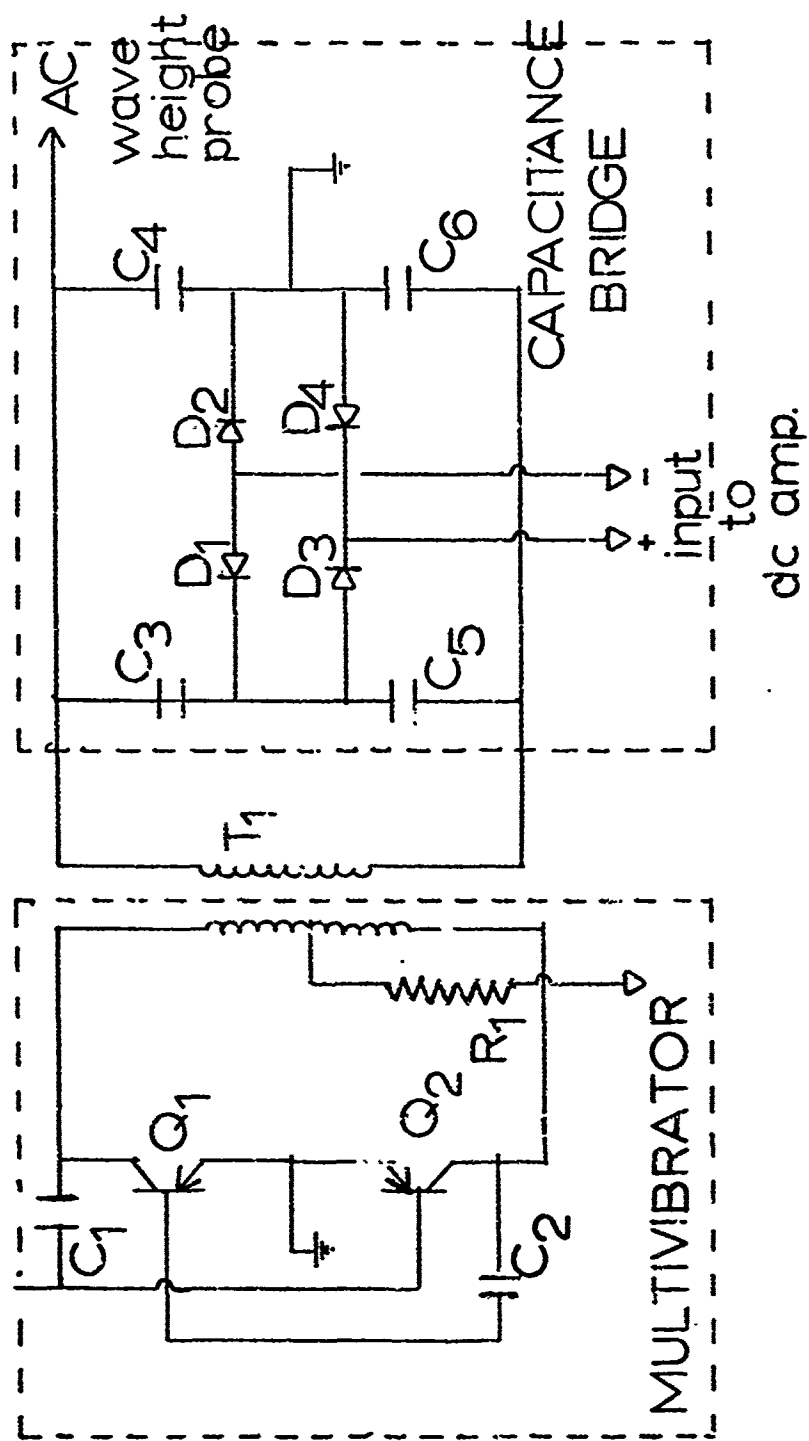


Fig. 9 WAVE HEIGHT PROBE CIRCUIT

The force cantilevers were rated by loading the cylinder with a series of weights, using a pulley arrangement shown in Figure 10. The load was transmitted to the cylinder through a series of tapped holes located around the circumference at positions horizontally fore and aft, and vertical. The Brush recorder output was calibrated by loading the cylinder in half-pound increments. This calibration was also checked prior to and after each series of runs.

After calibration was completed, the wave generator speed was set for the desired wave length and a data run commenced. During each run, wave generator eccentricity was varied from one inch to eight inches, or to a point where the waves broke in the channel.

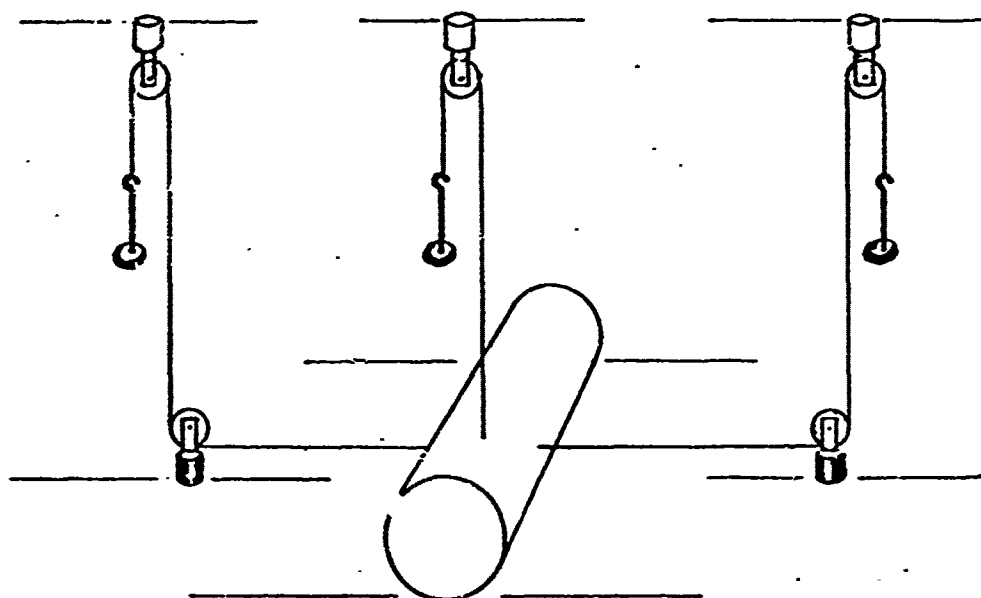


FIGURE 10. CANTILEVER CALIBRATION ARRANGEMENT

IV. PRESENTATION OF RESULTS AND CONCLUSIONS

As discussed in the theoretical analysis, dimensionless wave force coefficients can be represented as functions of the dimensionless water depth (h/a), the dimensionless wave height ($H/2a$), and dimensionless period (gT^2/h) parameters. A test program was developed which, for a given run, held water depth and period constant while varying wave height, in order to determine the effect of the dimensionless parameters on the horizontal and vertical force coefficients. Four series of experimental runs were conducted at relative water depths of 9.0, 7.0, 5.5, 4.0.

The dimensionless wave period parameter was varied for each series over a range of 100 to the maximum value attainable with the experimental apparatus. The upper limit in wave height was usually provided by breaking.

A series of representative traces are shown in Figures 11, 12, 13 and 14 due to the difficulty in presenting all the traces. These traces represent experimental data for three dimensionless periods from each of the four dimensionless water depths. The uppermost trace in each run represents wave height, the middle trace represents vertical force and the bottom trace represents horizontal force. The experimental values of the force coefficients for each experimental case are given in Appendix B.

Using the dimensionless period, water depth and waveheight as inputs, the computer program was used to generate

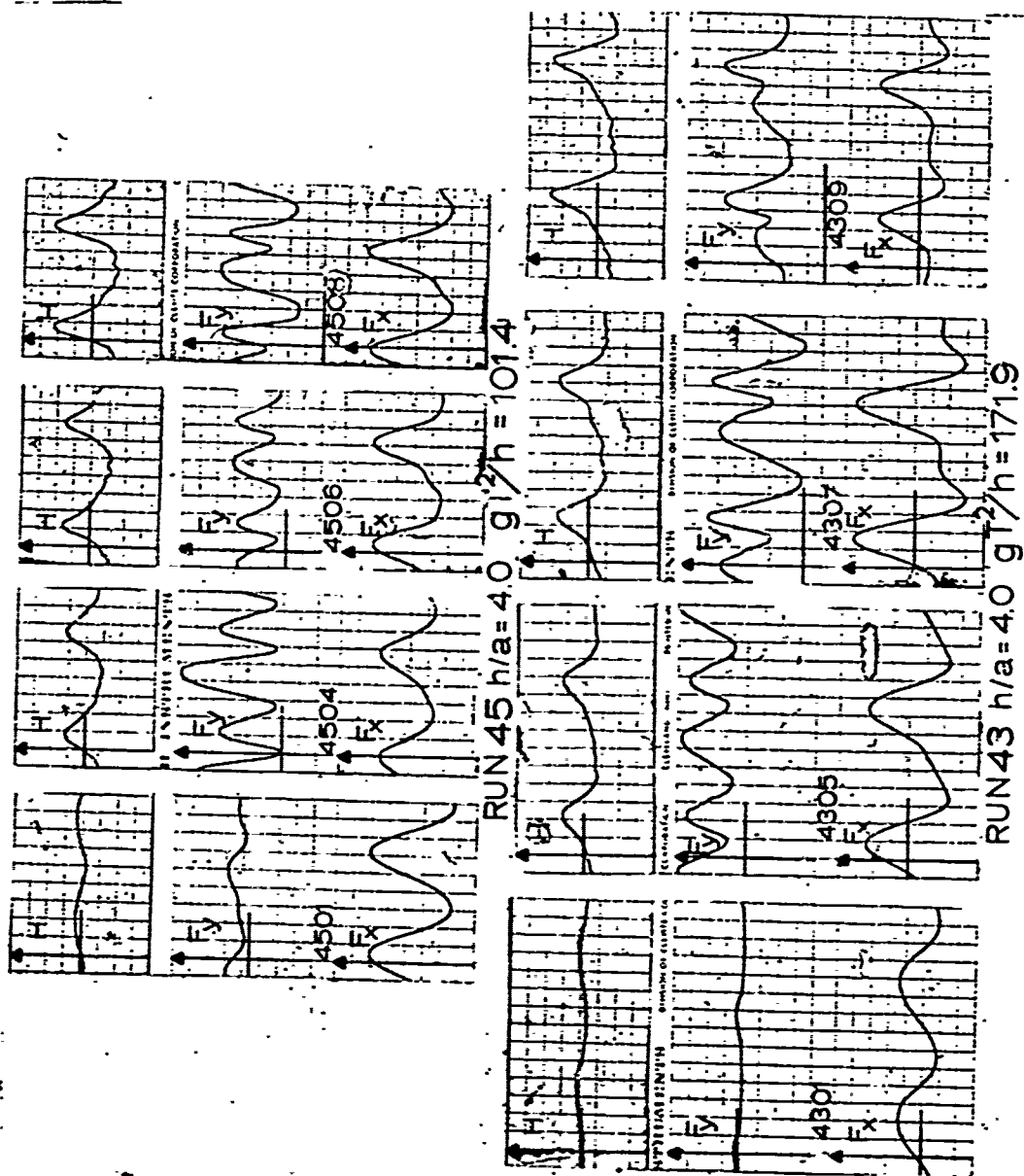


FIG. 11 Wave Height-Force Traces $h/a = 4.0$

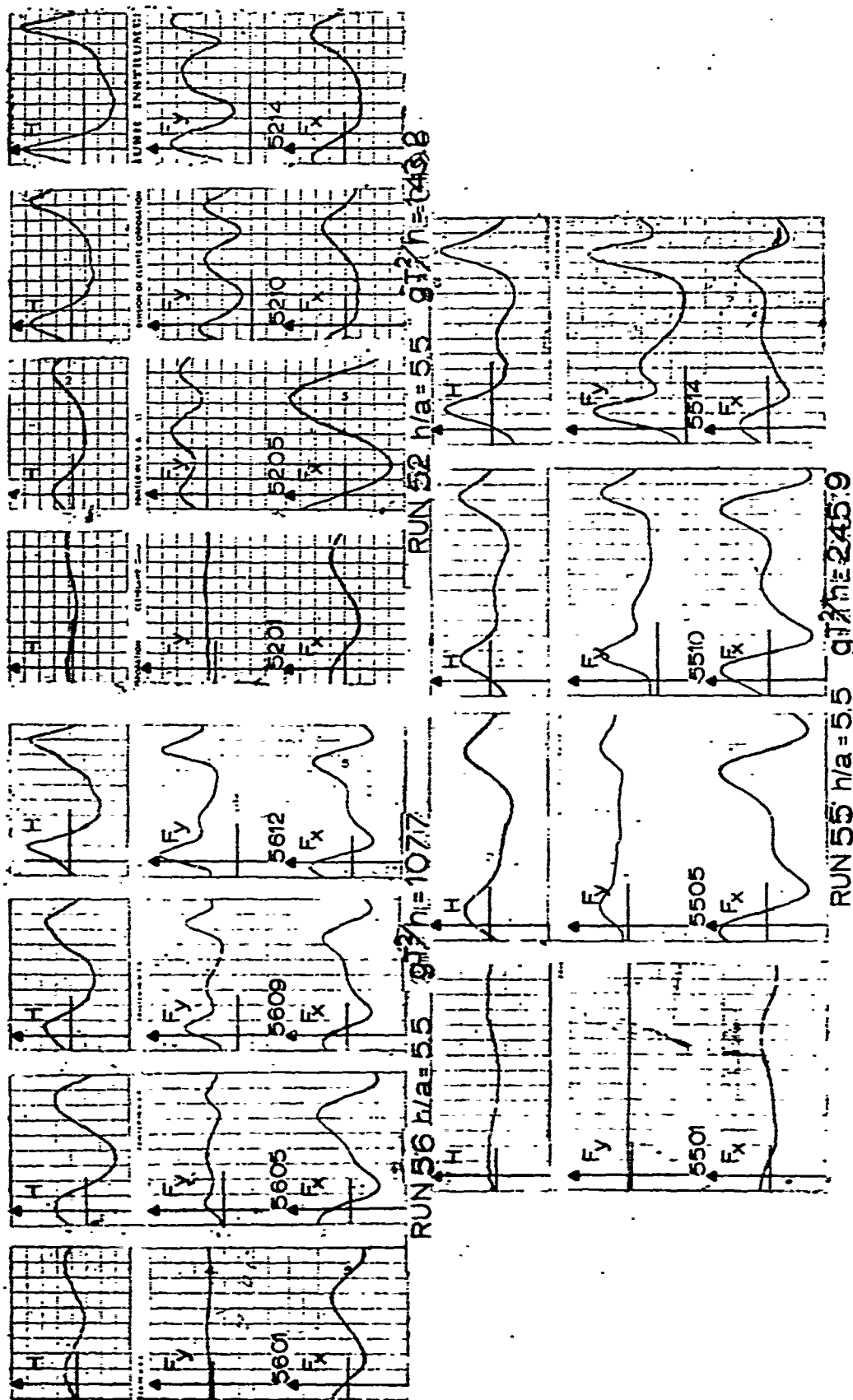


FIG. 12 Wave Height-Force Traces $h/a = 5.5$

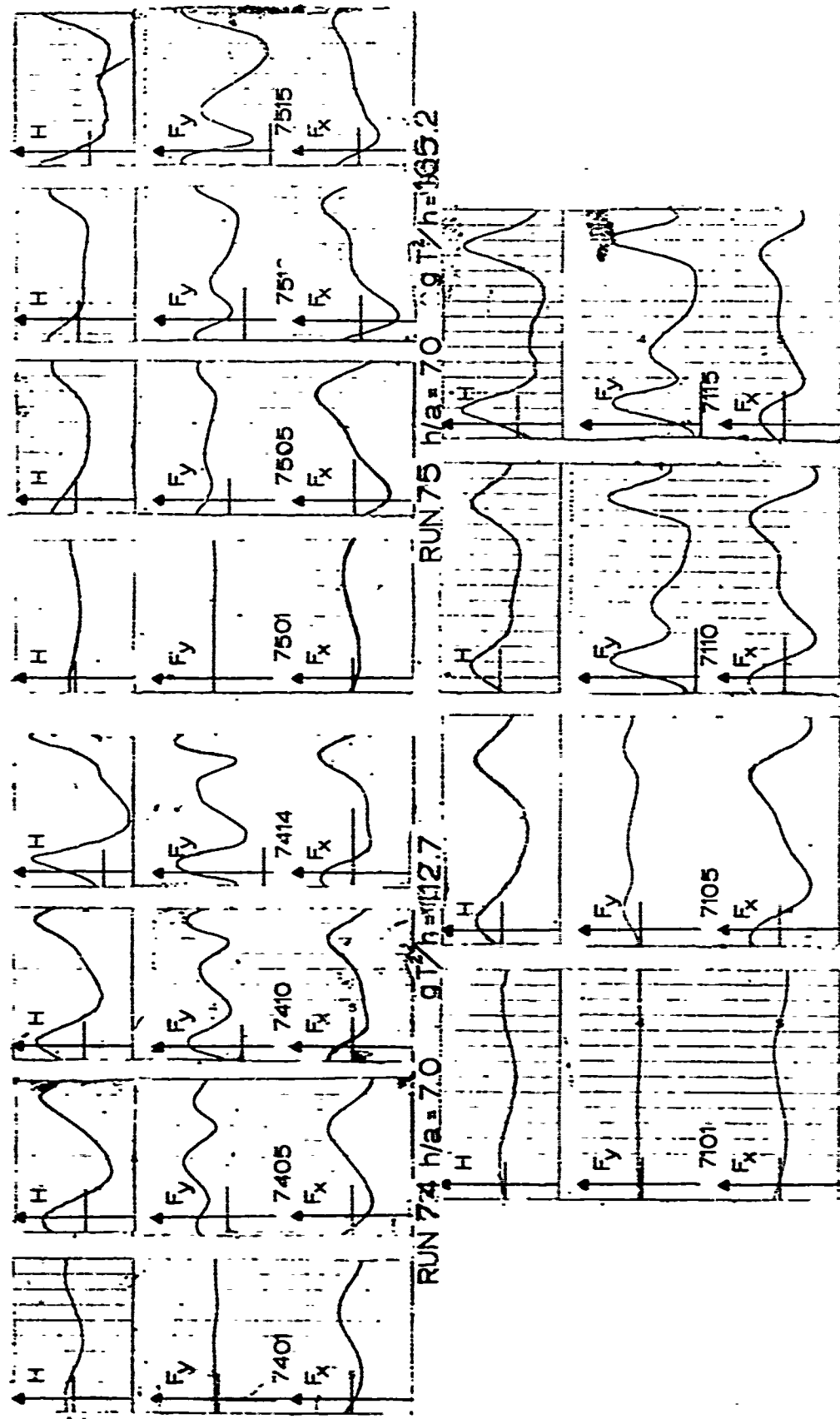


FIG. 13 Wave Height-Force Traces $h/a = 7.0$

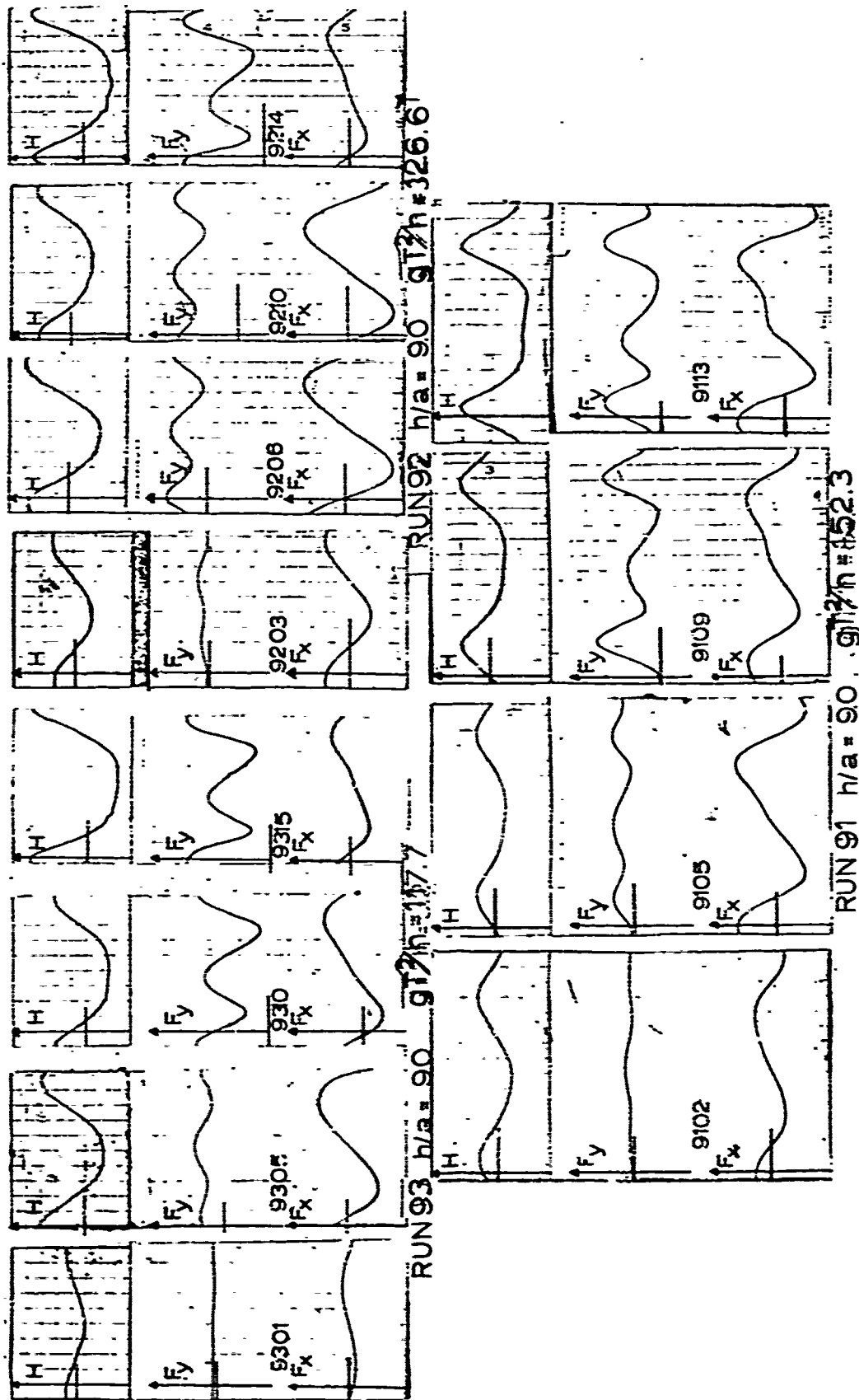


FIG. 14 Wave Height-Force Traces $h/a = 9.0$

corresponding theoretical values of the force coefficients for each experimental case. This provided a comparison between experimental and theoretical values for each run. Plots of experimental and theoretical values for maximum horizontal and vertical force coefficients as a function of wave height for each period and water depth studied are included in Appendix C.

Experimental results and theoretical computations indicate that, at the lower values of dimensionless period and wave height studied, the wave may be characterized as a linear wave. The horizontal force was found to vary sinusoidally, and increased linearly with waveheight. The vertical force varied approximately as a negative cosine function in this region, having its maximum value in the wave trough. The magnitude of the vertical force coefficient was found to vary approximately as the waveheight squared. These characteristics are shown most clearly in runs Number 44 through 47, 71 through 74 and 93 through 95 in Appendix C.

As the relative period and wave height increased, the wave displayed the sharper peaks and longer, shallower troughs that are characteristic of non-linear gravity waves. The horizontal force, proportional to the fluid particle acceleration, tended to reach maximum values closer to the wave peaks, but still remained symmetrical, with respect to the wave crest, as indicated by the theoretical traces. The theoretical analysis predicted a phase lag between the wave crest and the maximum force as small as 24° at the higher wave heights.

The vertical force component began to display positive values occurring at twice the frequency of the wave peaks, as shown in the experimental traces, Figures 11, 12, 13, 14. This is explained by the increasing importance of the lift component of vertical force, which, theoretically, is similar to a cosine squared function. At extremely long periods, the lift force is clearly dominant, and the maximum force no longer occurs in the middle of the wave trough. The maximum vertical force occurs when the cylinder is under the wave crests where the velocity is greatest.

At large periods and wave heights, a point is reached where flow separation effects are no longer negligible. This is seen most clearly in the vertical force component, whose value becomes suddenly lower than the theory predicts, though still varying as the waveheight squared. This sudden drop in lift is apparently caused by a corresponding decrease in the lift coefficient resulting from flow separation. This phenomenon is most clearly evident in the graphical presentation of runs 51 through 56, and 71 through 73 in Appendix C.

1). Horizontal Forces

As previously mentioned, the horizontal forces tended to be nearly sinusoidal in nature with a maximum value which is quite linear with wave height. It is therefore possible to characterize the horizontal force coefficient by it's maximum value ($F_{x_{max}} / \rho g a^2 l$). The variation in the horizontal force coefficient with dimensionless wave height is shown graphically in Appendix C.

The experimental values of horizontal force are seen to vary linearly with wave height for relative period parameter values from 100 to 120. For relative period values greater than 120, the force coefficient varies in an increasingly non-linear fashion. This is consistent with the theory, as shown in Figure 15. However, for the range of period parameters studied, the deviation from linearity is relatively small. It is therefore possible to display the experimental data in terms of the slope of the force coefficient versus wave height plots, as shown in Figures 16 and 17.

The theory predicts the maximum values of horizontal force coefficients prior to the wave heights where separation effects become apparent. The discrepancy between theoretical and experimental values is due to variation of the added mass coefficient in a separated flow as well as a net drag force which is no longer zero.

2). Vertical Forces

As indicated previously, the vertical force displays two regimes; one inertia dominated and one lift dominated. The maximum value of the vertical force coefficient ($F_{y_{max}} / \rho g a^2 l$) is seen to vary as the wave height squared throughout the range of data taken. This is shown graphically in Appendix C. For higher values of relative wave height, the magnitude of the vertical force coefficients is less than predicted by the theory, due to separation effects, as explained above.

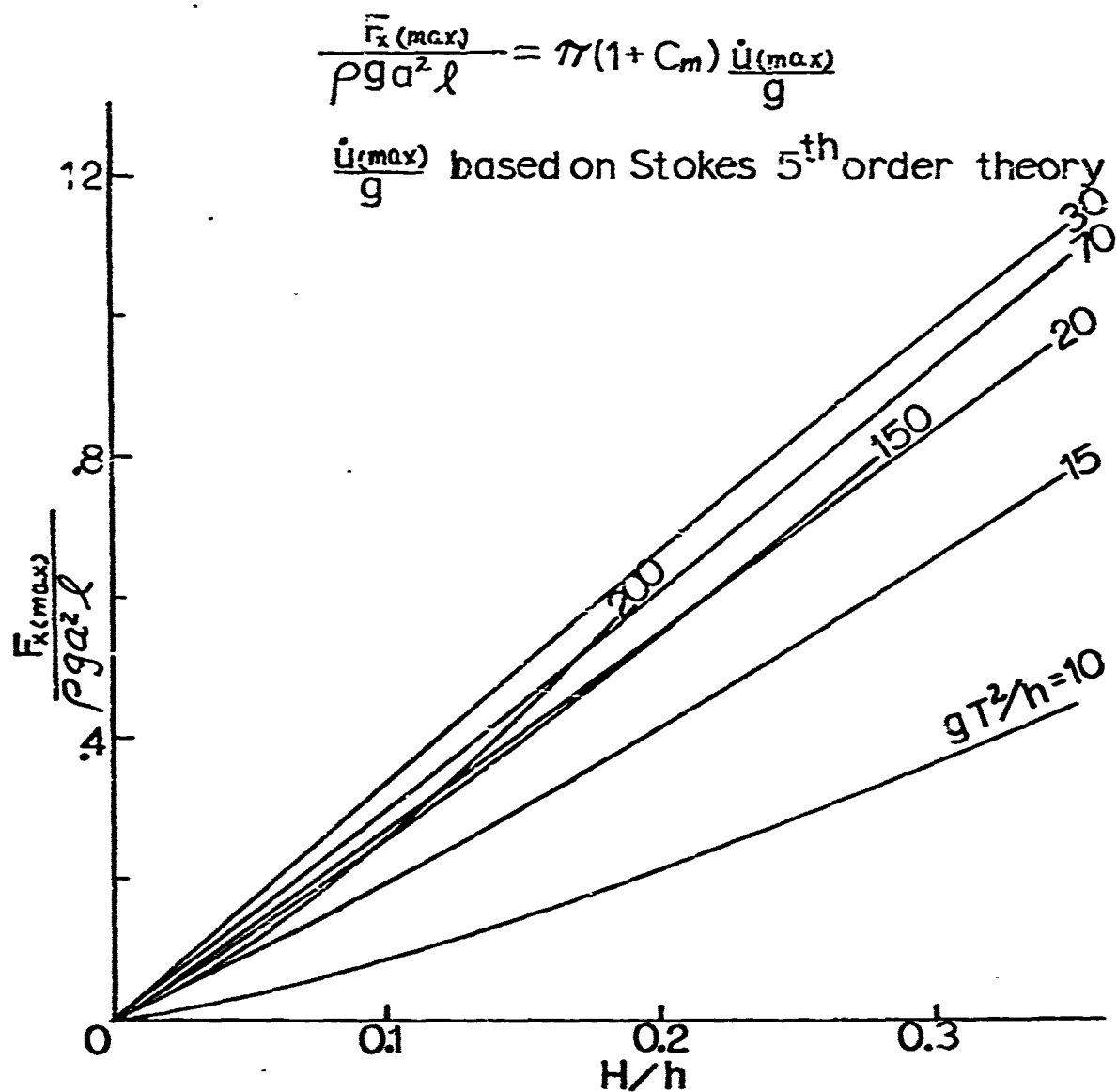


Fig. 15 HORIZ. WAVE FORCE

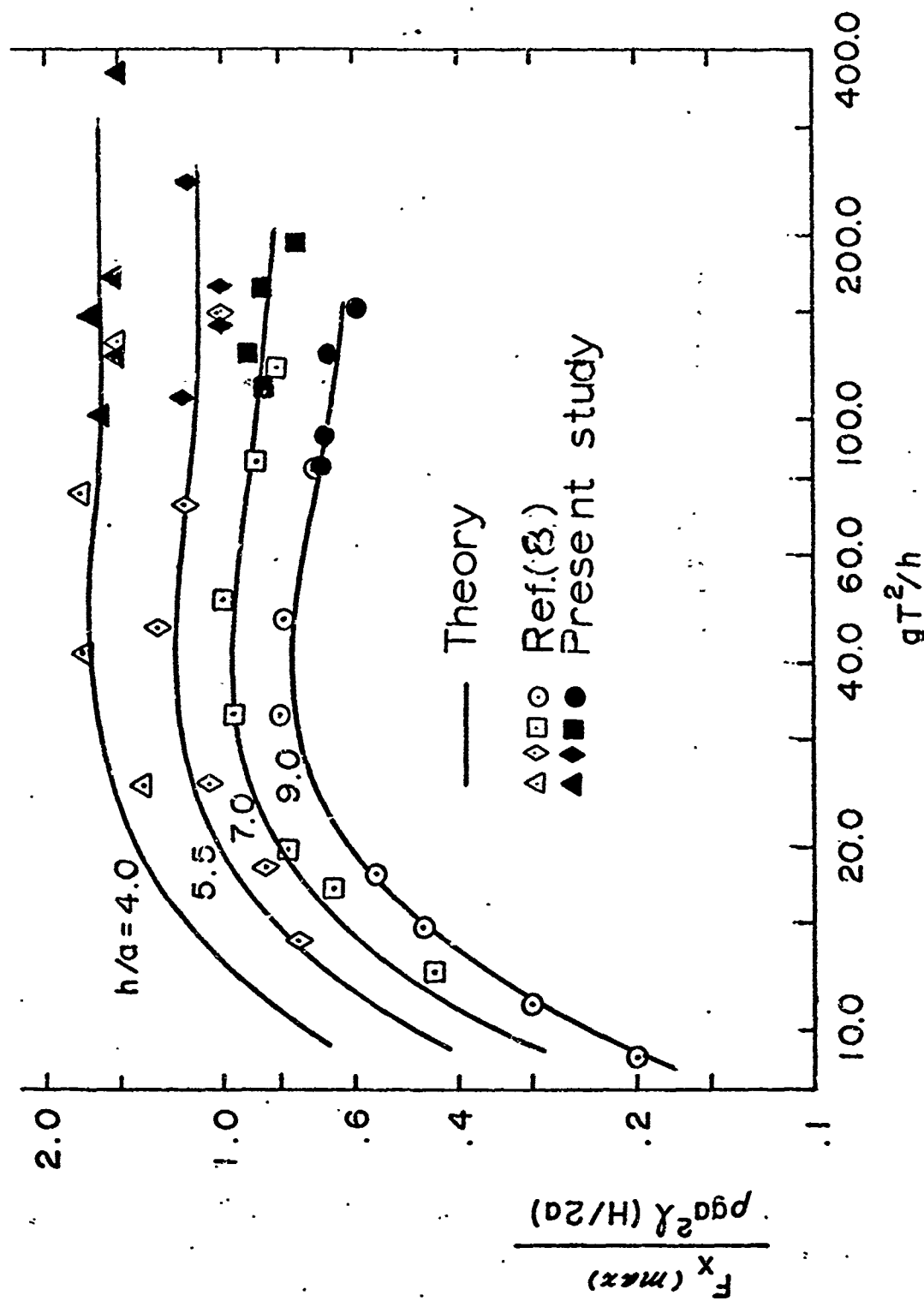


Fig.16 HORIZONTAL WAVE FORCE

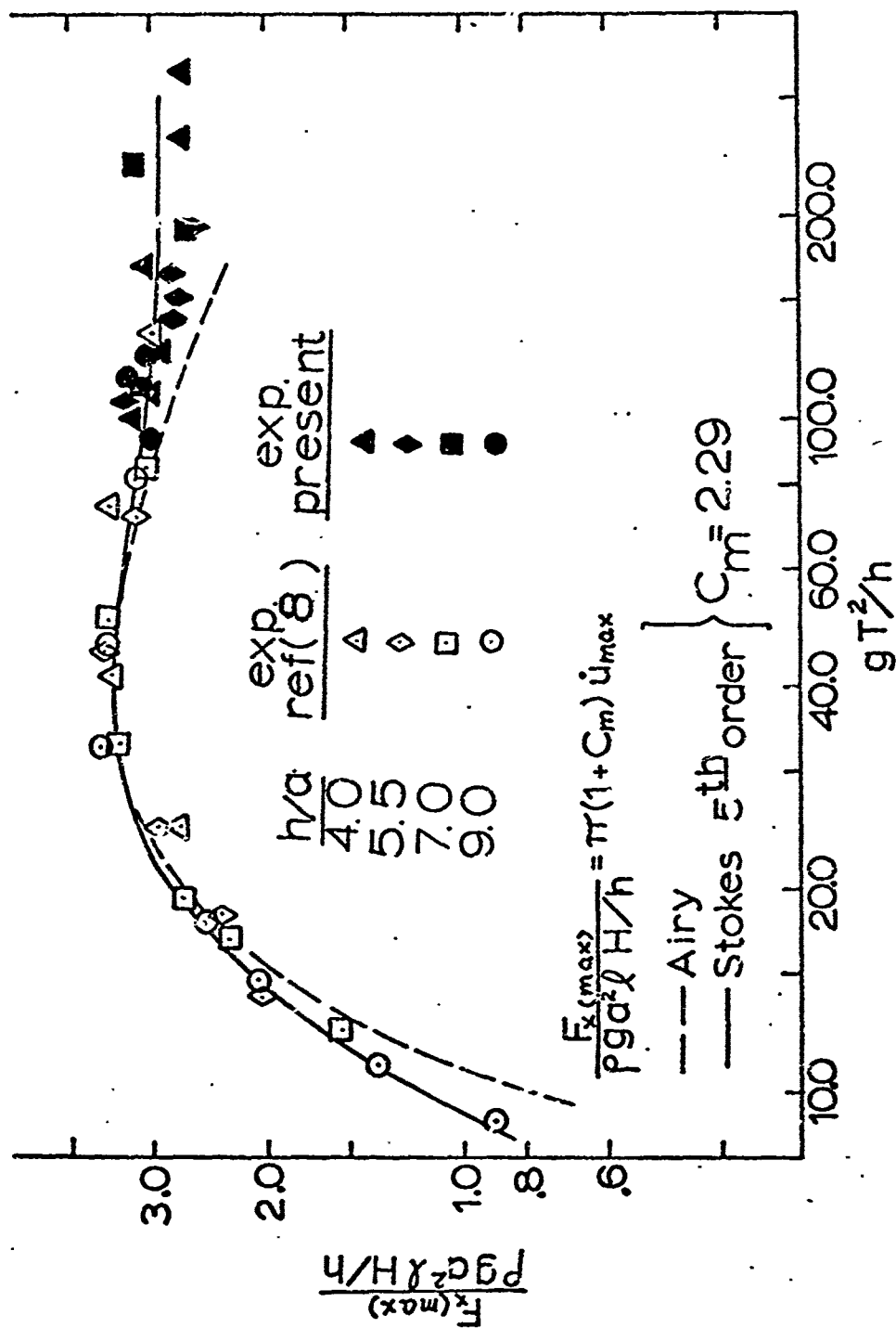


Fig. 17 HORIZONTAL WAVE FORCE

B. CONCLUSIONS

From the experimental and theoretical results, the following conclusions are considered warranted:

1. The horizontal forces on the cylinder, resulting from the incident gravity waves, increased linearly with wave height for relative period values less than 120. For relative period values greater than 120, the force coefficient was found to vary with wave height in an increasingly non-linear fashion.

2. The vertical forces displayed two regimes; one inertia dominated at lower periods and wave heights, and one lift dominated at higher values of these parameters.

3. For high period parameter values, separation effects can be expected for relative wave height values above 0.6, resulting in a sudden drop in experimental force coefficient values from those predicted by the theory.

4. The theory used in this study provides excellent agreement with experimental values for relative period (gT^2/h) values from 100 to 200, and prior to the onset of flow separation.

APPENDIX A
COEFFICIENTS FOR STOKES FIFTH ORDER WAVE THEORY

$$S = \sinh(\tilde{d})$$

$$C = \cosh(\tilde{d})$$

$$C_0 = \tanh(\tilde{d})$$

$$C_1 = \frac{(8C^4 - 8C^2 + 9)}{8S^4}$$

$$C_2 = \frac{(3840C^{12} - 4096C^{10} + 2592C^8 - 1008C^6 + 5944C^4 - 1830C^2 + 147)}{512S^{10}(6C^2 - 1)}$$

$$C_3 = -\frac{1}{4SC}$$

$$C_4 = \frac{(12C^8 + 36C^6 - 162C^4 + 141C^2 - 27)}{192CS^9}$$

$$A_{11} = \frac{1}{S}$$

$$A_{13} = \frac{-C^2(5C^2 + 1)}{8S^5}$$

$$A_{15} = \frac{-(1184C^{10} - 1440C^8 - 1992C^6 + 2641C^4 - 249C^2 + 18)}{1536S^{11}}$$

$$A_{22} = \frac{3}{8S^4}$$

$$A_{24} = \frac{(192C^8 - 424C^6 - 312C^4 + 480C^2 - 17)}{768S^{10}}$$

$$A_{33} = \frac{(13-4c^2)}{64s^7}$$

$$A_{35} = \frac{(512c^{12}+4224c^{10}-6800c^8-12,808c^6+16,704c^4-3154c^2+107)}{4096s^{13}(6c^2-1)}$$

$$A_{44} = \frac{(80c^6-816c^4+1338c^2-197)}{1536s^{10}(6c^2-1)}$$

$$A_{55} = \frac{-(2880c^{10}-72,480c^8+324,000c^6-432,000c^4+163,470c^2-16,245)}{61,440s^{11}(6c^2-1)(8c^4-11c^2+3)}$$

$$B_{22} = \frac{(2c^2+1)}{4s^3}$$

$$B_{24} = \frac{c(272c^8-504c^6-192c^4+322c^2+21)}{384s^9}$$

$$B_{33} = \frac{3(8c^6+1)}{63s^6}$$

$$B_{35} = \frac{(88,128c^{14}-208,224c^{12}+70,818c^{10}+54,000c^8-21,816c^6+6264c^4-54c^2-81)}{12,288s^{12}(6c^2-1)}$$

$$B_{44} = \frac{c(768c^{10}-448c^8-48c^6+48c^4+106c^2-21)}{384s^9(6c^2-1)}$$

$$B_{55} = \frac{(192,000c^{16}-262,720c^{14}+83,680c^{12}+20,160c^{10}-7280c^8)}{12,288s^{10}(6c^2-1)(8c^4-11c^2+3)} + \\ + \frac{(7160c^6-1800c^4-1050c^2+225)}{12,288s^{10}(6c^2-1)(8c^4-11c^2+3)}$$

$$A_1 = \lambda A_{11} + \lambda^3 A_{13} + \lambda^5 A_{15}$$

$$A_2 = \lambda^2 A_{22} + \lambda^4 A_{24}$$

$$A_3 = \lambda^3 A_{33} + \lambda^5 A_{35}$$

$$A_4 = \lambda^4 A_{44}$$

$$A_5 = \lambda^5 A_{55}$$

$$B_2 = \lambda^2 B_{22} + \lambda^4 B_{24}$$

$$B_3 = \lambda^3 B_{33} + \lambda^5 B_{35}$$

$$B_4 = \lambda^4 B_{44}$$

$$B_5 = \lambda^5 B_{55}$$

APPENDIX B EXPERIMENTAL DATA

DATA FOR RUN NUMBER 41. TOTAL NUMBER OF RUNS IS 23.
WAVE PERIOD IS 2.637SECONDS. WATER DEPTH IS 8.0INCHES.
DIMENSIONLESS PARAMETERS ARE NON-DIMENSIONAL PERIOD($=GT^{**2}/H$) IS 335.681
DEPTH TO RADIUS RATIO($=H/A$) IS 4.0000

SEGMENT NUMBER	WAVE HEIGHT	FORCE (X)	FORCE (Y)	H/2A	F. COEF (X)	F. COEF (Y)
4101	0.30	0.23	0.03	0.08	0.11	0.01
4102	0.51	0.56	0.05	0.13	0.26	0.03
4103	0.63	0.62	0.12	0.16	0.29	0.05
4104	1.01	0.93	0.23	0.25	0.42	0.11
4105	1.24	1.33	0.34	0.30	0.62	0.16
4106	1.34	1.71	0.48	0.33	0.79	0.22
4107	1.62	1.71	0.59	0.40	0.79	0.27
4108	1.86	1.81	0.80	0.46	0.84	0.37
4109	2.46	2.20	0.94	0.62	1.02	0.49
4110	2.60	2.37	1.05	0.65	1.10	0.44
4111	2.87	2.56	1.27	0.72	1.18	0.59

DATA FOR RUN NUMBER 42. TOTAL NUMBER OF RUNS IS 23.
 WAVE PERIOD IS 2.160SECONDS. WATER DEPTH IS 8.0INCHES.
 DIMENSIONLESS PARAMETERS ARE NON-DIMENSIONAL PERIOD(=GT**2/H) IS 225.138
 DEPTH TO RADIUS RATIO(=H/A) IS 4.0000

SEGMENT NUMBER	WAVE HEIGHT	FORCE (X)	FORCE (Y)	H/2A	F _x COEF (X)	F _y COEF (Y)
4201	0.31	0.25	0.04	0.08	0.12	0.02
4202	0.50	0.50	0.06	0.12	0.23	0.03
4203	0.83	0.63	0.11	0.21	0.29	0.05
4204	1.13	0.83	0.19	0.28	0.39	0.09
4205	1.47	1.05	0.30	0.37	0.49	0.14
4206	1.91	1.34	0.37	0.48	0.62	0.17
4207	2.13	1.49	0.57	0.53	0.69	0.26
4208	2.47	1.76	0.76	0.62	0.82	0.35
4209	2.83	1.92	0.94	0.71	0.89	0.44
4210	3.13	2.12	1.03	0.78	0.89	0.48
4211	3.39	2.12	1.18	0.85	0.78	0.55

DATA FOR RUN NUMBER 43. TOTAL NUMBER OF RUNS IS 23.
 WAVE PERIOD IS 1.887SECONDS. WATER DEPTH IS 8.0INCHES.
 DIMENSIONLESS PARAMETERS ARE NON-DIMENSIONAL PERIOD(=GT**2/H) IS 171.916
 DEPTH TO RADIUS RATIO(=H/A) IS 4.0000

SEGMENT NUMBER	WAVE HEIGHT	FORCE (X)	FORCE (Y)	H/2A	F. COEF (X)	F. COEF (Y)
4301	0.36	0.28	0.42	0.09	0.13	0.02
4302	0.89	0.74	0.19	0.15	0.23	0.06
4303	1.07	0.82	0.26	0.22	0.34	0.09
4304	1.40	1.23	0.36	0.27	0.38	0.12
4305	1.71	1.52	0.39	0.35	0.57	0.17
4306	2.06	1.81	0.52	0.43	0.70	0.24
4307	2.38	2.26	0.68	0.52	0.84	0.32
4308	2.57	2.36	0.97	0.64	1.05	0.41
4309	2.82	2.79	1.13	0.70	1.29	0.45
4310						0.52

DATA FOR RUN NUMBER 44. TOTAL NUMBER OF RUNS IS 23.
 WAVE PERIOD IS 1.637SECONDS. WATER DEPTH IS 8.0INCHES.
 DIMENSIONLESS PARAMETERS ARE NON-DIMENSIONAL PERIOD($=GT^{**2}/H$) IS 129.391
 DEPTH TO RADIUS RATIO($=H/A$) IS 4.0000

SEGMENT NUMBER	WAVE HEIGHT	FORCE (X)	FORCE (Y)	H/2A	F _x COEF (X)	F _y COEF (Y)
4401	0.46	0.25	0.05	0.12	0.12	0.02
4402	0.78	0.53	0.12	0.27	0.21	0.09
4403	1.08	0.88	0.20	0.34	0.41	0.12
4404	1.35	1.17	0.25	0.44	0.54	0.17
4405	1.78	1.29	0.37	0.56	0.60	0.21
4406	2.23	1.75	0.57	0.61	0.81	0.23
4407	2.36	2.11	0.70	0.59	0.98	0.30
4408	2.74	2.26	0.86	0.76	1.05	0.40
4409	3.04	2.58	1.03	0.76	1.19	0.47

DATA FOR RUN NUMBER 45. TOTAL NUMBER OF RUNS IS 23.
 WAVE PERIOD IS 1.450SECONDS. WATER DEPTH IS 8.0INCHES.
 DIMENSIONLESS PARAMETERS ARE NON-DIMENSIONAL PERIOD($=GT^{**2}/H$) IS 101.456
 DEPTH TO RADIUS RATIO($=H/A$) IS 4.0000

SEGMENT NUMBER	WAVE HEIGHT	FORCE (X)	FORCE (Y)	H/2A	F _x COEF (X)	F _y COEF (Y)
4501	0.44	0.59	0.13	0.19	0.27	0.05
4502	0.75	0.59	0.23	0.27	0.29	0.10
4503	1.06	1.47	0.20	0.35	0.80	0.09
4504	1.39	1.73	0.33	0.43	0.86	0.17
4505	1.73	1.86	0.43	0.52	0.89	0.20
4506	2.09	1.93	0.49	0.66	1.05	0.22
4507	2.66	2.26	0.78	0.77	1.23	0.29
4508	3.07					0.36

DATA FOR RUN NUMBER 46. TOTAL NUMBER OF RUNS IS 23.
 WAVE PERIOD IS 1.755SECONDS. WATER DEPTH IS 8.0INCHES.
 DIMENSIONLESS PARAMETERS ARE NON-DIMENSIONAL PERIOD($=GT^{**2}/H$) IS 148.626
 DEPTH TO RADIUS RATIO($=H/A$) IS 4.0000

SEGMENT NUMBER	WAVE HEIGHT	FORCE (X)	FORCE (Y)	H/2A	F _x COEF (X)	F _y COEF (Y)
4601	0.47	0.34	0.06	0.12	0.16	0.03
4602	0.79	0.56	0.11	0.20	0.26	0.05
4603	1.12	0.92	0.19	0.28	0.43	0.09
4604	1.36	1.04	0.17	0.34	0.47	0.08
4605	1.59	1.66	0.19	0.49	0.77	0.18
4606	2.22	2.05	0.34	0.55	0.95	0.25
4607	2.64	2.47	0.72	0.66	1.14	0.33
4608	3.04	2.78	0.91	0.76	1.25	0.42
4609	3.58	2.98	1.05	0.92	1.31	0.49
4610	3.68	2.83	1.05	0.92	1.31	0.49

DATA FOR RUN NUMBER 47. TOTAL NUMBER OF RUNS IS 23.
 WAVE PERIOD IS 1.535SECONDS. WATER DEPTH IS 8.0INCHES.
 DIMENSIONLESS PARAMETERS ARE NON-DIMENSIONAL PERIOD(=GT**2/H) IS 113.700
 DEPTH TO RADIUS RATIO(=H/A) IS 4.0000

SEGMENT NUMBER	WAVE HEIGHT	FORCE (X)	FORCE (Y)	H/2A	F _x COEF (X)	F _y COEF (Y)
4701	0.50	0.54	0.08	0.12	0.23	0.04
4702	0.92	0.83	0.12	0.23	0.33	0.05
4703	1.23	1.14	0.20	0.43	0.50	0.10
4704	1.41	1.31	0.32	0.49	0.70	0.14
4705	1.96	1.72	0.59	0.58	0.82	0.15
4706	2.35	2.09	0.69	0.60	0.92	0.22
4707	2.73	2.28	0.74	0.80	1.03	0.32
4708	3.20	2.83	1.01	0.84	1.33	0.34
4709	3.36	2.93			1.35	0.47

DATA FOR RUN NUMBER 51. TOTAL NUMBER OF RUNS IS 23.
 WAVE PERIOD IS 2.175SECONDS. WATER DEPTH IS 11.0INCHES.
 DIMENSIONLESS PARAMETERS ARE NON-DIMENSIONAL PERIOD($=GT^{**2}/H$) IS 166.019
 DEPTH TO RADIUS RATIO($=H/A$) IS 5.5000

SEGMENT NUMBER	WAVE HEIGHT	FORCE (X)	FORCE (Y)	H/2A	F _x COEF (X)	F _y COEF (Y)
5101	0.49	0.20	0.71	0.12	0.09	0.01
5102	0.67	0.32	0.09	0.17	0.15	0.02
5103	0.91	0.42	0.09	0.23	0.22	0.04
5104	1.23	0.67	0.15	0.32	0.29	0.07
5105	1.36	0.96	0.23	0.39	0.36	0.10
5106	1.85	1.24	0.34	0.46	0.43	0.16
5107	2.04	1.49	0.51	0.51	0.53	0.23
5108	2.45	1.45	0.65	0.57	0.60	0.30
5109	2.83	1.45	0.89	0.67	0.67	0.40
5110	3.22	1.55	0.89	0.71	0.70	0.41
5111	3.62	1.59	0.92	0.81	0.81	0.43
5112	3.96	1.59	1.12	0.99	0.92	0.45
5113	4.43	1.53	1.28	1.10	0.97	0.52
5114	4.73	2.25	1.68	1.19	1.08	0.57
5115	4.99	2.51	1.88	1.25	1.16	0.61

DATA FOR RUN NUMBER 52. TOTAL NUMBER OF RUNS IS 23.
 WAVE PERIOD IS 2.020SECONDS. WATER DEPTH IS 11.0INCHES.
 DIMENSIONLESS PARAMETERS ARE NON-DIMENSIONAL PERIOD($=GT^{**2}/H$) IS 143.200
 DEPTH TO RADIUS RATIO($=H/A$) IS 5.5000

SEGMENT NUMBER	WAVE HEIGHT	FORCE (X)	FORCE (Y)	H/2A	F. COEF (X)	F. COEF (Y)
5201	0.47	0.20	0.07	0.12	0.09	0.02
5202	0.73	0.34	0.13	0.18	0.16	0.03
5203	0.99	0.53	0.23	0.25	0.25	0.06
5204	1.55	0.66	0.32	0.39	0.30	0.11
5205	1.66	0.82	0.46	0.41	0.38	0.15
5206	2.02	1.04	0.59	0.50	0.48	0.21
5207	2.41	1.25	0.74	0.60	0.58	0.27
5208	2.61	1.53	0.87	0.65	0.71	0.34
5209	3.04	1.70	0.95	0.76	0.82	0.40
5210	3.46	2.04	1.14	0.87	0.94	0.44
5211	3.75	2.31	1.24	0.94	1.07	0.53
5212	4.15	2.64	1.47	1.04	1.22	0.71
5213	4.62	2.86	1.54	1.16	1.32	0.68
5214	5.14	3.05	1.65	1.28	1.41	0.76

DATA FOR RUN NUMBER 53. TOTAL NUMBER OF RUNS IS 23.
 WAVE PERIOD IS 1.880SECONDS. WATER DEPTH IS 11.0INCHES.
 DIMENSIONLESS PARAMETERS ARE NON-DIMENSIONAL PERIOD(=GT**2/H) IS 124.038
 DEPTH TO RADIUS RATIO(=H/A) IS 5.5000

SEGMENT NUMBER	WAVE HEIGHT	FORCE (X)	FORCE (Y)	H/2A	F. COEF (X)	F. COEF (Y)
5301	0.40	0.27	0.04	0.10	0.12	0.02
5302	0.63	0.44	0.09	0.16	0.21	0.04
5303	0.92	0.62	0.14	0.23	0.28	0.06
5304	1.25	0.81	0.24	0.31	0.37	0.11
5305	1.46	1.09	0.30	0.36	0.51	0.14
5306	1.80	1.35	0.39	0.45	0.62	0.18
5307	2.06	1.57	0.55	0.52	0.72	0.25
5308	2.37	1.86	0.75	0.59	0.83	0.35
5309	2.72	2.10	0.98	0.67	0.86	0.45
5310	3.10	2.26	1.10	0.77	1.00	0.51
5311	3.51	2.56	1.21	0.88	1.18	0.56
5312	3.72	2.86	1.36	0.93	1.32	0.63
5313	4.25	3.12	1.54	1.06	1.44	0.71
5314	4.50	3.26	1.67	1.13	1.51	0.77

DATA FOR RUN NUMBER 54. TOTAL NUMBER OF RUNS IS 23.
 WAVE PERIOD IS 2.322SECONDS. WATER DEPTH IS 11.0INCHES.
 DIMENSIONLESS PARAMETERS ARE NON-DIMENSIONAL PERIOD(=GT**2/H) IS 189.300
 DEPTH TO RADIUS RATIO(=H/A) IS 5.5000

SEGMENT NUMBER	WAVE HEIGHT	FORCE (X)	FORCE (Y)	H/2A	F. COEF (X)	F. COEF (Y)
5401	0.31	0.11	0.04	0.08	0.05	0.02
5402	0.50	0.31	0.08	0.13	0.14	0.02
5403	0.71	0.45	0.14	0.18	0.21	0.07
5404	0.93	0.59	0.22	0.23	0.23	0.10
5405	1.14	0.73	0.31	0.29	0.34	0.11
5406	1.43	0.97	0.45	0.36	0.45	0.16
5407	1.72	1.08	0.57	0.43	0.50	0.21
5408	2.01	1.30	0.77	0.50	0.60	0.22
5409	2.30	1.55	0.92	0.57	0.72	0.23
5410	2.54	1.77	1.10	0.63	0.79	0.30
5411	2.86	1.95	1.22	0.68	0.81	0.43
5412	3.25	2.18	1.17	0.88	0.72	0.51
5413	3.88	1.88	1.11	0.97	0.81	0.51
5414	4.34	1.88	1.17	1.09	0.87	0.54

DATA FOR RUN NUMBER 55. TOTAL NUMBER OF RUNS IS 23.
 WAVE PERIOD IS 2.647SECONDS. WATER DEPTH IS 11.0INCHES.
 DIMENSIONLESS PARAMETERS ARE NON-DIMENSIONAL PERIOD(=GT**2/H) IS 245.986
 DEPTH TO RADIUS RATIO(=H/A) IS 5.5000

SEGMENT NUMBER	WAVE HEIGHT	FORCE (X)	FORCE (Y)	H/2A	F _x COEF (X)	F _y COEF (Y)
5501	0.30	0.10	0.01	0.07	0.05	0.00
5502	0.41	0.26	0.03	0.10	0.12	0.01
5503	0.67	0.43	0.03	0.17	0.20	0.02
5504	0.75	0.60	0.10	0.19	0.28	0.05
5505	1.05	0.75	0.19	0.26	0.35	0.09
5506	1.37	0.84	0.29	0.34	0.39	0.13
5507	1.76	1.09	0.45	0.44	0.50	0.26
5508	2.06	1.20	0.55	0.51	0.55	0.35
5509	2.32	1.36	0.78	0.58	0.63	0.36
5510	2.69	1.58	0.92	0.67	0.79	0.43
5511	3.17	1.77	0.98	0.79	0.82	0.45
5512	3.34	1.94	1.21	0.84	0.90	0.56
5513	3.70	2.17	1.40	0.92	1.01	0.65
5514	4.17			1.04		

DATA FOR RUN NUMBER 56. TOTAL NUMBER OF RUNS IS 23.
 WAVE PERIOD IS 1.752SECONDS. WATER DEPTH IS 11.0INCHES.
 DIMENSIONLESS PARAMETERS ARE NON-DIMENSIONAL PERIOD(=GT**2/H) IS 107.734
 DEPTH TO RADIUS RATIO(=H/A) IS 5.5000

SEGMENT NUMBER	WAVE HEIGHT	FORCE (X)	FORCE (Y)	H/2A	F _x COEF (X)	F _y COEF (Y)
5601	0.56	0.28	0.07	0.14	0.13	0.01
5602	0.94	0.51	0.13	0.23	0.34	0.03
5603	1.20	0.74	0.23	0.30	0.43	0.06
5604	1.66	0.93	0.36	0.42	0.51	0.11
5605	2.11	1.11	0.40	0.53	0.61	0.17
5606	2.46	1.35	0.56	0.60	0.72	0.18
5607	2.82	1.53	0.76	0.70	0.76	0.26
5608	3.17	1.88	0.77	0.79	0.87	0.35
5609	3.43	2.06	0.85	0.86	0.95	0.39
5610	3.78	2.24	0.92	0.95	1.13	0.43
5611	4.66	2.55	1.03	1.17	1.18	0.48

DATA FOR RUN NUMBER 71. TOTAL NUMBER OF RUNS IS 23.
 WAVE PERIOD IS 2.645SECONDS. WATER DEPTH IS 14.0INCHES.
 DIMENSIONLESS PARAMETERS ARE NON-DIMENSIONAL PERIOD(=GT**2/H) IS 192.910
 DEPTH TO RADIUS RATIO(=H/A) IS 7.0000

SEGMENT NUMBER	WAVE HEIGHT	FORCE (X)	FORCE (Y)	H/2A	F. COEF (X)	F. COEF (Y)
7101	0.30	0.10	0.23	0.07	0.05	0.01
7102	0.60	0.21	0.00	0.15	0.10	0.02
7103	0.82	0.27	0.05	0.27	0.13	0.02
7104	1.09	0.40	0.08	0.32	0.18	0.04
7105	1.27	0.56	0.16	0.39	0.26	0.07
7106	1.54	0.78	0.22	0.48	0.31	0.10
7107	1.94	0.93	0.36	0.56	0.36	0.16
7108	2.24	1.06	0.45	0.66	0.43	0.22
7109	2.63	1.20	0.67	0.71	0.49	0.29
7110	3.26	1.33	0.93	0.81	0.55	0.36
7111	3.87	1.45	0.95	0.97	0.62	0.44
7112	4.05	1.50	0.97	1.01	0.69	0.43
7113	4.40	1.78	1.24	1.10	0.80	0.57
7114	4.75	1.88	1.42	1.19	0.87	0.66
7115						

DATA FOR RUN NUMBER 720. TOTAL NUMBER OF RUNS IS 23.
 WAVE PERIOD IS 2.365 SECONDS. WATER DEPTH IS 14.0 INCHES.
 DIMENSIONLESS PARAMETERS ARE NON-DIMENSIONAL PERIOD ($=GT^{**2}/H$) IS 154.229
 DEPTH TO RADIUS RATIO ($=H/A$) IS 7.0000

SEGMENT NUMBER	WAVE HEIGHT	FORCE (X)	FORCE (Y)	H/2A	F _x COEF (X)	F _y COEF (Y)
7201	0.34	0.16	0.01	0.08	0.07	0.01
7202	0.60	0.16	0.03	0.15	0.03	0.01
7203	0.79	0.23	0.06	0.25	0.13	0.03
7204	0.99	0.34	0.08	0.32	0.16	0.04
7205	1.27	0.50	0.12	0.37	0.25	0.09
7206	1.50	0.60	0.28	0.40	0.38	0.13
7207	1.89	0.73	0.42	0.50	0.40	0.19
7208	2.38	0.87	0.50	0.59	0.45	0.23
7209	2.73	0.98	0.62	0.68	0.51	0.29
7210	2.99	1.10	0.87	0.75	0.58	0.39
7211	3.61	1.22	0.95	0.90	0.66	0.47
7212	4.14	1.32	1.02	1.03	0.71	0.47
7213	4.58	1.47	1.34	1.14	0.74	0.65
7214	5.02	1.75	1.40	1.25	0.81	0.65
7215						

DATA FOR RUN NUMBER 73. TOTAL NUMBER OF RUNS IS 23.
 WAVE PERIOD IS 2.170SECONDS. WATER DEPTH IS 14.0INCHES.
 DIMENSIONLESS PARAMETERS ARE NON-DIMENSIONAL PERIOD(=GT**2/H) IS 129.844
 DEPTH TO RADIUS RATIO(=H/A) IS 7.0000

SEGMENT NUMBER	WAVE HEIGHT	FORCE (X)	FORCE (Y)	H/2A	F. COEF (X)	F. COEF (Y)
7301	0.43	0.236	0.03	0.185	0.17	0.01
7302	0.71	0.352	0.05	0.185	0.21	0.02
7303	1.00	0.420	0.09	0.231	0.29	0.04
7304	1.25	0.480	0.14	0.297	0.37	0.06
7305	1.57	0.589	0.22	0.47	0.47	0.10
7306	1.90	0.82	0.26	0.54	0.52	0.12
7307	2.16	1.023	0.40	0.58	0.59	0.19
7308	2.34	1.138	0.50	0.73	0.72	0.23
7309	2.90	1.241	0.69	0.82	0.85	0.34
7310	3.30	1.595	0.74	0.91	0.91	0.42
7311	3.64	1.535	0.92	1.01	0.98	0.47
7312	4.06	2.153	1.09	1.13	1.18	0.50
7313	4.50	2.556	1.43	1.20	1.18	0.62
7314	4.80					
7315	5.16					

DATA FOR RUN NUMBER 74. TOTAL NUMBER OF RUNS IS 23.
 WAVE PERIOD IS 2.022SECONDS. WATER DEPTH IS 14.0INCHES.
 DIMENSIONLESS PARAMETERS ARE NON-DIMENSIONAL PERIOD(=GT**2/H) IS 112.793
 DEPTH TO RADIUS RATIO(=H/A) IS 7.0000

SEGMENT NUMBER	WAVE HEIGHT	FORCE (X)	FORCE (Y)	H/2A	F _x COEF (X)	F _y COEF (Y)
7401	0.52	0.238	0.04	0.13	0.18	0.02
7402	0.90	0.355	0.05	0.23	0.125	0.025
7403	1.19	0.569	0.11	0.38	0.032	0.039
7404	1.54	0.823	0.19	0.57	0.033	0.14
7405	1.85	0.937	0.33	0.79	0.045	0.19
7406	2.30	1.030	0.45	0.99	0.052	0.25
7407	2.74	1.130	0.70	1.06	0.069	0.33
7408	3.16	1.181	0.94	1.06	0.084	0.39
7409	3.60	1.200	1.07	1.24	0.093	0.45
7410	4.06	2.239	1.30	1.44	1.118	0.56
7411	4.26	2.356	1.35		1.118	0.60
7412	4.50					
7413	5.20					
7414	5.76					

DATA FOR RUN NUMBER 75. TOTAL NUMBER OF RUNS IS 23.
 WAVE PERIOD IS 2.447SECONDS. WATER DEPTH IS 14.0INCHES.
 DIMENSIONLESS PARAMETERS ARE NON-DIMENSIONAL PERIOD(=GT**2/H) IS 165.177
 DEPTH TO RADIUS RATIO(=H/A) IS 7.0000

SEGMENT NUMBER	WAVE HEIGHT	FORCE (X)	FORCE (Y)	H/2A	F _x COEF (X)	F _y COEF (Y)
7501	0.38	0.16	0.01	0.09	0.08	0.01
7502	0.625	0.34	0.03	0.15	0.14	0.01
7503	1.04	0.55	0.07	0.21	0.20	0.03
7504	1.42	0.74	0.13	0.26	0.25	0.06
7505	1.61	0.82	0.19	0.30	0.29	0.09
7506	1.83	0.95	0.24	0.34	0.33	0.12
7507	2.00	1.02	0.29	0.38	0.37	0.16
7508	2.25	1.12	0.34	0.41	0.40	0.21
7509	2.50	1.23	0.40	0.45	0.44	0.26
7510	2.80	1.36	0.46	0.49	0.48	0.31
7511	3.10	1.47	0.51	0.53	0.52	0.36
7512	3.40	1.58	0.57	0.57	0.56	0.41
7513	3.80	1.71	0.64	0.61	0.60	0.46
7514	4.20	1.85	0.71	0.65	0.64	0.51
7515	4.60	2.00	0.78	0.69	0.68	0.56

DATA FOR RUN NUMBER 91. TOTAL NUMBER OF RUNS IS 23.
 WAVE PERIOD IS 2.665SECONDS. WATER DEPTH IS 18.0INCHES.
 DIMENSIONLESS PARAMETERS ARE NON-DIMENSIONAL PERIOD(=GT**2/H) IS 152.319
 DEPTH TO RADIUS RATIO(=H/A) IS 9.0000

SEGMENT NUMBER	WAVE HEIGHT	FORCE (X)	FORCE (Y)	H/2A	F _x COEF (X)	F _y COEF (Y)
9101	0.47	0.187	0.011	0.127	0.085	0.001
9102	0.66	0.238	0.003	0.126	0.083	0.001
9103	1.041	0.351	0.007	0.043	0.013	0.003
9104	1.471	0.567	0.015	0.043	0.028	0.005
9105	1.830	0.671	0.025	0.047	0.039	0.007
9106	2.358	0.883	0.038	0.064	0.051	0.018
9107	2.520	0.992	0.058	0.076	0.043	0.023
9108	3.250	1.002	0.085	0.087	0.047	0.031
9109	3.570	1.123	0.086	0.092	0.051	0.039
9110	4.256	1.133	1.007	0.140	0.057	0.040
9111	5.20	1.13	1.241	0.150	0.063	0.049
9112						
9113						
9114						
9115						

DATA FOR RUN NUMBER 92. TOTAL NUMBER OF RUNS IS 23.
 WAVE PERIOD IS 2.342SECONDS. WATER DEPTH IS 18.0INCHES.
 DIMENSIONLESS PARAMETERS ARE NON-DIMENSIONAL PERIOD($\pi GT^2/H$) IS 117.684
 DEPTH TO RADIUS RATIO($\pi H/A$) IS 9.0000

SEGMENT NUMBER	WAVE HEIGHT	FORCE (X)	FORCE (Y)	H/2A	F _x COEF (X)	F _y COEF (Y)
9201	0.58	1.58	1.58	1.44	0.00	0.00
9202	0.59	1.24	0.00	1.23	0.00	0.00
9203	1.16	0.00	0.00	0.00	0.00	0.00
9204	1.63	0.00	0.00	0.00	0.00	0.00
9205	1.99	0.00	0.00	0.00	0.00	0.00
9206	2.75	0.00	0.00	0.00	0.00	0.00
9207	3.94	0.00	0.00	0.00	0.00	0.00
9208	3.26	0.00	0.00	0.00	0.00	0.00
9209	3.00	0.00	0.00	0.00	0.00	0.00
9210	3.08	0.00	0.00	0.00	0.00	0.00
9211	4.37	0.00	0.00	0.00	0.00	0.00
9212	4.70	0.00	0.00	0.00	0.00	0.00
9213	5.11	0.00	0.00	0.00	0.00	0.00
9214	5.30	0.00	0.00	0.00	0.00	0.00
9215	5.30	0.00	0.00	0.00	0.00	0.00

DATA FOR RUN NUMBER 93. TOTAL NUMBER OF RUNS IS 23.
 WAVE PERIOD IS 2.430SECONDS. WATER DEPTH IS 18.0INCHES.
 DIMENSIONLESS PARAMETERS ARE NON-DIMENSIONAL PERIOD($=GT^{**2}/H$) 1.1126.640
 DEPTH TO RADIUS RATIO($=H/A$) 11.9.0000

SEGMENT NUMBER	WAVE HEIGHT	FORCE (X)	FORCE (Y)	H/2A	F _x COEF (X)	F _y COEF (Y)
9301	0.0000	0.0000	0.0000	0.0000	0.0000	0.0000
9302	0.0000	0.0000	0.0000	0.0000	0.0000	0.0000
9303	0.0000	0.0000	0.0000	0.0000	0.0000	0.0000
9304	0.0000	0.0000	0.0000	0.0000	0.0000	0.0000
9305	0.0000	0.0000	0.0000	0.0000	0.0000	0.0000
9306	0.0000	0.0000	0.0000	0.0000	0.0000	0.0000
9307	0.0000	0.0000	0.0000	0.0000	0.0000	0.0000
9308	0.0000	0.0000	0.0000	0.0000	0.0000	0.0000
9309	0.0000	0.0000	0.0000	0.0000	0.0000	0.0000
9310	0.0000	0.0000	0.0000	0.0000	0.0000	0.0000
9311	0.0000	0.0000	0.0000	0.0000	0.0000	0.0000
9312	0.0000	0.0000	0.0000	0.0000	0.0000	0.0000
9313	0.0000	0.0000	0.0000	0.0000	0.0000	0.0000
9314	0.0000	0.0000	0.0000	0.0000	0.0000	0.0000
9315	0.0000	0.0000	0.0000	0.0000	0.0000	0.0000
9316	0.0000	0.0000	0.0000	0.0000	0.0000	0.0000
9317	0.0000	0.0000	0.0000	0.0000	0.0000	0.0000
9318	0.0000	0.0000	0.0000	0.0000	0.0000	0.0000
9319	0.0000	0.0000	0.0000	0.0000	0.0000	0.0000
9320	0.0000	0.0000	0.0000	0.0000	0.0000	0.0000
9321	0.0000	0.0000	0.0000	0.0000	0.0000	0.0000
9322	0.0000	0.0000	0.0000	0.0000	0.0000	0.0000
9323	0.0000	0.0000	0.0000	0.0000	0.0000	0.0000

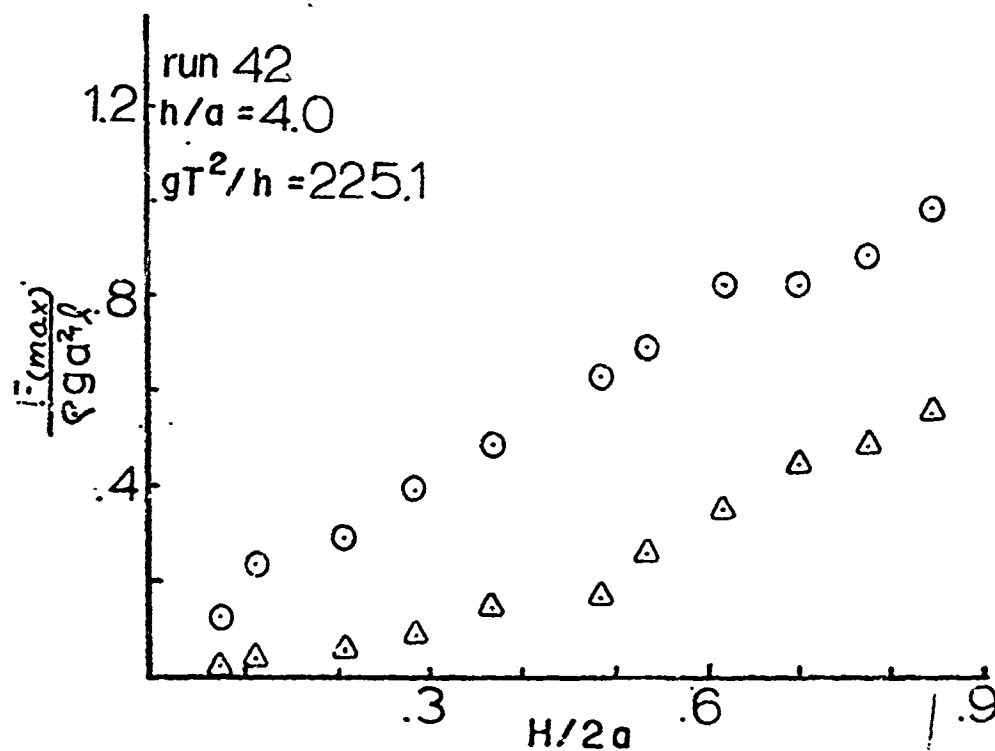
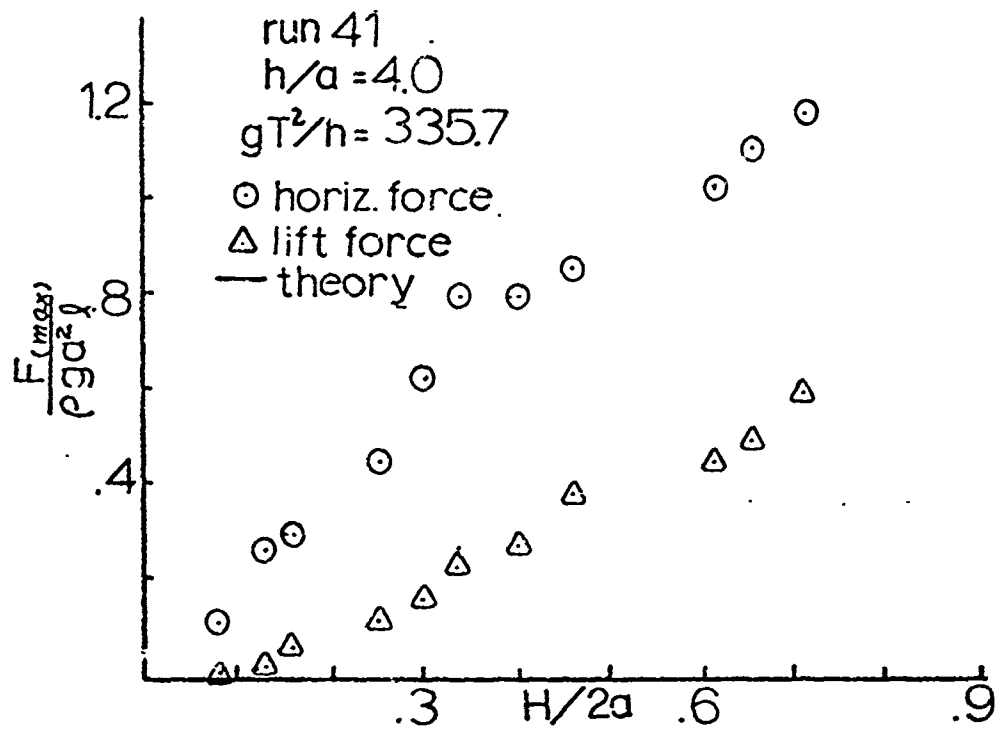
DATA FOR RUN NUMBER 94. TOTAL NUMBER OF RUNS IS 23.
 WAVE PERIOD IS 2.097SECONDS. WATER DEPTH IS 18.0INCHES.
 DIMENSIONLESS PARAMETERS ARE NON-DIMENSIONAL PERIOD(=GT**2/H) IS 94.355
 DEPTH TO RADIUS RATIO(=H/A) IS 9.0000

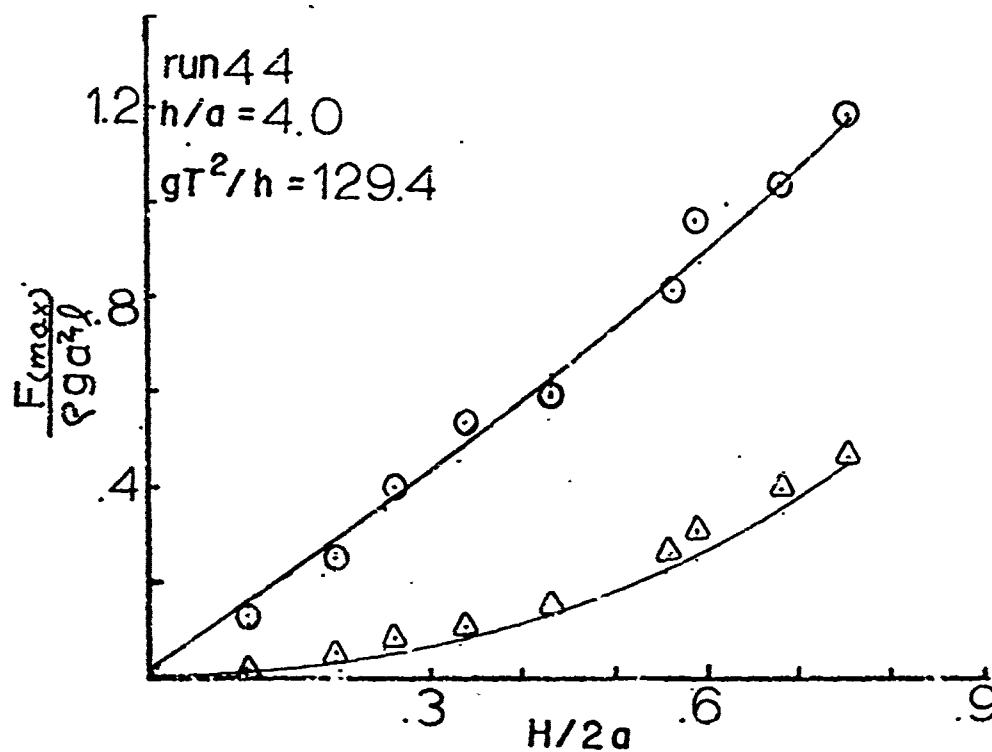
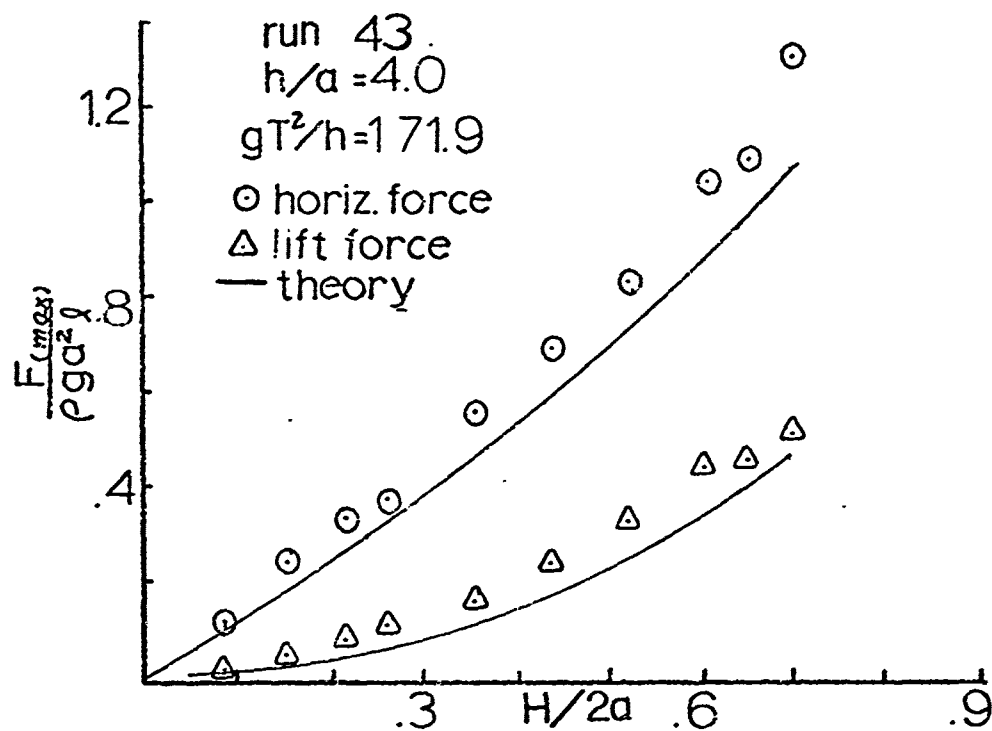
SEGMENT NUMBER	WAVE HEIGHT	FORCE (X)	FORCE (Y)	H/2A	F _x COEF (X)	F _y COEF (Y)
9401	0.38	0.16	0.04	1.5	0.08	0.02
9402	0.91	0.37	0.13	1.23	0.15	0.06
9403	1.29	0.40	0.18	1.0	0.23	0.08
9404	1.66	0.63	0.21	0.8	0.28	0.14
9405	1.91	0.63	0.24	0.7	0.29	0.19
9406	1.32	0.63	0.24	0.8	0.34	0.14
9407	1.30	0.63	0.24	0.7	0.41	0.14
9408	3.30	1.12	0.51	0.2	0.55	0.22
9409	3.60	1.12	0.53	0.2	0.55	0.27
9410	3.90	1.12	0.53	0.2	0.55	0.27
9411	3.20	1.12	0.53	0.2	0.55	0.27
9412	3.47	1.12	0.53	0.2	0.55	0.27
9413	3.50	1.12	0.53	0.2	0.55	0.27
9414	3.50	1.12	0.53	0.2	0.55	0.27
9415	3.70	1.12	0.53	0.2	0.55	0.27

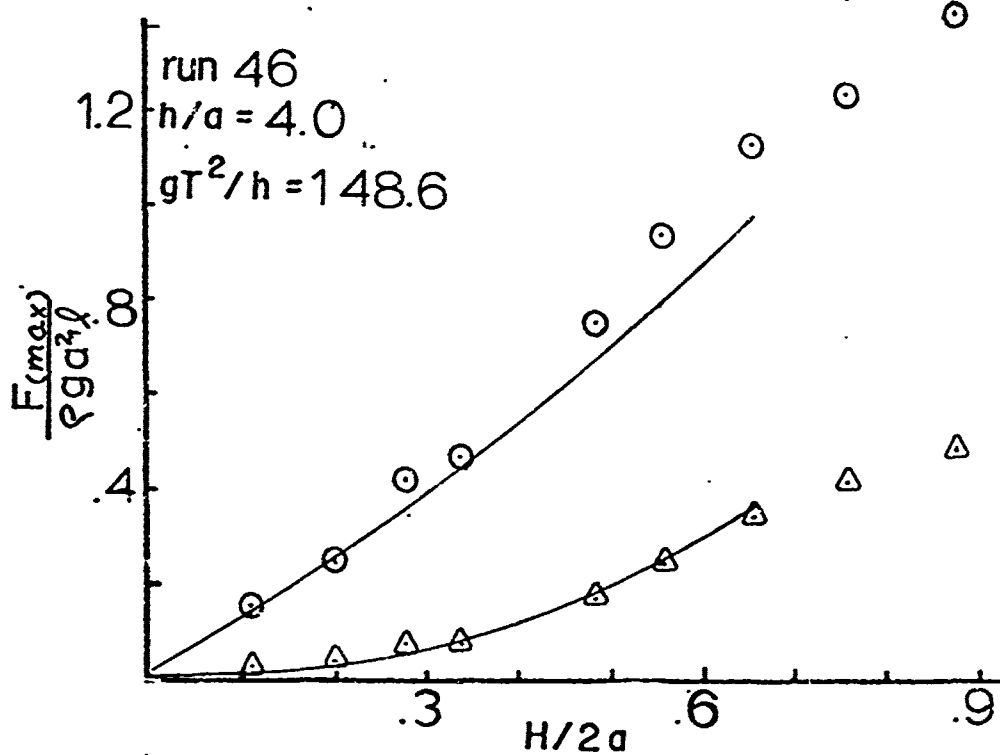
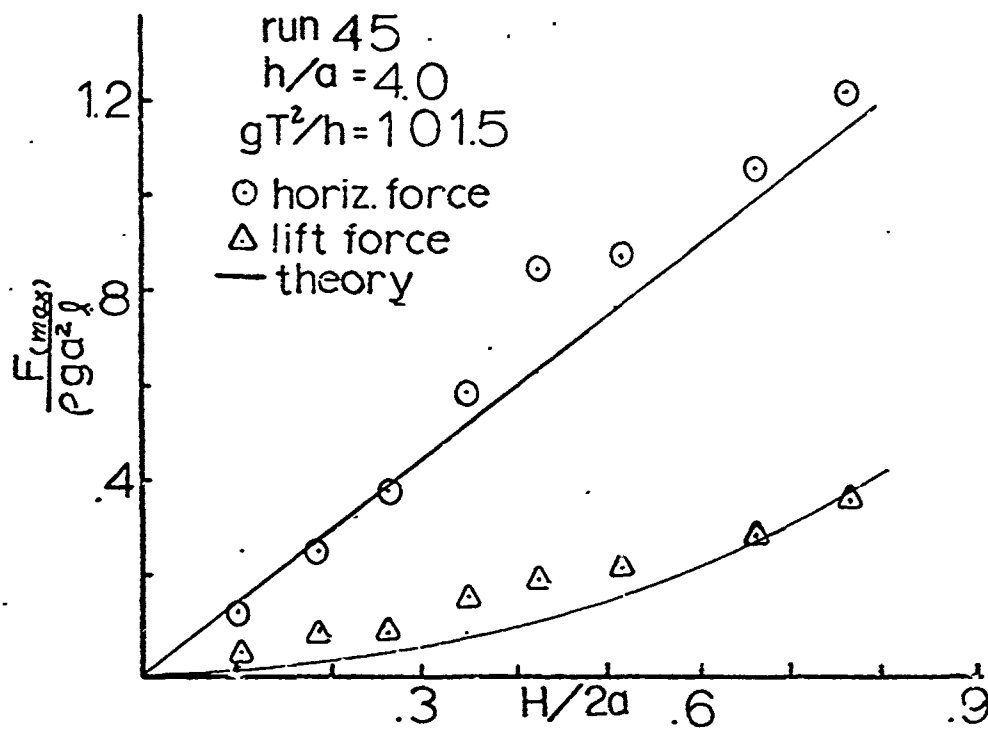
DATA FOR RUN NUMBER 95. TOTAL NUMBER OF RUNS IS 23.
 WAVE PERIOD IS 1.957SECONDS. WATER DEPTH IS 18.0 INCHES.
 DIMENSIONLESS PARAMETERS ARE NON-DIMENSIONAL PERIOD(=GT**2/H) IS 82.179
 DEPTH TO RADIUS RATIO(=H/A) IS 9.0000

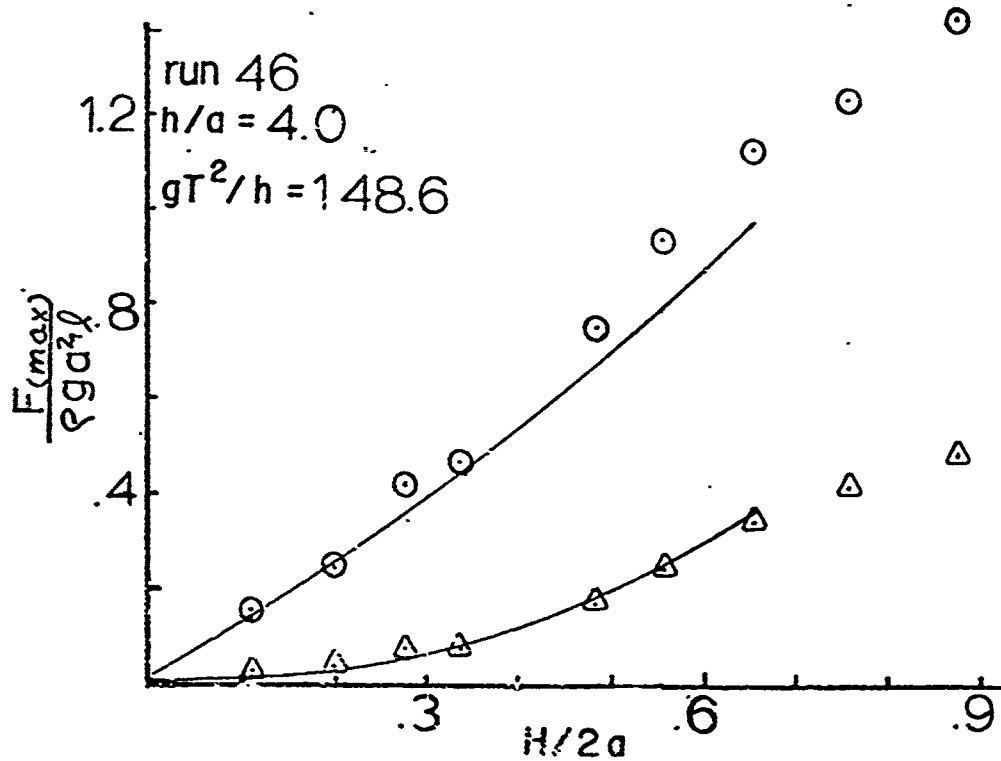
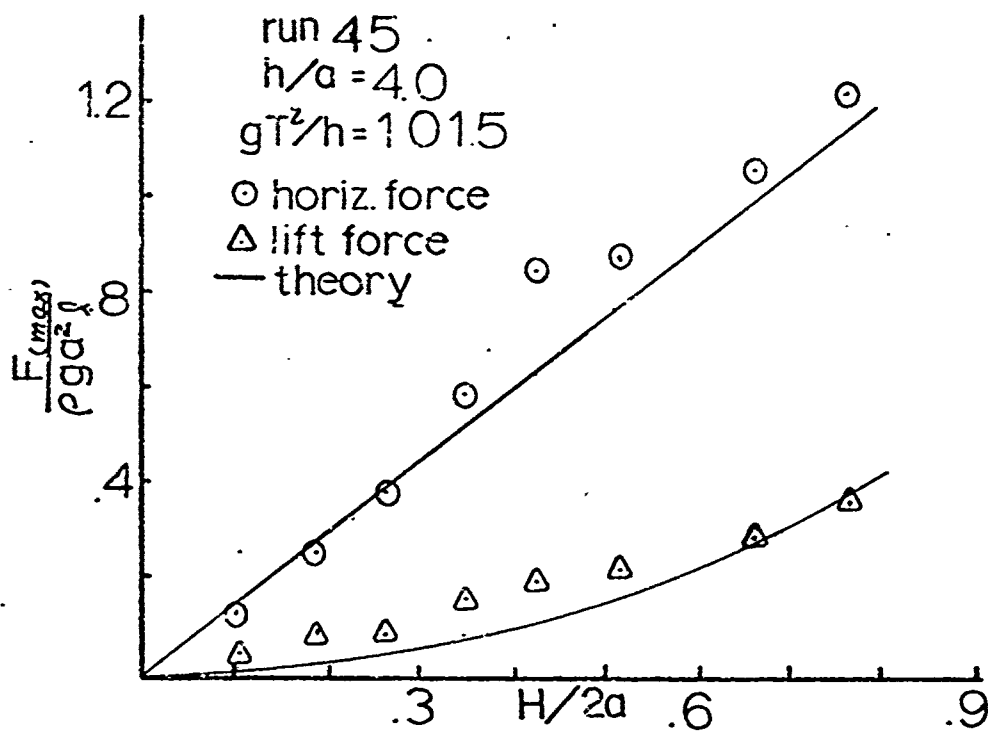
SEGMENT NUMBER	WAVE HEIGHT	FORCE (X)	FORCE (Y)	H/2A	F. COEF (X)	F. COEF (Y)
9501	0.58	0.17	0.01	0.15	0.08	0.01
9502	1.04	0.34	0.04	0.26	0.16	0.02
9503	1.45	0.47	0.09	0.36	0.22	0.04
9504	1.74	0.66	0.15	0.44	0.31	0.07
9505	1.91	0.69	0.17	0.48	0.32	0.12
9506	3.00	0.83	0.23	0.75	0.39	0.16
9507	3.40	0.93	0.35	0.85	0.46	0.18
9508	3.80	1.11	0.54	0.95	0.51	0.23
9509	4.20	1.32	0.70	1.05	0.61	0.32
9510	4.60	1.46	0.86	1.15	0.77	0.40
9511	5.00	1.66	0.93	1.34	0.98	0.43
9512	5.70	2.11	0.97	1.45	1.11	0.45
9513	6.20	2.30	1.08	1.57	1.16	0.50
9514	6.80	2.53	1.40	1.85	1.17	0.65
9515	1.40	2.53	1.73	1.85	1.17	0.80

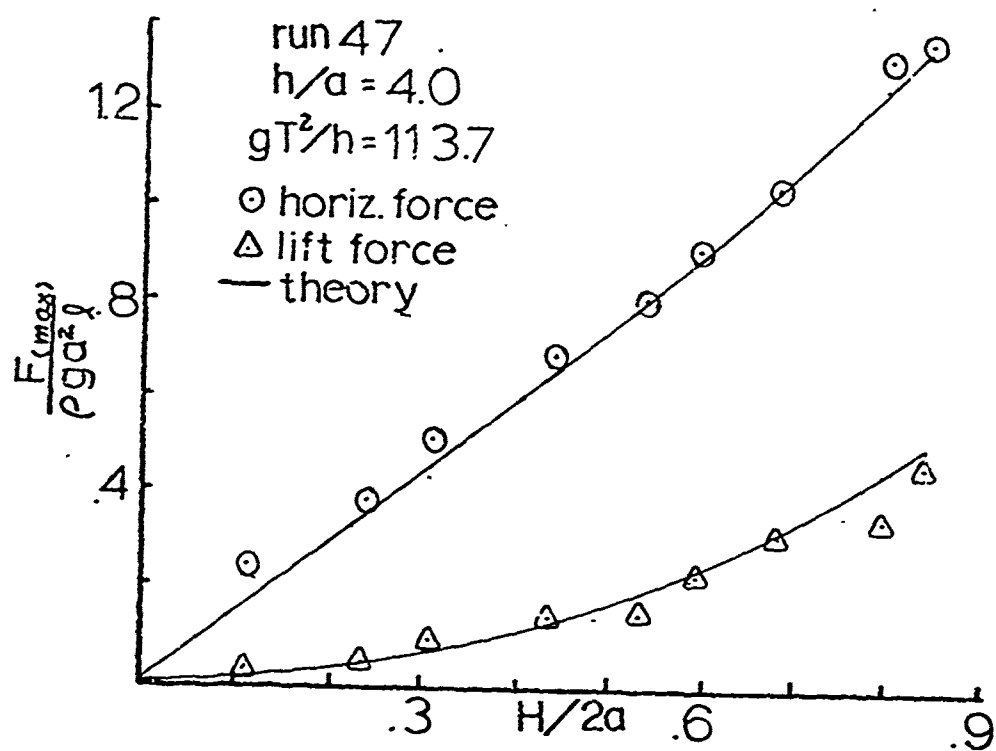
APPENDIX C. WAVE HEIGHT-FORCE PLOTS

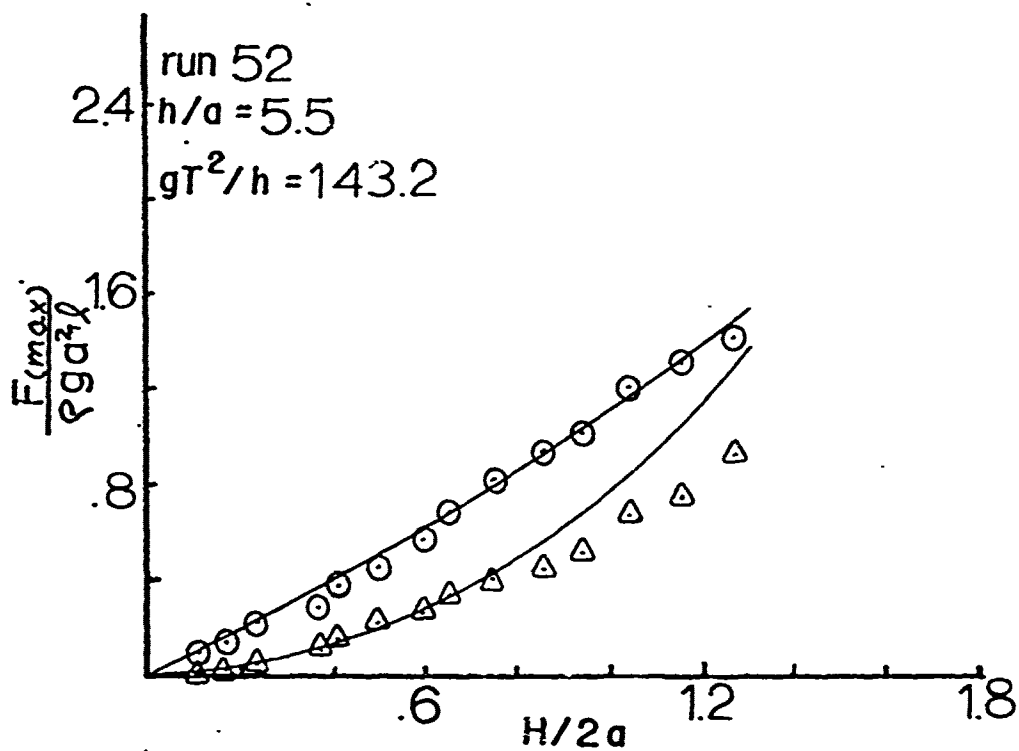
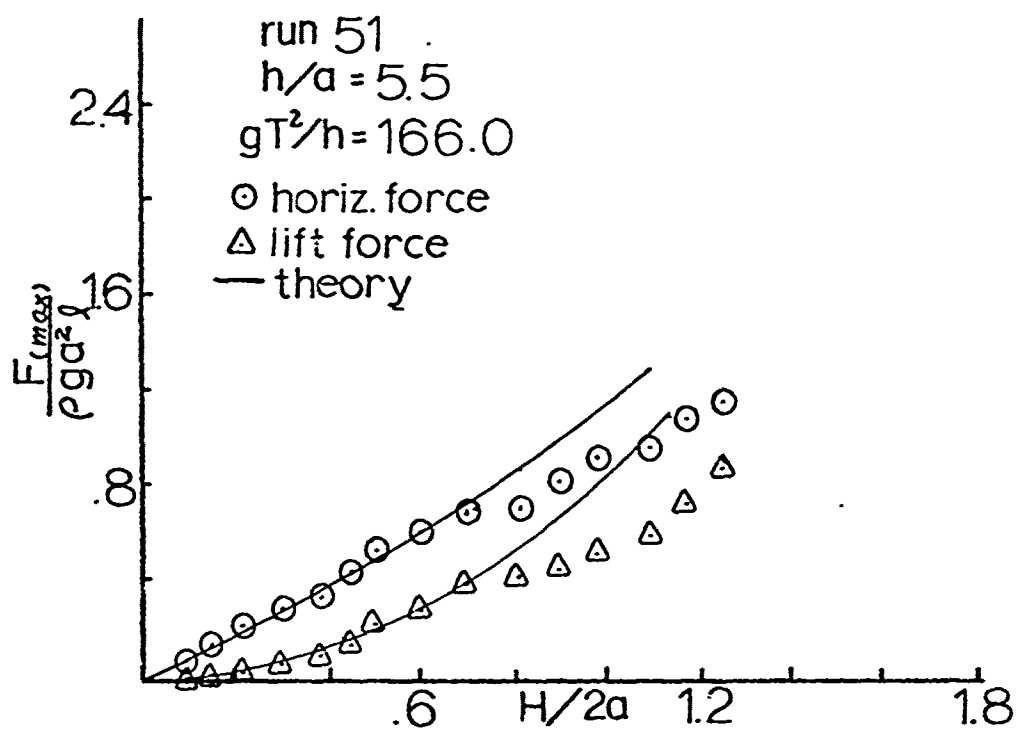


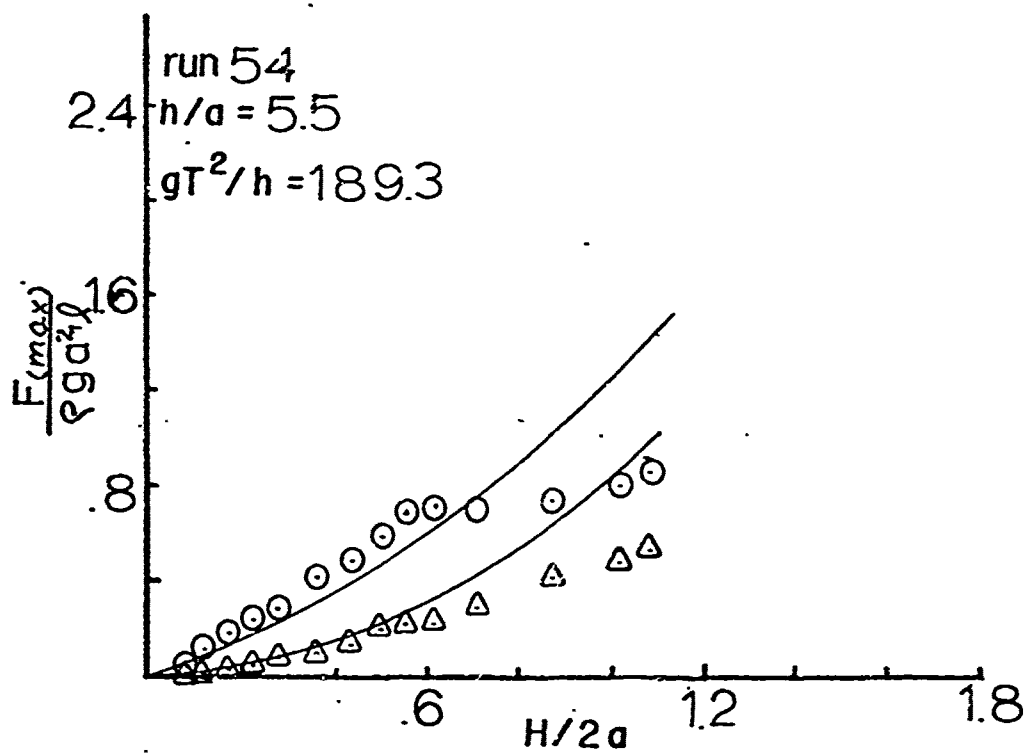
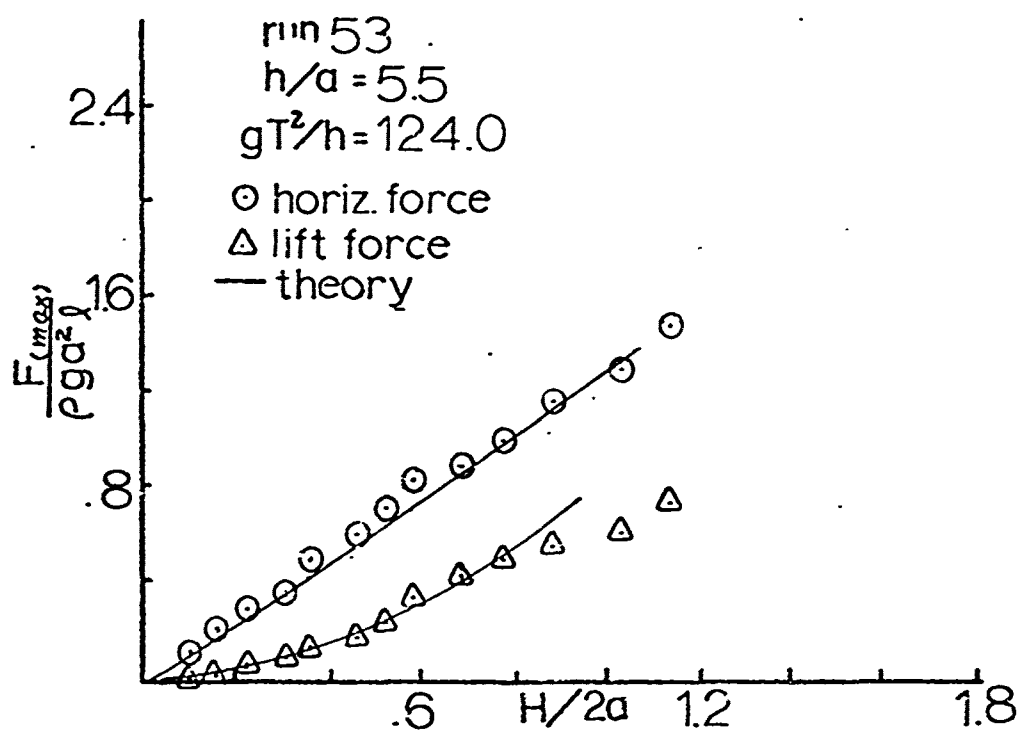


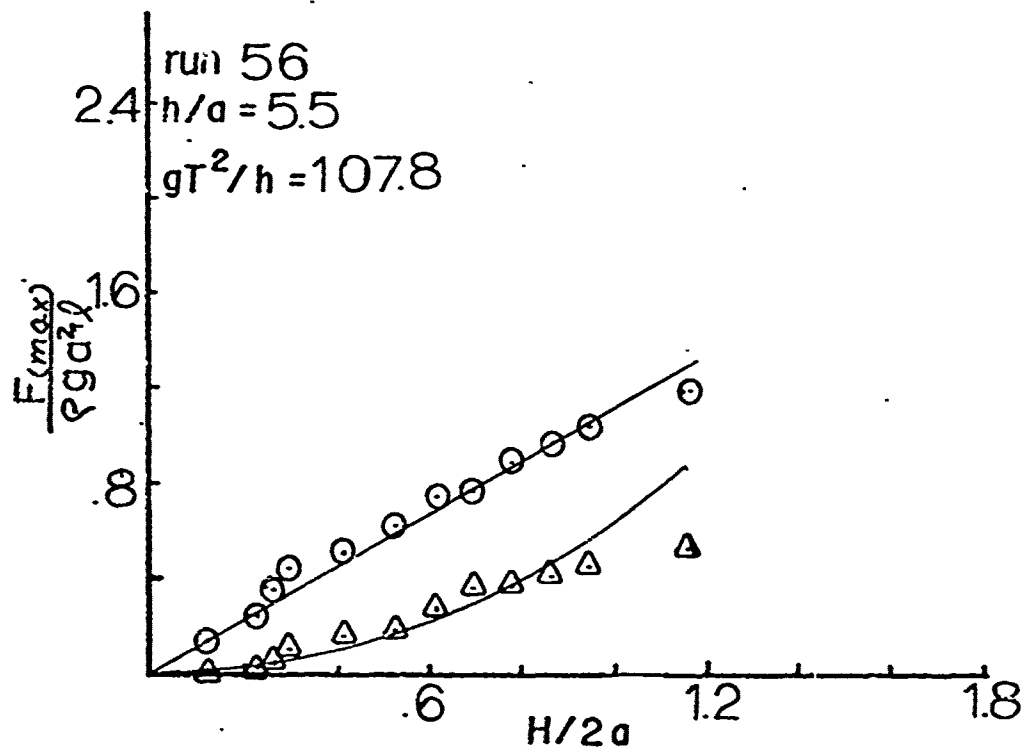
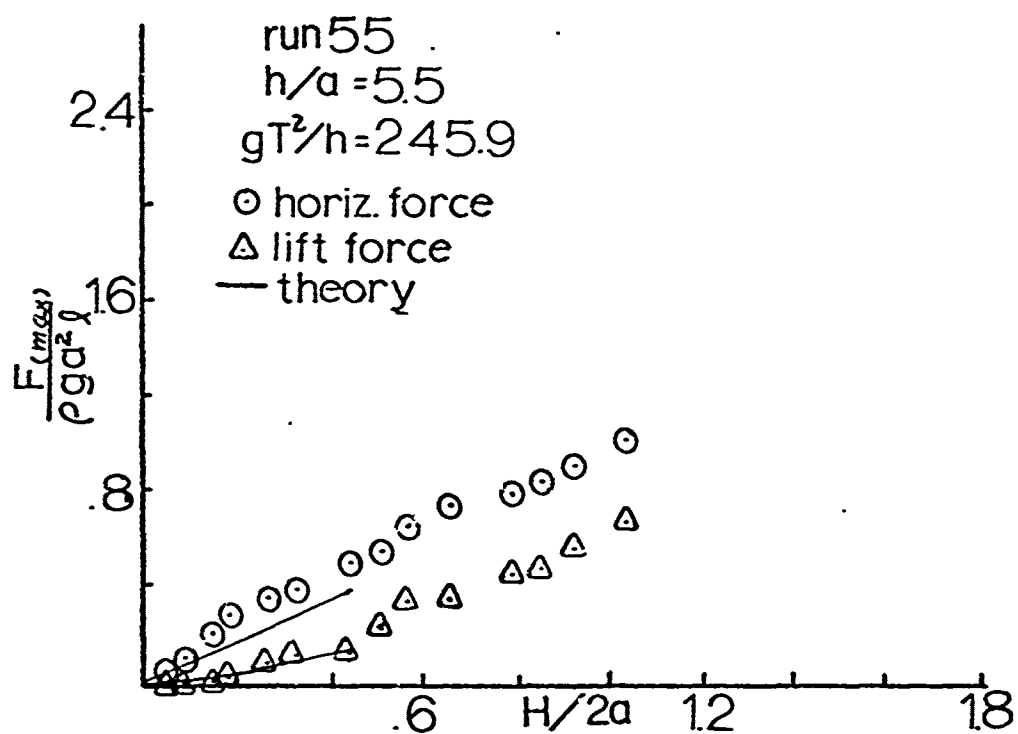


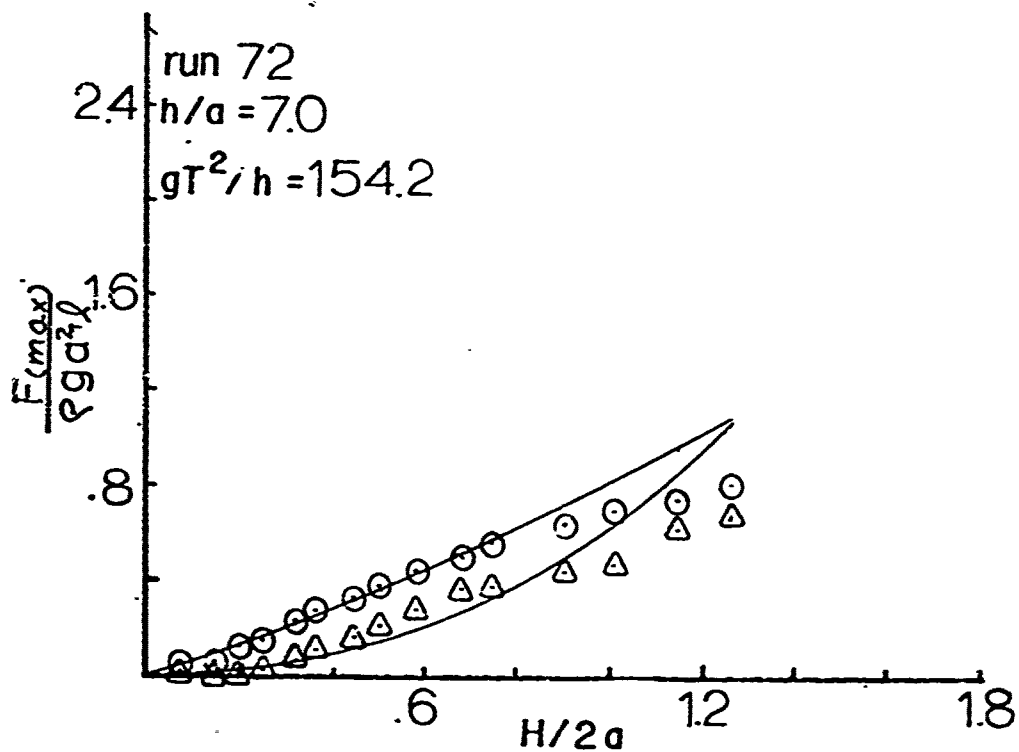
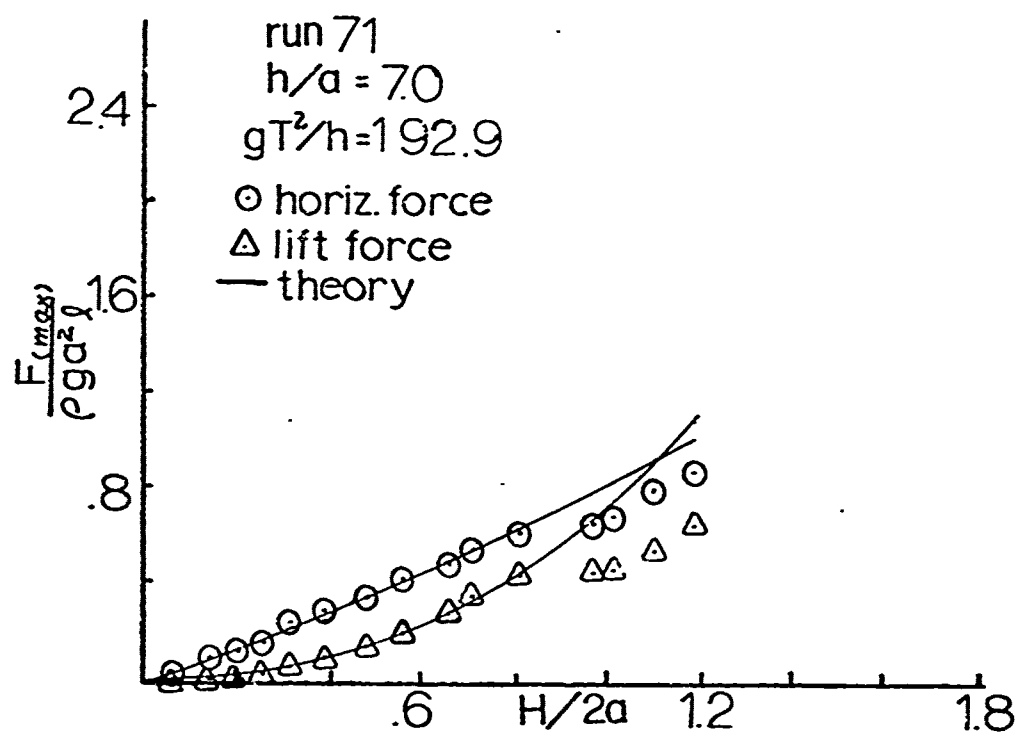


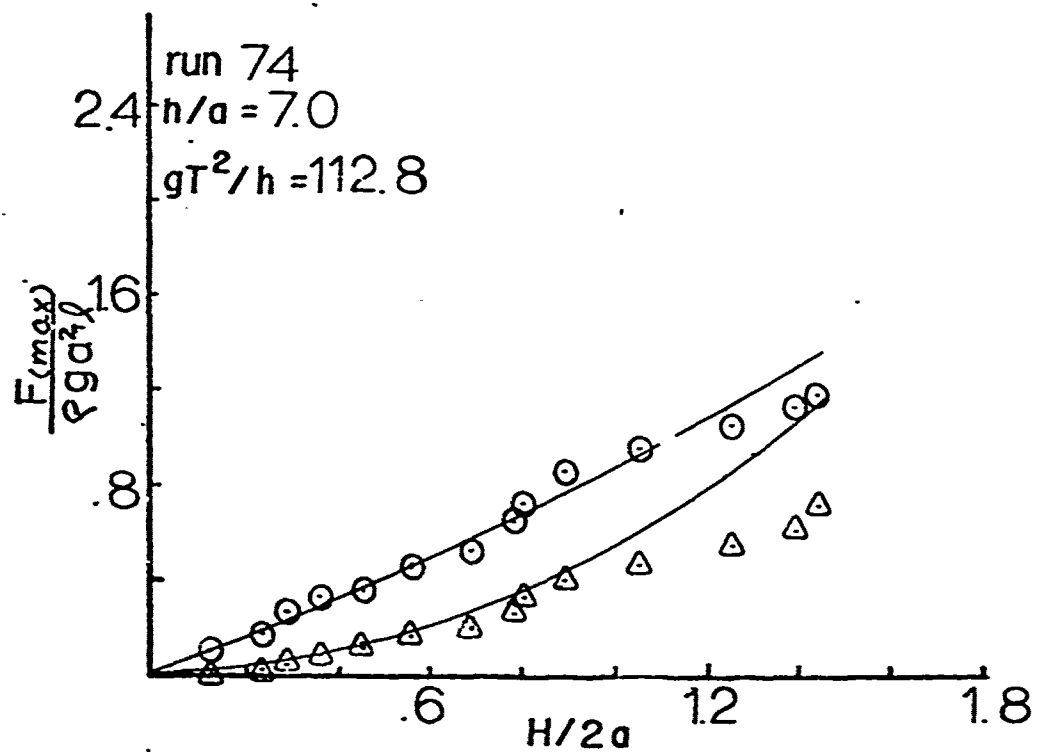
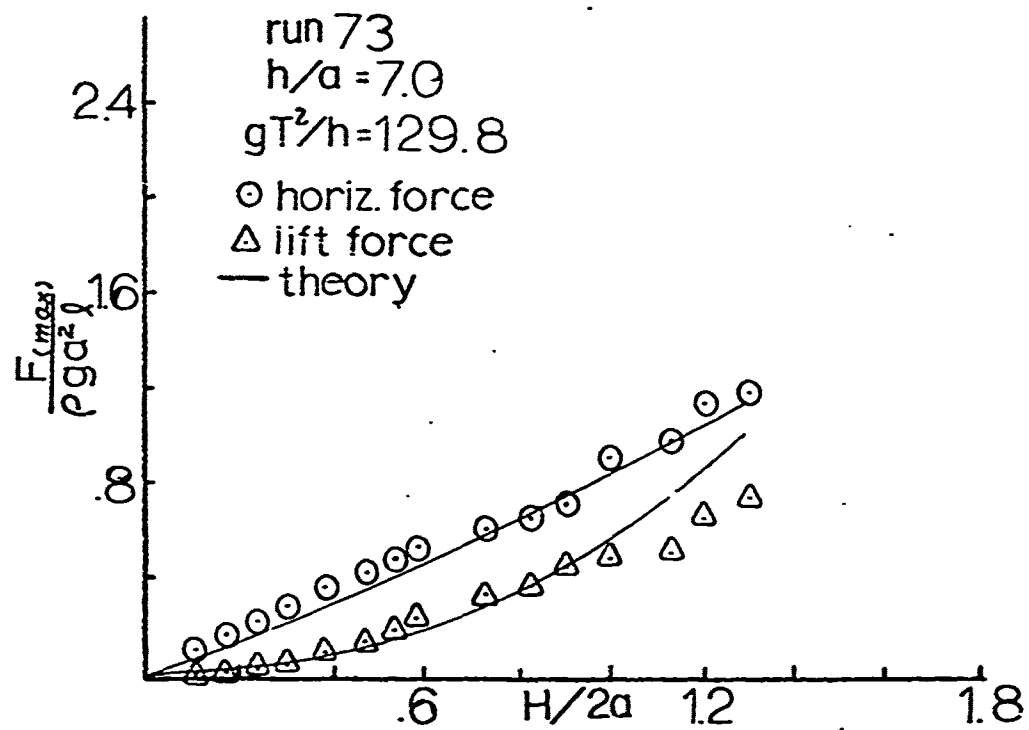


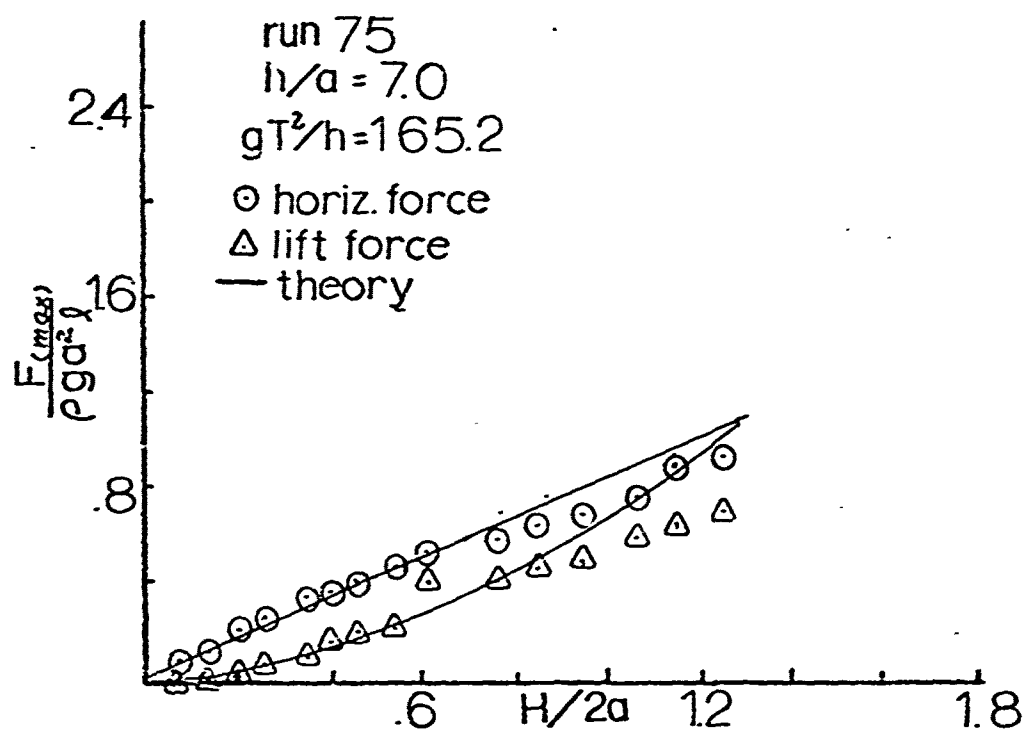


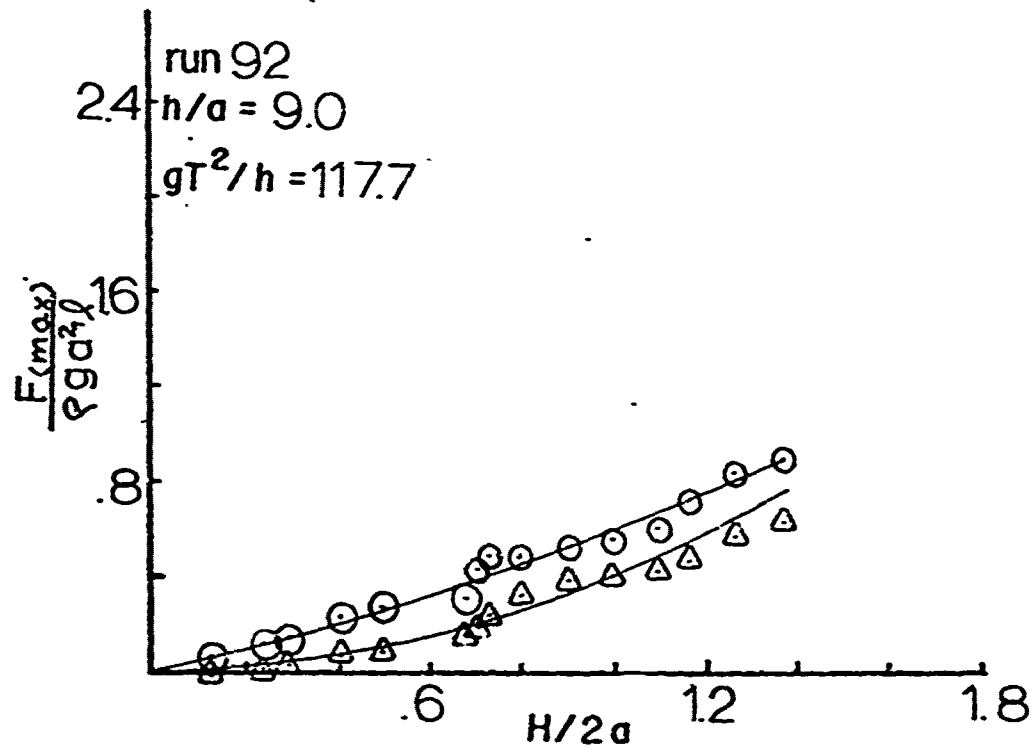
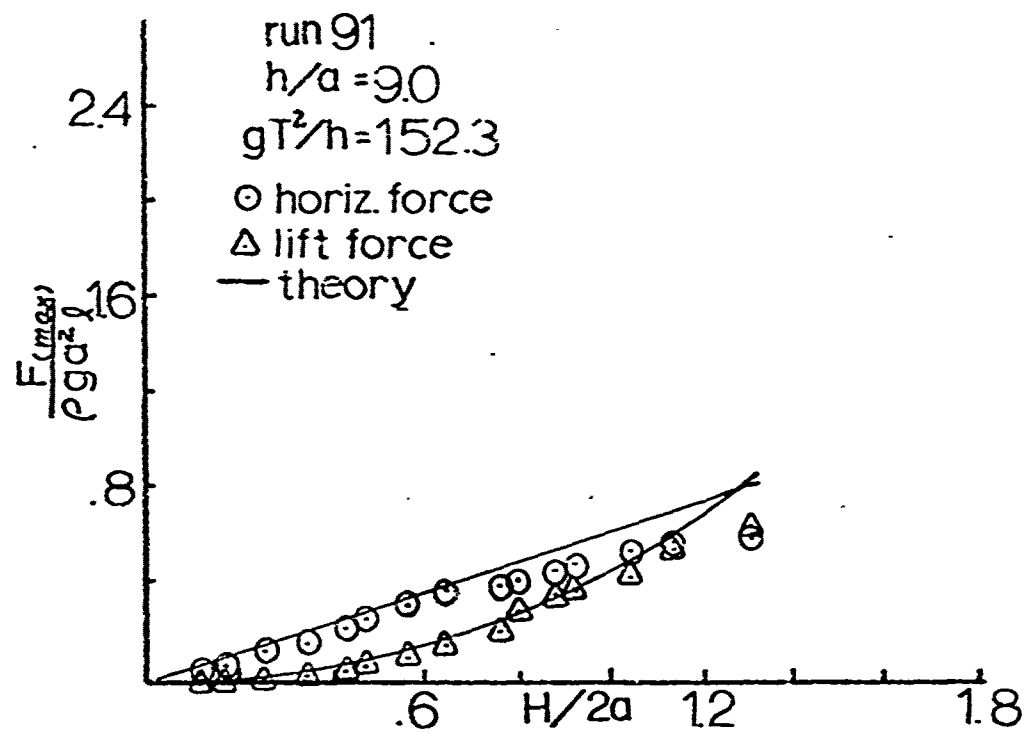


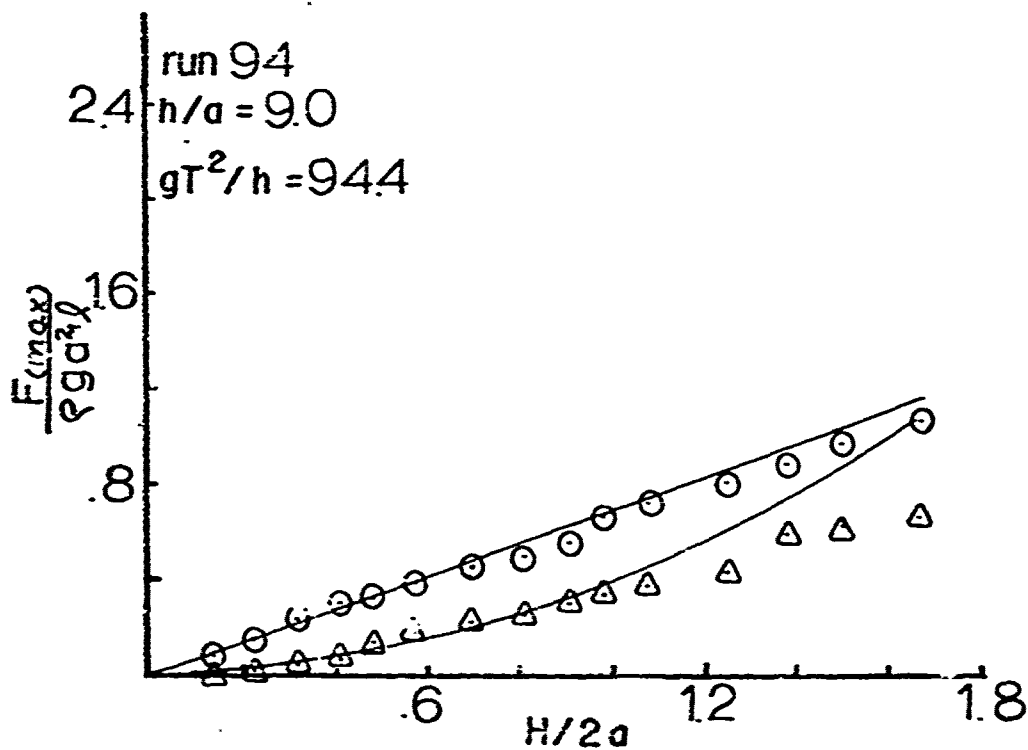
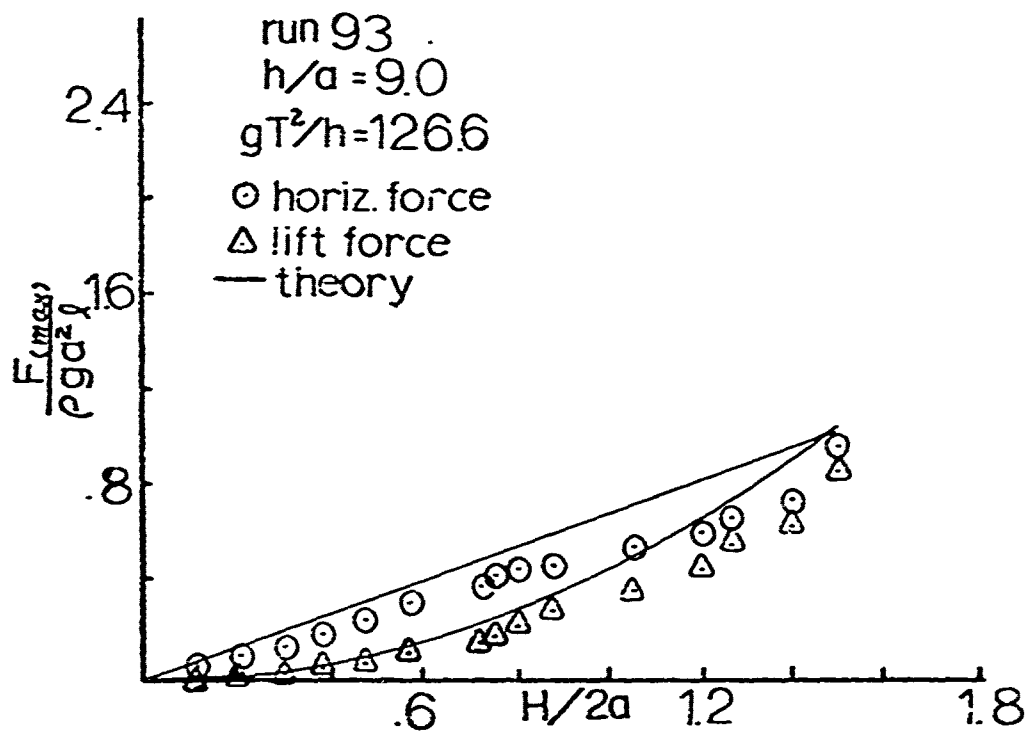


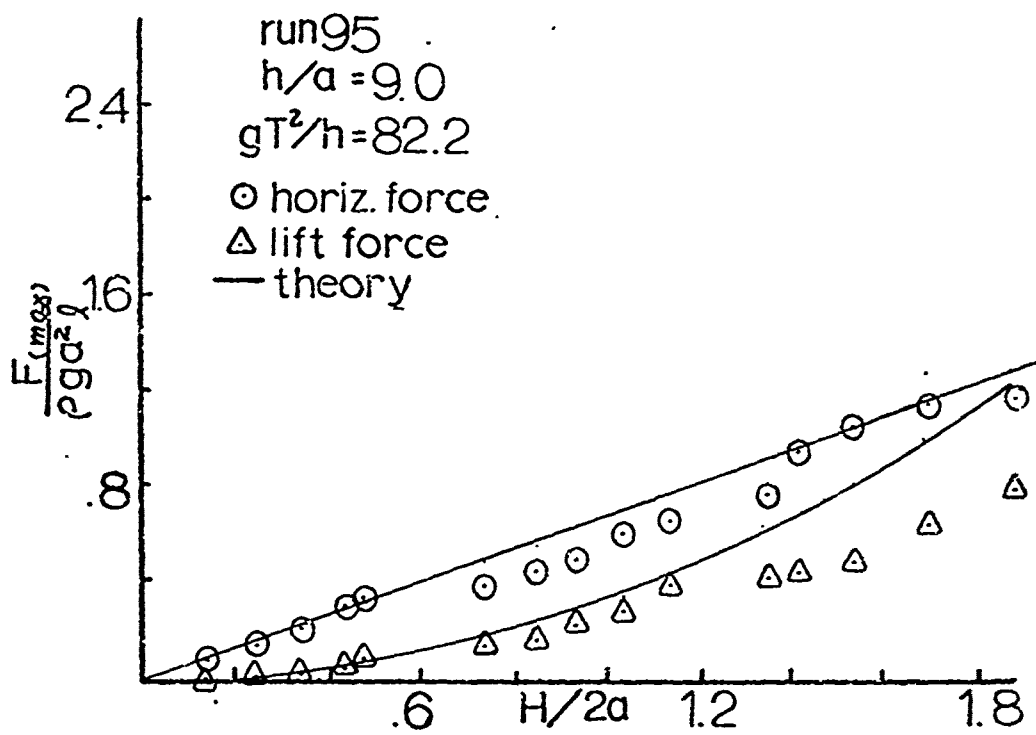












APPENDIX D
COMPUTER PROGRAM

FORCES ON A HORIZONTAL CYLINDER DUE TO NON-LINEAR WAVES

THESIS TOPIC

FRED HERMAN GEHRMAN JR.

NAVAL POSTGRADUATE SCHOOL

DECEMBER, 1972

THIS PROGRAM COMPUTES THE FORCES ON A BOTTOM-MOORED RIGHT CIRCULAR CYLINDER DUE TO WAVE MOTION USING STOKES'S FIFTH ORDER GRAVITY WAVE THEORY. THE INPUTS TO THE PROGRAM ARE

TN=NONDIMENSIONAL PERIOD PARAMETER= $G \cdot (T^2)^2 / \text{DEPTH}$
DN=DEPTH/CYLINDER RADIUS
HN=WAVEHEIGHT/CYLINDER DIAMETER

OTHER PARAMETERS OF THE PROGRAM ARE

H=WAVEHEIGHT/DEPTH

TI=TIME/PERIOD

X=HORIZONTAL DISTANCE/WAVELENGTH

D= $2 \cdot \pi \cdot \text{DEPTH} / \text{WAVELENGTH}$

BETA= $D / DN = 2 \cdot \pi \cdot \text{CYLINDER RADIUS} / \text{WAVELENGTH}$

CL=LIFT COEFFICIENT

CM=ADDED MASS COEFFICIENT

G=GRAVITATIONAL CONSTANT

```

00000010
00000020
00000030
00000040
00000050
00000060
00000070
00000080
00000090
00000100
00000110
00000120
00000130
00000140
00000150
00000160
00000170
00000180
00000190
00000200
00000210
00000220
00000230
00000240
00000250
00000260
00000270
00000280
00000290
00000300
00000310
00000320
00000330
00000340
00000350
00000360
00000370
00000380

```

```

IMPLICIT REAL*8 (A-H,L-Z)
REAL*4 DUM1,DUM2,DUM3,DUM4
DIMENSION Y(5),U(5),S(100),VEL(100),PR(100),DE(100),DUM1(100),
4DUM2(100,1),UDATA(100),FVN(100),FVN(100),DUM3(100,2),
BDUM4(100,1)
1 FORMAT(3(F20.10))
CM=2.29
CL=4.48
G=32.2
PI=3.141592653
PI2=2.0*PI
DO 9000 JJJ=1,15
C READ IN VALUES
READ (5,1) TN,HN,DN
H=2.0*HN/DN
C ADJUST TN FOR STAKES
T=TN/(PI2**2)
WRITE (6,1) TN
FORMAT (10,F16.8)
11 CALL STAKS5 (H,D,Y,U,C,CS,LO,T)
DX=D/PI2
WRITE (6,12)
FORMAT (10,6X,D,11X,Y(1),11X,Y(2),11X,Y(3),11X,Y(4),
A 11X,Y(5),11X,U(1),11X,U(2))
WRITE (6,14) DX,Y(1),Y(2),Y(3),Y(4),Y(5),U(1),U(2)
14 FORMAT (10,3X,F6.3,1P7D14.4)
WRITE (6,13)
FORMAT (10,6X,D,11X,U(3),11X,U(4),11X,U(5),11X,C,11X,
A 11X,CS,11X,H)
13 WRITE (6,14) DX,U(3),U(4),U(5),C,LO,CS,H
C COMPUTE WAVE PROFILE
BETA=D/DN
WRITE (6,298) BETA
298 FORMAT (10,F16.8)
C INITIALIZE VALUES
X=0.0
TI=0.0
C K DETERMINES THE NUMBER OF DATA POINTS

```

```

K=31
J=K-1
DO 200 I=1,K
TH1=PI2*(X+I)
C COMPUTE PHASE ANGLE
DE(I)=(180.0/PI)*TH1
C SET UP FOR PLOT
DUM1(I)=DE(I)
TH2=2.0*TH1
TH3=3.0*TH1
TH4=4.0*TH1
TH5=5.0*TH1
C COMPUTE WAVEPROFILE
PR(I)=(1.0/D)*(Y(I)*DCOS(TH1)+Y(2)*DCOS(TH2)+Y(3)*DCOS(TH3)+
AY(4)*DCOS(TH4)+Y(5)*DCOS(TH5))
C SET UP FOR PLOT
DUM2(I,1)=PR(I)
C STEP TIME
TI=TI+1.0/J
200 CONTINUE
C PLOT OF VALUES
CALL OSPLT (DUM1,DUM2,K,K,1,0,0,0,0,0,0,0)
C LABEL PLOT
WRITE (6,500)
500 FORMAT (10,20X,'WAVE PROFILE')
501 WRITE (6,501)
501 FORMAT (10,20X,'X - PHASE ANGLE, DEG; Y - NONDIMENSIONAL WAVEHEIGHT
A,Y/D')
502 WRITE (6,502) TN,DN,HN,D
502 FORMAT (10,20X,'TN,DN,HN,D')
C TABLE OF VALUES
WRITE (6,201)

```

```

00000390
00000400
00000410
00000420
00000430
00000440
00000450
00000460
00000470
00000480
00000490
00000500
00000510
00000520
00000530
00000540
00000550
00000560
00000570
00000580
00000590
00000600
00000610
00000620
00000630
00000640
00000650
00000660
00000670
00000680
00000690
00000700

```

```

00000710
00000720
00000730
00000740
00000750
00000760
00000770
00000780
00000790
00000800
00000810
00000820
00000830
00000840
00000850
00000860
00000870
00000880
00000890
00000900
00000910
00000920
00000930
00000940
00000950
00000960
00000970
00000980
00000990
00001000
00001010
00001020
00001030
00001040
00001050
00001060

```

```

201 FORMAT ('1.10X, PHASE ANGLE', 10X, 'Y VALUE')
202 WRITE (6,202) (DE(I),PR(I),I=1,K)
203 FORMAT ('0.8X,IPD14.4,6X,D14.4')

C DETERMINE VELOCITY VS. DEPTH

ETA=PR(1)*D
STARGL=D+ETA
299 WRITE (6,299) ETA, F16.8)
299 FORMAT ('0.8X,ETA=1.16.8)

C REINITIALIZE X AND TI
X=0.0
TI=0.0
TH1=PI/2*(X+TI)
TH2=2.0*TH1
TH3=3.0*TH1
TH4=4.0*TH1
TH5=5.0*TH1

C J DETERMINES THE NUMBER OF DATA POINTS
J=30

C Z=NON-DIMENSIONAL DISTANCE FROM BOTTOM=S/0
Z=0.0
DO 400 I=1,100
K=I
S(I)=Z

C SET UP FOR OSPL0T
DUM2(I,1)=S(I)
ARG1=D*Z
ARG2=2.0*ARG1
ARG3=3.0*ARG1
ARG4=4.0*ARG1
ARG5=5.0*ARG1
QUIT=STARGL-ARG1
IF(QUIT-0.0) 401,300,300

C COMPUTE VELOCITY
300 VEL(I)=C*(U(1)*DCOSH(ARG1)*DCOSH(TH1)+U(2)*DCOSH(ARG2)*DCOSH(TH2)+
AU(3)*DCOSH(ARG3)*DCOSH(TH3)+U(4)*DCOSH(ARG4)*DCOSH(TH4)+U(5)*
BDCOSH(ARG5)*DCOSH(TH5))

```

```

C      SET UP FOR OSPLOT
C      DUM1(I)=VEL(I)
C      STEP DEPTH
C      Z=Z+1.0/J
C      400 CONTINUE
C      PLOT OF VALUES
C      401 DUM1(K)=0.0
C      VEL(K)=0.0
C      CALL OSPLOT (DUM1,DUM2,K,K,1,0,0,0,0,0,0,0.)
C      LABEL PLOT
C      600 WRITE (6,600)
C      600 FORMAT ('0','HORIZONTAL VELOCITY DISTRIBUTION ON VERTICAL SECTION
C      A THROUGH WAVE CREST')
C      601 WRITE (6,601)
C      601 FORMAT ('0','Y - WATER DEPTH, , X - HORIZONTAL PARTICLE VELOCITY
C      A, FT/SEC.')
C      602 WRITE (6,602) TN,DN,HN,D
C      602 FORMAT ('0','TN=','1PG14.4','DN=','G14.4','HN=','G14.4','D=','G14.4')
C      TABLE OF VELOCITY VALUES
C      402 WRITE (6,402)
C      402 FORMAT ('1','10X','DISTANCE FROM BOTTOM','10X','U')
C      403 WRITE (6,403) {S(I),VEL(I),I=1,K}
C      403 FORMAT ('0','13X','1PG14.4,6X','D14.4')
C      COMPUTE FORCES ON CYLINDER
C      REINITIALIZE PARAMETERS
C      X=0.0
C      YI=0.0
C      I DETERMINES THE NUMBER OF ITERATIONS ON PHASE ANGLE
C      I=31
C      I1=I-1
C      DO 3000 I1=1}
C      RAD=((-1.0*PI))/2.0
C      DETERMINE FUNCTION ARGUMENTS

```

```

ARG1=BETA*(1.0+DSIN(RAD))
ARG2=ARG1*2.0
ARG3=ARG1*3.0
ARG4=ARG1*4.0
ARG5=ARG1*5.0
TH1=BETA*DCOS(RAD)+PI2*TI
TH2=TH1*2.0
TH3=TH1*3.0
TH4=TH1*4.0
TH5=TH1*5.0
UV=C*(U(1)*DCOSH(ARG1)*DCOS(TH1)+U(2)*DCOSH(ARG2)*DCOS(TH2)+
AU(3)*DCOSH(ARG3)*DCOS(TH3)+U(4)*DCOSH(ARG4)*DCOS(TH4)+U(5)*
BDCOSH(ARG5)*DCOS(TH5))
UVELS=UVEL*2
C      UDT= NONDIMENSIONAL X ACCELERATION
1100  UDT=(U(1)*DCOSH(ARG1)*DSIN(TH1)+U(2)*DCOSH(ARG2)*DSIN(TH2)+
AU(3)*DCOSH(ARG3)*DSIN(TH3)+U(4)*DCOSH(ARG4)*DSIN(TH4)+U(5)*
BDCOSH(ARG5)*DSIN(TH5))*5.)*DCS
C      FV=NONDIMENSIONAL INERTAIL FORCE
FV=DN*UVELS*CL
DUM3(11.1)=FV
C      FHN=NONDIMENSIONAL HORIZONTAL FORCE
FHN(11)=PI*(1.0+CM)*UDT
DUM2(11)=FHN(11)
DE(11)=180.0/PI)*TH1
DUM1(11)=DE(11)
C      K DETERMINES THE NUMBER OF POINTS ALONG THE CYLINDER
K=30
C      INITIALIZE VALUES
C      PN=NONDIMENSIONAL PRESSURE BASED ON BERNOULLI EQUATION
PN=0.0
RAD=3AD+PI/K
DO 2000 KK=1,<
C      SET UP FUNCTION ARGUMENTS
ARG1=0.7A*(1.0+DSIN(RAD))+PI/K

```

```

ARG2=2.0*ARG1
ARG3=3.0*ARG1
ARG4=4.0*ARG1
ARG5=5.0*ARG1
TH1=BETAN*DCOS(RAD)+PI2*TI+PI/K
TH2=2.0*TH1
TH3=3.0*TH1
TH4=4.0*TH1
TH5=5.0*TH1
C POTS= TIME DERIVATIVE OF POTENTIAL FUNCTION NON-DIMENSIONALIZED
POTS=CS*(U(1)*DCOSH(ARG1)*DCOS(TH1)+U(2)*DCOSH(ARG2)*DCOS(TH2)+
AU(3)*DCOSH(ARG3)*DCOS(TH3)+U(4)*DCOSH(ARG4)*DCOS(TH4)+U(5)*
BDCOSH(ARG5)*DCOS(TH5))
UVEL=NONDIMENSIONAL X VELOCITY
UVEL=C*(U(1)*DCOSH(ARG1)*DCOS(TH1)+U(2)*DCOSH(ARG2)*DCOS(TH2)+
AU(3)*DCOSH(ARG3)*DCOS(TH3)+U(4)*DCOSH(ARG4)*DCOS(TH4)+U(5)*
BDCOSH(ARG5)*DCOS(TH5))
C VVEL=NONDIMENSIONAL Y VELOCITY
VVEL=C*(U(1)*DSINH(ARG1)*DCOS(TH1)+U(2)*DSINH(ARG2)*DCOS(TH2)+U(3)*
A*DSINH(ARG3)*DCOS(TH3)+U(4)*DSINH(ARG4)*DCOS(TH4)+U(5)*DSINH(ARG5)
B*DSINH(ARG5))
UVELS=UVEL**2
VVELS=VVEL**2
PN=PN-(0.5*(UVELS+VVELS)+POTS)*DSIN(RAD)*DN*PI2/K
C ITERATE AROUND CYLINDER SURFACE
RAD=RAD+PI2/K
2000 CONTINUE
DUM3(I,2)=PN
C COMPUTE TOTAL VERTICAL FORCE
FVN(1)=FY+PN
DUM4(1)=FVN(1)
C ITERATE THROUGH 360 DEGREES
TI=TI+.0111
3000 CONTINUE
CALL OSPLDT (DUM1,DUM2,1,1,1,0,0,0,0,0,0,0)
WRITE (9,3004)
3004 FORMAT (10,' HORIZONTAL FORCE VS. PHASE ANGLE')

```



```

3005 WRITE (6,3005) X,FHN,IX,PHASE ANGLE')
3006 FORMAT (6,3006) (FHN(11),DE(11),11=1,1)
3007 FORMAT (6,3007) X,IPG,4.6,13X,014.6)
3008 WRITE (6,3008) TABLE OF VALUES FOR FV AND PN VS. PHASE ANGLE')
3009 FORMAT (6,3009) X,IX,LIFT COMPONENT',10X,INERTIA COMPONENT',10X,PHASE ANGLE')
3010 WRITE (6,3010) (DUM3(11,1),DUM2(11,2),DE(11),11=1,1)
3011 CALL OSPLDT (DUM1,DUM4,1,1,1,0,0,0,0,0,0,0)
3012 WRITE (6,3012) TOTAL VERTICAL FORCE VS. PHASE ANGLE')
3013 FORMAT (6,3013) X,FVN,IX,PHASE ANGLE')
3014 WRITE (6,3014) (FVN(11),DE(11),11=1,1)
3015 FORMAT (6,3015) X,IPG,4.6,13X,014.6)
3016 STOP
3017 END

```

99

```

C SUBROUTINE STAKS5
C
C SUBROUTINE STAKS5 (H,D,Y,U,C,CS,LO,T)
C DETERMINES COEFFICIENTS FOR FIFTH ORDER STOKES GRAVITY HAVE
C INPUTS ARE: H/D(=H) AND T=G*M**2/D
C
C IMPLICIT REAL*8 (A-H,I-Z)
C DIMENSION Y(3,1),U(5,1)
C P1=3.141592653
C P2=2.0*pi
C
C ITERATE FOR D AND A
C DO 2 J=1,100
C D=(1.0)/T
C
C NEWTON RAPHSOON ITERATION ON D
C RT=(1.0/T)-D*DTANH(D)
C RTA=0.485*(RT)
C HY=-1.0*(DTANH(D)+D/(DCOSH(D)**2))

```

```

C      TEST FOR CONVERGENCE
C      IF (RTA-0.01) 3,1,1
C      CORRECTION
C      1 D=0.1*(RT/HT)
C      2 CONTINUE
C      VERIFY CONVERGENCE
C      WRITE (6,4) RTA
C      3 FORMAT (10.1)
C      4 WRITE (6,5) D
C      5 FORMAT (10.1)
C      COMPUTE COEFFICIENTS
C      DO 40 J=1,500
C      SET UP EQUATION ARGUMENTS
C      1 D=0.1*(RT/HT)
C      2 D=0.1*(RT/HT)
C      3 D=0.1*(RT/HT)
C      4 D=0.1*(RT/HT)
C      5 D=0.1*(RT/HT)
C      6 D=0.1*(RT/HT)
C      7 D=0.1*(RT/HT)
C      8 D=0.1*(RT/HT)
C      9 D=0.1*(RT/HT)
C      10 D=0.1*(RT/HT)
C      11 D=0.1*(RT/HT)
C      12 D=0.1*(RT/HT)
C      13 D=0.1*(RT/HT)
C      14 D=0.1*(RT/HT)
C      15 D=0.1*(RT/HT)
C      16 D=0.1*(RT/HT)
C      17 D=0.1*(RT/HT)
C      18 D=0.1*(RT/HT)
C      19 D=0.1*(RT/HT)
C      20 D=0.1*(RT/HT)
C      21 D=0.1*(RT/HT)
C      22 D=0.1*(RT/HT)
C      23 D=0.1*(RT/HT)
C      24 D=0.1*(RT/HT)
C      25 D=0.1*(RT/HT)
C      26 D=0.1*(RT/HT)
C      27 D=0.1*(RT/HT)
C      28 D=0.1*(RT/HT)
C      29 D=0.1*(RT/HT)
C      30 D=0.1*(RT/HT)
C      31 D=0.1*(RT/HT)
C      32 D=0.1*(RT/HT)
C      33 D=0.1*(RT/HT)
C      34 D=0.1*(RT/HT)
C      35 D=0.1*(RT/HT)
C      36 D=0.1*(RT/HT)
C      37 D=0.1*(RT/HT)
C      38 D=0.1*(RT/HT)
C      39 D=0.1*(RT/HT)
C      40 D=0.1*(RT/HT)
C      41 D=0.1*(RT/HT)
C      42 D=0.1*(RT/HT)
C      43 D=0.1*(RT/HT)
C      44 D=0.1*(RT/HT)
C      45 D=0.1*(RT/HT)
C      46 D=0.1*(RT/HT)
C      47 D=0.1*(RT/HT)
C      48 D=0.1*(RT/HT)
C      49 D=0.1*(RT/HT)
C      50 D=0.1*(RT/HT)
C      51 D=0.1*(RT/HT)
C      52 D=0.1*(RT/HT)
C      53 D=0.1*(RT/HT)
C      54 D=0.1*(RT/HT)
C      55 D=0.1*(RT/HT)
C      56 D=0.1*(RT/HT)
C      57 D=0.1*(RT/HT)
C      58 D=0.1*(RT/HT)
C      59 D=0.1*(RT/HT)
C      60 D=0.1*(RT/HT)
C      61 D=0.1*(RT/HT)
C      62 D=0.1*(RT/HT)
C      63 D=0.1*(RT/HT)
C      64 D=0.1*(RT/HT)
C      65 D=0.1*(RT/HT)
C      66 D=0.1*(RT/HT)
C      67 D=0.1*(RT/HT)
C      68 D=0.1*(RT/HT)
C      69 D=0.1*(RT/HT)
C      70 D=0.1*(RT/HT)
C      71 D=0.1*(RT/HT)
C      72 D=0.1*(RT/HT)
C      73 D=0.1*(RT/HT)
C      74 D=0.1*(RT/HT)
C      75 D=0.1*(RT/HT)
C      76 D=0.1*(RT/HT)
C      77 D=0.1*(RT/HT)
C      78 D=0.1*(RT/HT)
C      79 D=0.1*(RT/HT)
C      80 D=0.1*(RT/HT)
C      81 D=0.1*(RT/HT)
C      82 D=0.1*(RT/HT)
C      83 D=0.1*(RT/HT)
C      84 D=0.1*(RT/HT)
C      85 D=0.1*(RT/HT)
C      86 D=0.1*(RT/HT)
C      87 D=0.1*(RT/HT)
C      88 D=0.1*(RT/HT)
C      89 D=0.1*(RT/HT)
C      90 D=0.1*(RT/HT)
C      91 D=0.1*(RT/HT)
C      92 D=0.1*(RT/HT)
C      93 D=0.1*(RT/HT)
C      94 D=0.1*(RT/HT)
C      95 D=0.1*(RT/HT)
C      96 D=0.1*(RT/HT)
C      97 D=0.1*(RT/HT)
C      98 D=0.1*(RT/HT)
C      99 D=0.1*(RT/HT)
C      100 D=0.1*(RT/HT)
C      101 D=0.1*(RT/HT)
C      102 D=0.1*(RT/HT)
C      103 D=0.1*(RT/HT)
C      104 D=0.1*(RT/HT)
C      105 D=0.1*(RT/HT)
C      106 D=0.1*(RT/HT)
C      107 D=0.1*(RT/HT)
C      108 D=0.1*(RT/HT)
C      109 D=0.1*(RT/HT)
C      110 D=0.1*(RT/HT)
C      111 D=0.1*(RT/HT)
C      112 D=0.1*(RT/HT)
C      113 D=0.1*(RT/HT)
C      114 D=0.1*(RT/HT)
C      115 D=0.1*(RT/HT)
C      116 D=0.1*(RT/HT)
C      117 D=0.1*(RT/HT)
C      118 D=0.1*(RT/HT)
C      119 D=0.1*(RT/HT)
C      120 D=0.1*(RT/HT)
C      121 D=0.1*(RT/HT)
C      122 D=0.1*(RT/HT)
C      123 D=0.1*(RT/HT)
C      124 D=0.1*(RT/HT)
C      125 D=0.1*(RT/HT)
C      126 D=0.1*(RT/HT)
C      127 D=0.1*(RT/HT)
C      128 D=0.1*(RT/HT)
C      129 D=0.1*(RT/HT)
C      130 D=0.1*(RT/HT)
C      131 D=0.1*(RT/HT)
C      132 D=0.1*(RT/HT)
C      133 D=0.1*(RT/HT)
C      134 D=0.1*(RT/HT)
C      135 D=0.1*(RT/HT)
C      136 D=0.1*(RT/HT)
C      137 D=0.1*(RT/HT)
C      138 D=0.1*(RT/HT)
C      139 D=0.1*(RT/HT)
C      140 D=0.1*(RT/HT)
C      141 D=0.1*(RT/HT)
C      142 D=0.1*(RT/HT)
C      143 D=0.1*(RT/HT)
C      144 D=0.1*(RT/HT)
C      145 D=0.1*(RT/HT)
C      146 D=0.1*(RT/HT)
C      147 D=0.1*(RT/HT)
C      148 D=0.1*(RT/HT)
C      149 D=0.1*(RT/HT)
C      150 D=0.1*(RT/HT)
C      151 D=0.1*(RT/HT)
C      152 D=0.1*(RT/HT)
C      153 D=0.1*(RT/HT)
C      154 D=0.1*(RT/HT)
C      155 D=0.1*(RT/HT)
C      156 D=0.1*(RT/HT)
C      157 D=0.1*(RT/HT)
C      158 D=0.1*(RT/HT)
C      159 D=0.1*(RT/HT)
C      160 D=0.1*(RT/HT)
C      161 D=0.1*(RT/HT)
C      162 D=0.1*(RT/HT)
C      163 D=0.1*(RT/HT)
C      164 D=0.1*(RT/HT)
C      165 D=0.1*(RT/HT)
C      166 D=0.1*(RT/HT)
C      167 D=0.1*(RT/HT)
C      168 D=0.1*(RT/HT)
C      169 D=0.1*(RT/HT)
C      170 D=0.1*(RT/HT)
C      171 D=0.1*(RT/HT)
C      172 D=0.1*(RT/HT)
C      173 D=0.1*(RT/HT)
C      174 D=0.1*(RT/HT)
C      175 D=0.1*(RT/HT)
C      176 D=0.1*(RT/HT)
C      177 D=0.1*(RT/HT)
C      178 D=0.1*(RT/HT)
C      179 D=0.1*(RT/HT)
C      180 D=0.1*(RT/HT)
C      181 D=0.1*(RT/HT)
C      182 D=0.1*(RT/HT)
C      183 D=0.1*(RT/HT)
C      184 D=0.1*(RT/HT)
C      185 D=0.1*(RT/HT)
C      186 D=0.1*(RT/HT)
C      187 D=0.1*(RT/HT)
C      188 D=0.1*(RT/HT)
C      189 D=0.1*(RT/HT)
C      190 D=0.1*(RT/HT)
C      191 D=0.1*(RT/HT)
C      192 D=0.1*(RT/HT)
C      193 D=0.1*(RT/HT)
C      194 D=0.1*(RT/HT)
C      195 D=0.1*(RT/HT)
C      196 D=0.1*(RT/HT)
C      197 D=0.1*(RT/HT)
C      198 D=0.1*(RT/HT)
C      199 D=0.1*(RT/HT)
C      200 D=0.1*(RT/HT)
C      201 D=0.1*(RT/HT)
C      202 D=0.1*(RT/HT)
C      203 D=0.1*(RT/HT)
C      204 D=0.1*(RT/HT)
C      205 D=0.1*(RT/HT)
C      206 D=0.1*(RT/HT)
C      207 D=0.1*(RT/HT)
C      208 D=0.1*(RT/HT)
C      209 D=0.1*(RT/HT)
C      210 D=0.1*(RT/HT)
C      211 D=0.1*(RT/HT)
C      212 D=0.1*(RT/HT)
C      213 D=0.1*(RT/HT)
C      214 D=0.1*(RT/HT)
C      215 D=0.1*(RT/HT)
C      216 D=0.1*(RT/HT)
C      217 D=0.1*(RT/HT)
C      218 D=0.1*(RT/HT)
C      219 D=0.1*(RT/HT)
C      220 D=0.1*(RT/HT)
C      221 D=0.1*(RT/HT)
C      222 D=0.1*(RT/HT)
C      223 D=0.1*(RT/HT)
C      224 D=0.1*(RT/HT)
C      225 D=0.1*(RT/HT)
C      226 D=0.1*(RT/HT)
C      227 D=0.1*(RT/HT)
C      228 D=0.1*(RT/HT)
C      229 D=0.1*(RT/HT)
C      230 D=0.1*(RT/HT)
C      231 D=0.1*(RT/HT)
C      232 D=0.1*(RT/HT)
C      233 D=0.1*(RT/HT)
C      234 D=0.1*(RT/HT)
C      235 D=0.1*(RT/HT)
C      236 D=0.1*(RT/HT)
C      237 D=0.1*(RT/HT)
C      238 D=0.1*(RT/HT)
C      239 D=0.1
```

```

855=(182000.0*CO16-282729.0*CO14+83689.0*CO12+225.01712288.0*SO10-7280.0*CO2
2*CO8+7160.0*CO6-11800.0*CO4-11800.0*CO2+3.01718.0*SO4}
C1=0.0*CO4-8.0*CO2+9.01718.0*SO4}
C2=0.0*CO4-8.0*CO2+9.01718.0*SO4}
1*CO2+147.01718.0*SO10*(6.0*CO2-1.0)}
00002910
00002920
00002930
00002940
00002950
00002960
00002970
00002980
00002990
00003000
00003010
00003020
00003030
00003040
00003050
00003060
00003070
00003080
00003090
00003100
00003110
00003120
00003130
00003140
00003150
00003160
00003170

```

C COMPUTE A

A=H*D/(2.0)

DO 50 K=1,500

C NEWTON RAPSON ITERATION ON A

RA=H*(-2.0*(A+(A**3)*B33+(A**5)*(B35+B55)))/D

R=DABS(RA)

HP=(-2.0/D)*(1.0+3.0*(A**2)*B33+5.0*(A**4)*(B35+B55))

C TEST FOR CONVERGENCE

IF(R-0.001) 53,49.49

C CORRECTION

49 A=A-(RA/HP)

50 CONTINUE

C VERIFY CONVERGENCE

WRITE (4,51) 3A

51 FORMAT (10F10.4, 'A DID NOT CONVERGE IN 100 ITERATIONS, ABSOLUTE ERROR

53 A1S=F16.4

53 CO=D*TANH(D)

A2=A**2

A4=A**4

C ITERATE FOR PERIOD

TE=1.0/(D*CO*(1.0+A2*CO1+A4*CO2))

ER=TE-T

ERA=DABS(ER)

ERA=DABS(ER/T)

C TEST FOR CONVERGENCE

IF (ERA-0.010) 65,59.59

C CORRECTION

```

59 D=D10.100*ER
60 CONTINUE
61 WRITE (6,61) ER
C
62 VERIFY CONVERGENCE
63 FORMAT (10,'D DID NOT CONVERGE,ERROR IS',F16.8)
64 DX=DX/P12
65 WRITE (6,66) DX,F16.8)
66 FORMAT (10,'D',F16.8)
67 WRITE (6,67) A
68 FORMAT (10,'A',F16.8)
C
69 DETERMINE B COEFFICIENTS
70 B22=(C01*(2.0*CO2+1.0)/(4.0*SO3)
71 B24=(C01*(2.72.0*CO8-192.0*CO4+322.0*CO2+21.0)/(384.0*SO9)
72 B44=(C01*(7.60.0*CO10-448.0*CO8-48.0*CO6+48.0*CO4+106.0*CO2-21.0)/
73 1(384.0*SO9*(6.0*CO2-1.0))
C
74 DETERMINE WAVE CELERITY.C
75 CO=DTANH(D)
76 C3=(-1.0)/(4.0*SO1*CO1)
77 C4=(12.0*CO8+36.0*CO6-162.0*CO4+141.0*CO2-27.0)/(192.0*CO1*SO9)
C
78 NOW DETERMINE WAVE EQUATION COEFFICIENTS
79 A11=1.0/SO1
80 A12=(-1.0)*CO2*(5.0*CO2+1.0)/(8.0*SO3)
81 A13=(-1.0)*(1184.0*CO10-1440.0*CO8-1992.0*CO6+2641.0*CO4-249.0*CO2
82 1+18.0)/(1536.0*SO1)
83 A22=3.0/(8.0*SO4)
84 A23=(192.0*CO8-424.0*CO6-312.0*CO4+400.0*CO2-27.0)/(768.0*SO10)
85 A33=(112.0*CO12+4224.0*CO10-6800.0*CO8-12808.0*CO6+16704.0*CO4-
86 13154.0*CO2+107.0)/(4396.0*SO13*(6.0*CO2-1.0))
87 A44=(80.0*CO6-816.0*CO4+(338.0*CO2-197.0)/(1536.0*SO10*(6.0*CO2-
88 1.0))
89 A55=(-1.0)*(2880.0*CO12-72480.0*CO8+324000.0*CO6-432000.0*CO4+
90 1163470.0*CO2-16245.0)/(61440.0*SO11*(6.0*CO2-1.0)*(8.0*CO4-11.0*
91 2*CO2+3.0))
C
92 FIND VELOCITY AND WAVE PROFILE COEFFICIENTS AND WAVELENGTH
C
93 LO=WAVELENGTH

```

```

A3=A**3
A5=A**5
CS=(C0/D)*(1.0+A2*C1+A4*C2)
C=DS/CRT(CS)
Y(1,1)=A2*B22+A4*B24
Y(2,1)=A3*B33+A5*B35
Y(3,1)=A4*B44
Y(4,1)=A5*B55
Y(1,1)=A*A11+A3+A13+A5*A15
U(2,1)=2.0*(A2*A22+A4*A24)
U(3,1)=3.0*(A3*A33+A5*A35)
U(4,1)=4.0*(A4*A44)
U(5,1)=5.0*(A5*A55)
LD=TE
WRITE (6,20)

```

C PRINT OUT COEFFICIENTS

```

20 FORMAT ('0',6X,'D',11X,'B22',11X,'B24',11X,'B33',11X,'B35',11X,
A,B44,11X,'B55',11X,'A11',
6 WRITE ('6,6) DX,B22,B24,B33,B35,B44,B55,A11
6 FORMAT ('0',3X,'FS.3,IP7D14.4)
7 WRITE ('6,7)
7 FORMAT ('0',6X,'D',11X,'A13',11X,'A15',11X,'A22',11X,'A24',11X,
A,A33,11X,'A35',11X,'A44',
7 WRITE ('6,6) DX,A13,A15,A22,A24,A33,A35,A44
8 WRITE ('6,8)
8 FORMAT ('0',6X,'D',11X,'A55',11X,'C1',11X,'C2',11X,'C3',11X,'C4',
A,A11X,'S01',11X,'C01',
8 WRITE ('6,6) DX,A55,C1,C2,C3,C4,S01,C01
RETURN
END

```

```

00003540
00003550
00003560
00003570
00003580
00003590
00003600
00003610
00003620
00003630
00003640
00003650
00003660
00003670
00003680
00003690
00003700
00003710
00003720
00003730
00003740
00003750
00003760
00003770
00003780
00003790
00003800
00003810
00003820
00003830
00003840

```

LIST OF REFERENCES

1. Harleman, D.R.F. and Shapiro, W.C., Experimental and Analytical Studies of Wave Forces on Offshore Structures, Part I, MIT Hydrodynamics Lab. T.R. No. 19, May 1955.
2. Carpenter, L.H. and Keulegan, G.H. "Forces on Cylinders and Plates in an Oscillating Fluid," Journal of Research of the National Bureau of Standards, J. 60, p. 423-444, May 1958.
3. Morrison, J.R., Johnson, J.W. and O'Brien, M.P., "Experimental Studies of Forces on Piles," Proc. Fourth Conf. Coastal Council on Wave Research, Berkeley, California, p. 345-370, 1954.
4. Sarpkaya, T. and Garrison, C. J., "Vortex Formation and Resistance in Unsteady Flow," Transactions of the ASME, pp. 16-23, March, 1963.
5. Dalton, C. and Helfenstein, R.A., Potential Flow Past a Group of Circular Cylinders.
6. Johnson, R.E., "Regression Model of Wave Forces on Ocean Outfalls," Journal of the Waterways and Harbors Division Proceedings of the ASCE, V-96, No. WW 2, p. 284-305, May 1970.
7. Shiller, F.C., Wave Forces on a Submerged Horizontal Cylinder, M.S. Thesis, Naval Postgraduate School, June 1971.
8. Perkinson, B.T., Wave Forces on a Horizontal Submerged Cylinder, M.S. Thesis, Naval Postgraduate School, June 1972.
9. Stokes, G.G., "On the Theory of Oscillatory Waves," Trans. Cambridge Phil. Soc., Vol. 8, and Supplement, Sci. Papers, Vol 1, 1847.
10. Borgman, L.E. and Chappellear, J.E., "The Use of Stokes-Struik Approximation for Waves of Finite Height," Proc. Sixth Conf. Coastal Eng., Chap. 16, 1958.
11. Skjelbreia, L. and Hendrickson, J.A., "Fifth Order Gravity Wave Theory," Proc. Seventh Conf. on Coastal Eng., Vol. 1, Chap. 10, 1961.
12. Bretschneider, C.L. "A Theory for Waves of Finite Height," Proc. Seventh Conf. on Coastal Eng., Vol. 2, Ch. 9, 1961.
13. Garrison, C.J., "Added Mass of a Cylinder in Contact with a Rigid Boundary," Journal of Hydronautics, V. 6, No. 1, pp. 59, Jan., 1972.